Holographic Entanglement Entropy

Structure and Applications from Noncommutative Field Theories to Energy Conditions

by

Charles Rabideau

BSc Honours Mathematics and Physics, McGill University, 2010

MSc Physics, The University of British Columbia, 2012

A THESIS SUBMITTED IN PARTIAL FULFILLMENT
OF THE REQUIREMENTS FOR THE DEGREE OF

Doctor of Philosophy

in

THE FACULTY OF GRADUATE AND POSTDOCTORAL STUDIES

(Physics)

The University of British Columbia

(Vancouver)

August 2016

Abstract

The holographic Ryu-Takayanagi formula for entanglement entropy connects the entanglement of a field theory to the geometry of a dual gravitational theory in a straightforward and universal way.

The first part of this thesis applies this formula to study the entanglement entropy in strongly coupled noncommutative field theories. It is found that the ground state of these theories have substantial entanglement at the length scale of the noncommutativity. The entanglement entropy in a different perturbative regime is also computed, where in contrast it is found that noncommutative interactions do not induce long range entanglement in the ground state to leading order in perturbations theory.

The second part of this thesis explores some general consequences of this holographic formula for the entanglement entropy. Identities involving entanglement entropies are related to nontrivial geometric constraints on gravitational duals. In particular, the strong subadditivity of entanglement entropy is used to show that dual three dimensional asymptotically anti-de Sitter gravitational states must obey an averaged null energy condition. Finally, this holographic formula allows us at least in principle to express the entanglement entropy of a region in a holographic field theory in terms of the one-point functions in that theory. This is explored in the context of a two dimensional conformal field theory where explicit calculations are possible. Our results in this case allow us to extend a recent proposal that the entanglement entropy of states near the vacuum of conformal theories can be understood by propagation in an auxiliary de Sitter space.

Preface

This thesis includes work that has been published. This preface explains my contributions to the research presented here.

Chapter 1 is a review and includes original research only when summarising the results of the rest of this thesis.

Chapter 2 is published as J. L. Karczmarek and C. Rabideau,"Holographic entanglement entropy in nonlocal theories," JHEP **1310**, 078 (2013). The research topic was proposed by J. L. Karczmarek. This work was the result of a close collaboration between the authors throughout the entire work. I completed the numerical calculations and prepared the figures. The publication was prepared by J. L. Karczmarek with contributions from notes I prepared.

Chapter 3 is published as C. Rabideau, "Perturbative entanglement entropy in nonlocal theories," JHEP **1509**, 180 (2015). I am the sole author of this work. This work was completed with the advice and supervision of J. L. Karczmarek.

Chapter 4 is published as N. Lashkari, C. Rabideau, P. Sabella-Garnier and M. Van Raamsdonk, "Inviolable energy conditions from entanglement inequalities," JHEP **1506**, 067 (2015). This work is based on the close collaboration of these authors under the supervision of M. Van Raamsdonk. I was most heavily involved in the results of Section 3 and 4 and Appendix B. The publication was prepared by N. Lashkari and M. Van Raamsdonk with contributions from notes prepared by all of the authors.

Chapter 5 is published as M. J. S. Beach, J. Lee, C. Rabideau and M. Van Raamsdonk, "Entanglement entropy from one-point functions in holographic states," JHEP **1606**, 085 (2016). This work is based on the close collaboration of the authors under the supervision of M. Van Raamsdonk. I was most heavily involved

in the work presented in Sections 4 and 5 and the Appendix, which are based on calculations completed by J. Lee and myself. All the co-authors participated in the writing and editing of this publication.

Table of Contents

List of Figures

Acknowledgments

I would like to thank my supervisor Joanna Karczmarek; my collaborators Matthew Beach, Nima Lashkari, Jaehoon Lee, Philippe Sabella-Garnier and Mark Van Raamsdonk; and all of the people I have had the great pleasure of discussing physics with in my office at UBC and at conferences and summer schools.

To my parents and family, thank you for your constant encouragement throughout this degree and your unconditional support throughout my life.

I was supported by funding from the Natural Sciences and Engineering Research Council of Canada's Alexander Graham Bell Canada Graduate Scholarship, the Izaak Walton Killam Memorial Fund for Advanced Studies, the University of British Columbia and the Walter C. Sumner Foundation.

My co-authors and I are grateful for helpful discussions with Raphael Bousso, Daniel Carney, Laurent Chaurette, Keshav Dasgupta, Ori Ganor, Thomas Hartman, Michal Heller, Juan Maldacena, Don Marolf, Shunji Matsuura, Robert Myers, Fernando Nogueira, Hirosi Ooguri, Ali Izadi Rad, Jared Stang and Brian Swingle.

This thesis is dedicated to Green College and all the wonderful people I have met there.

Chapter 1

Introduction

The standard model of particle physics has applied the techniques of quantum field theory very successfully to describe all observed particles and their interactions with one important caveat: it does not include the effects of gravity. In the classical limit, Einstein's theory of general relativity and Maxwell's equations describe the behaviour of matter subject to gravity and electromagnetism. At small scales in laboratory settings on earth, gravitational interactions become weak and can be ignored, while electromagnetism dominates. At these small scales in the quantum regime, Maxwell's classical description breaks down. The study of this regime lead to the development of the standard model, however as gravity is very weak in this regime the question of how to include it in the framework of the standard model could be postponed while still matching the results of experiments in particle accelerators to exquisite precision.

Applying the techniques of perturbative quantum field theory to general relativity leads to a nonrenormalisable theory, indicating that general relativity can only be understood as an effective field theory and does not describe the correct degrees of freedom to understand quantum gravity at short distance scales. String theory provides an ultraviolet completion which reduces to general relativity at long distances, but is not understood in a full nonperturbative sense. A full understanding of quantum gravity is still lacking and this is especially apparent in the context of geometries far from flat space such as black holes.

One of the symptoms of the problem of quantum gravity is the information loss

problem for black holes [1]. In classical general relativity no signal can escape the event horizon of a black hole. However, the study of quantum fields in curved space near a black hole reveals that black holes emit thermal radiation. As this radiation carries away energy, the black hole must shrink until it reaches a small size where the calculation breaks down. This poses a problem for any quantum theory which proposes to describe this system: time evolution in quantum systems is unitary and therefore reversible, yet the semi-classical description of the collapse of matter into a black hole which eventually evaporates away into thermal radiation is not unitary as the information about the configuration of the initial matter cannot be contained in thermal radiation. Either the unitarity of quantum gravity or the validity of the semi-classical approximation near the event horizon of the black hole must be abandoned.

Another symptom is the holographic bound on entropy in gravitational systems [2, 3]. In quantum field theories, thermal entropies are extensive. However, gravity contains black holes which are thermal systems with an entropy proportional to the area of their event horizon. In fact, in a gravitational system, thermal entropy in a region is bounded by the area of the boundary of that region. This lead to the holographic principle, which conjectures that a gravitational system in a region should be described by degrees of freedom on the boundary of that region.

Taken together, these suggest that we do not understand how to correctly organise the degrees of freedom of quantum gravity. However, a concrete example of the holographic principle has been found in the context of string theory where quantum gravity in an asymptotically anti-de Sitter (AdS) geometry was found to be dual to a conformal field theory living on its conformal boundary [4, 5]. This explicit example of holography can be used to shed light on quantum gravity as the dual conformal field theory is a well defined quantum system.[1]

Although in order to make contact with reality we might be most interested in quantum gravity with asymptotically flat or de Sitter boundary conditions, asymptotically AdS boundary conditions provide a good starting point for understanding

[1] The classical limit of the gravitational description is dual to a strong coupling limit in the conformal field theory, which although well defined in principle is often inaccessible to perturbative field theory techniques. This presents an obstacle to our original goal of understanding quantum gravity, but it also opens up new opportunities for understanding strongly coupled field theories by studying the dual classical gravitational description.

some of the problems of quantum gravity because they simplify the problem of defining diffeomorphism invariant operators. Diffeomorphisms are a gauge symmetry of general relativity and so the physical states and operators of quantum gravity should be diffeomorphism invariant, which precludes the existence of local operators in quantum gravity. However, the conformal structure of the asymptotic boundary of a geometry is invariant under diffeomorphisms and so this boundary provides a natural setting for diffeomorphism invariant observables. In asymptotically AdS spaces, the conformal boundary is timelike and the observables of quantum gravity can be matched to those of a conformal field theory.

This thesis will focus on a particular diffeomorphism invariant quantity, the area of the minimal surface anchored on a region of the boundary. The holographic duality relates this quantity to entanglement entropy in the dual conformal field theory through the Ryu-Takayanagi (RT) formula [6, 7, 8] and its covariant generalisation given by Huberny, Rangamani and Takayanagi [9].

From topological condensed matter systems, to black holes, to phase transitions and the emergence of spacetime in holography, the study of entanglement entropy has proven fruitful across many fields of physics [10, 11, 12, 8, 13]. Entanglement is one of the principal features distinguishing the quantum from the classical and entanglement entropy has proven to be an important tool for quantifying entanglement between two systems.

A useful property of entanglement entropy is that its definition is independent of the details of the theory in question giving us an tool to study universal properties of field theories and to compare the entanglement structure of very different field theories. This universality is reflected in the RT formula which relates the entanglement entropy directly to the geometry of the gravity dual.

Part I of this thesis uses this holographic relation to compute the entanglement entropy in noncommutative field theories using known gravitational duals and contrasts these results to those found in a different perturbative regime of these theories.

One of the original motivations for studying noncommutative field theories was to help regulate divergences in local quantum field theories. Much as introducing a commutation relation between positions and momenta regulated the ultraviolet catastrophe in black body radiation by introducing a minimal scale in phase space,

a commutation relation between coordinates can introduce a minimal length scale. Since this involves quantising coordinates, it was hoped that this might be related to the quantisation of spacetime required to understand quantum gravity. In addition, noncommutativity appears naturally in string theory in the context of D-branes.

Part II studies general properties of this holographic relation, with the goal of better understanding the holographic map and ultimately quantum gravity. Chapter 4 relates universal properties of entanglement entropy to constraints on the classical limit of dual holographic geometries in the form of gravitational energy inequalities. This tells us that although the effective theory given by general relativity can describe any geometry given appropriate matter, the ultraviolet completion given by string theory can only accommodate geometries obeying some constraints.

Chapter 5 uses properties of classical geometries to express entanglement entropy in terms of one-point functions, exhibiting constraints on quantum states which have a classical gravitational description. The results of this chapter also extend a surprising connection between entanglement entropy in conformal field theories and a field propagating in an auxiliary de Sitter (dS) space.

1.1 Entanglement

Given two Hilbert spaces $\mathscr{H}_A$ and $\mathscr{H}_B$, we can construct a tensor product space $\mathscr{H} = \mathscr{H}_A \otimes \mathscr{H}_B$ [2]. A state in the tensor product space is called a product state if it can be written as the tensor product of states in the constituent Hilbert spaces. $|\psi\rangle \in \mathscr{H}$ is a product state if $|\psi\rangle = |\psi_A\rangle \otimes |\psi_B\rangle$ for $|\psi_i\rangle \in \mathscr{H}_i$. A state which is not a product state is called an entangled state. Given an operator $\mathscr{O}_A$ on $\mathscr{H}_A$ and a product state $|\psi\rangle \in \mathscr{H}$, $\langle\psi|\mathscr{O}_A \otimes \mathbb{I}_B|\psi\rangle = \langle\psi_A|\mathscr{O}_A|\psi_A\rangle$. The expectation value of $\mathscr{O}_A$ in a product state only depends on the state in the A-subspace. This is not the case in an entangled state.

A density matrix is an operator on $\mathscr{H}$ which encodes the state, but which can also encode classical uncertainty like that found in statistical mechanics. Given an

[2] Given a basis $\{|\chi_a\rangle\}$ for $\mathscr{H}_{\mathscr{A}}$ and $\{|\xi_b\rangle\}$ for $\mathscr{H}_B$ the tensor product space is the space spanned by $\{|\chi_a\rangle\} \times \{|\xi_b\rangle\}$.

ensemble of states $|\psi_i\rangle$ with classical probabilities p_i, the density matrix is

$$\rho = \sum_i p_i |\psi_i\rangle\langle\psi_i|. \tag{1.1}$$

A density matrix describes a pure state if it can be written as $\rho = |\psi\rangle\langle\psi|$ for a single state, otherwise it describes a mixed state. The expectation value of an observable is $\mathrm{tr}\,(\rho\mathscr{O})$. Note that ρ itself is not an observable as it depends on the state.

Given a tensor product space and a basis $\{|\chi_a\rangle\}$ for $\mathscr{H}_A$ and $\{|\xi_b\rangle\}$ for $\mathscr{H}_B$, the partial trace is

$$\mathrm{tr}_B(\mathscr{O}) = \sum_b \langle\xi_b|\mathscr{O}|\xi_b\rangle, \tag{1.2}$$

which defines an operator on A.

The reduced density matrix $\rho_A = \mathrm{tr}_B\,\rho$ reproduces the expectation values of operators $\mathscr{O}_A$ on $\mathscr{H}_A$,

$$\mathrm{tr}\,\rho\mathscr{O}_A = \mathrm{tr}_A\,\rho_A\mathscr{O}_A. \tag{1.3}$$

The expectation value of local operators in a subspace can be reproduced with a state in that subspace at the cost of introducing classical uncertainty when the original state was entangled.

Quantifying this uncertainty using the von Neumann entropy of the reduced density matrix leads us to a natural way of quantifying the entanglement of a state. This is called the entanglement entropy[3]

$$S(A) = -\,\mathrm{tr}_A\,(\rho_A \log \rho_A)\,. \tag{1.4}$$

If ρ corresponds to a pure state on $\mathscr{H} = \mathscr{H}_A \otimes \mathscr{H}_B$, then the entanglement entropy computed using either subspace must be equal, $S(A) = S(B)$. In this case the classical uncertainty in the reduced density matrices on either subspace comes only from the entanglement. If the state is mixed, this equality does not hold as there is additional classical uncertainty which can be unevenly distributed between

[3] A useful reference on the topic of quantum information is [14].

the subsystems.

Of course this one number cannot fully describe the entanglement of a state. Other useful quantities include the Renyi entropies

$$S_n = \frac{1}{1-n} \log \mathrm{tr}_A \left(\rho_A^n\right) \tag{1.5}$$

and the entanglement negativity.

Knowledge of all the Renyi entropies allows one to compute the spectrum of the reduced density matrix also known as the entanglement spectrum. In fact the Renyi entropies are often used to calculate the entanglement entropy since

$$\lim_{n\to 1} S_n = S_A. \tag{1.6}$$

1.1.1 Field theory

The Hilbert space of a field theory can be decomposed into a tensor product of the degrees of freedom inside a region and those in its compliment. The entanglement entropy of a region in a field theory is that resulting from this decomposition. This entanglement entropy is defined for any state of the field theory, but unless otherwise specified we will usually be interested in the entanglement entropy in the ground state of the theory in question.

Since the von Neumann entropy of the reduced density matrix in a thermal state[4] will receive an extensive contribution related to the thermal entropy, some reserve the terminology of entanglement entropy for the vacuum state where the entanglement entropy can only be attributed to entanglement. This work will use the term somewhat more loosely to refer to the von Neumann entropy of the reduced density matrix in any state. The entanglement entropy in the ground state is sometimes referred to as geometric entanglement entropy in the literature.

When decomposing the Hilbert space of a gauge theory there are ambiguities related to the fact that the physical gauge invariant Hilbert space is not strictly local. The resolution of these ambiguities has been discussed in detail in the literature

[4] A thermal state is a mixed state described by a density matrix where every state appears with a classical probability given by the canonical ensemble, $\rho_{\text{thermal}} = e^{-\beta H}$.

[15, 16, 17].

In the ground states of local relativistic field theories, the entanglement entropy usually has an area law divergence.[5] In d dimensions,

$$S(A) = C\frac{|\partial A|}{\varepsilon^{d-1}} + \ldots, \qquad (d > 2) \tag{1.7}$$

$$S(A) = C\log\varepsilon + \ldots, \qquad (d = 2) \tag{1.8}$$

where ∂A is the boundary of A, $|\partial A|$ is the area of this boundary, C is a regulator dependent constant and ε is a UV regulator such as a lattice spacing. This area law divergence reflects the short range entanglement present in local quantum field theories.

In field theories, the entanglement entropy is often computed using the replica trick. Computing the Renyi entropies defined in (1.5) requires evaluating the n^{th} power of the reduced density matrix, which can be computed by appropriately sewing together along A the boundary conditions of n copies of the theory in a path integral. Analytically continuing the result for the n^{th} Renyi entropy to make n continuous and taking the appropriate limit as $n \to 1$ allows us to compute the entanglement entropy. This procedure is described in detail in Section 3.3 where it is used in the context of perturbative quantum field theory.

1.1.2 Relative entropy

The relative entropy

$$S(\rho||\sigma) = \mathrm{tr}(\rho\log\rho) - \mathrm{tr}(\rho\log\sigma). \tag{1.9}$$

provides a measure of the distinguishability between two density matrices as $S(\rho||\sigma) \geq 0$ with $S(\rho||\sigma) = 0$ iff $\rho = \sigma$. If ρ and σ are two different pure states this measure will diverge.

Fixing a state σ, the modular Hamiltonian can be defined $H_\sigma = \log\sigma$. The

[5] See [18] for a review of area laws. Exceptions include Fermi surfaces [19].

relative entropy is

$$S(\rho||\sigma) = \Delta E - \Delta S \tag{1.10}$$

$$\Delta S = S_\rho - S_\sigma \tag{1.11}$$

$$\Delta E = \langle H_\sigma \rangle_\rho - \langle H_\sigma \rangle_\sigma . \tag{1.12}$$

The relative entropy is positive and monotonic. For any regions A and B such that $A \subset B$,

$$S(\rho_A||\sigma_A) \geq 0, \tag{1.13}$$

$$S(\rho_B||\sigma_B) \geq S(\rho_A||\sigma_A) . \tag{1.14}$$

The relative entropy of a density matrix with itself vanishes. Since the relative entropy is positive,

$$\frac{d}{d\lambda} S(\rho + \lambda\delta\rho||\rho)\Big|_{\lambda=0} = 0, \tag{1.15}$$

which leads to the first law for entanglement entropies: [6]

$$\delta S = \delta E, \tag{1.16}$$

where where δS and δE are the first order changes under the perturbation of the state to the entanglement entropy and the expectation of the modular Hamiltonian respectively.

The monotonicity of relative entropy is equivalent to the strong sub-additivity of entanglement entropy (SSA), which says that for tripartite systems with $\mathscr{H} = \mathscr{H}_A \otimes \mathscr{H}_B \otimes \mathscr{H}_C$, [20, 21]

$$S(A \cup B) + S(B \cup C) \geq S(B) + S(A \cup B \cup C). \tag{1.17}$$

[6] This name is in analogy to the first law of thermodynamics.

This can be recast in terms of the mutual information

$$I(A,B) \equiv S(A) + S(B) - S(A \cup B), \tag{1.18}$$

so that strong sub-additivity reads

$$I(A, B \cup C) \geq I(A,B). \tag{1.19}$$

Restricting ourselves to a subset (B) of a subsystem ($B \cup C$) cannot increase our knowledge about the correlations between this subsystem and a reference subsystem (A).

1.2 Holography

This section will review gauge-gravity duality. The best established example is the $AdS_5 \times S_5$—$\mathcal{N} = 4, d = 4$ Super-Yang Mills duality [4, 5]. A number of variations of this example are also understood, which lead us to some entries in the dictionary of the duality[7] in its most general form.

D-branes are extended dynamical objects in string theory, described in textbooks on perturbative string theory, e.g. [22]. At small string coupling (g_s),[8] their degrees of freedom can be understood using string perturbation theory. These include a gauge theory living on the world-volume of the brane. The rank of the gauge group of this theory counts the number of units of brane charge, so we think of the low energy excitations of a stack of N branes as including a $U(N)$ gauge theory. The Yang-Mills coupling of this $U(N)$ gauge theory obeys $g_{YM}^2 \sim g_s$.

A large stack of these branes has a complimentary description at large string coupling [5]. In this case, the stack of branes represents a large classical source and can be described using classical gravity. We will focus on the case of D3-branes which fill 3 spatial directions. The curvature length scale of this classical solution obeys $R^4 = 4\pi g_s \alpha'^2 N$, where α' is the dimensionful string tension parameter in

[7] The gauge-gravity dictionary is the set of relationships that allows us to convert concepts between the two sides of the duality.

[8] String theory doesn't have externally fixed dimensionless coupling constants. However, in string perturbation theory amplitudes are expanded in the constant part of the expectation value of the dilaton field.

string theory which sets the length scale of fundamental strings. For this classical description to be a good approximation, the curvature must be large compared to the scale of both gravity and strings. In terms of string parameters, the string scale is $l_s \sim \sqrt{\alpha'}$ and the plank length is $l_p = \sqrt{G_N} \sim \sqrt{\alpha' \sqrt{g_s}}$. We need that

$$\frac{R^4}{l_s^4} \sim g_s N \sim g_{YM}^2 N \sim \lambda \gg 1 \tag{1.20}$$

$$\frac{R^4}{l_p^4} \sim N \gg 1, \tag{1.21}$$

where λ is the 't-Hooft coupling. In the low-energy limit of this gravitational description, the dynamics of a near horizon $AdS_5 \times S_5$ spacetime decouples from the rest. This is understood to be a complimentary strong coupling description of the low energy sector of this stack of branes, which at weak coupling is a $U(N)$ gauge theory.

This example related a specific spacetime to a specific conformal field theory (CFT). However, by considering different brane configurations, by varying the dimensionality of the branes or by turning on other sugergravity fields, many gauge-gravity dualities can be found [23, 5, 24, 25].

There is an important entry in the holographic dictionary which allows us to extend this duality. Deforming the action of a conformal theory by an operator $\mathcal{O}$ with source J corresponds to adding a scalar field to the gravitational action [26]. J and $\langle \mathcal{O} \rangle$ determine the boundary conditions for the scalar at the conformal boundary of the asymptotically AdS space. The mass of the scalar field is related to the conformal dimension of the operator $\mathcal{O}$ by $R^2 m^2 = \Delta(\Delta - d)$.

A general feature of the duality is that to describe a field theory defined on a manifold M the gravitational description will need a conformal boundary of M. This means that if the gravitational theory is defined on a manifold N, there must be a diffeomorphism which preserves the metric up to a local rescaling between ∂N and M.[9] This feature allows us to use local data in the field theory as boundary conditions for the gravitational theory.

[9] Given a region or a manifold M, ∂M denotes its boundary.

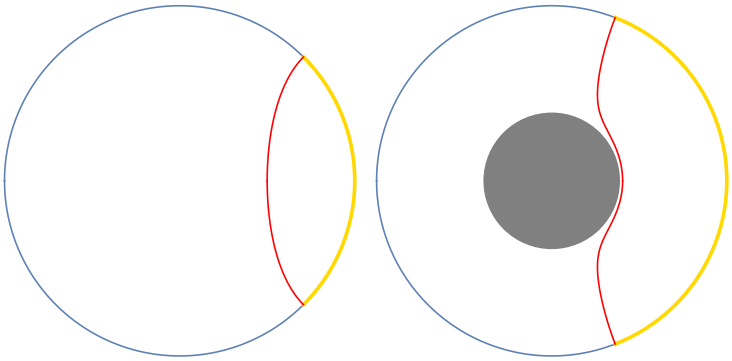

Figure 1.1: Two time slices of asymptotically AdS_3 geometries in coordinates which bring the conformal boundary (in blue) into view. The minimal surface (in red) homologous to a boundary region (in orange) is shown. On the left the geometry is empty AdS_3 corresponding to the vacuum state of a CFT_2. On the right, the geometry is a BTZ black hole corresponding to a thermal state of a CFT_2. The grey region is enclosed by the horizon of the black hole.

1.2.1 Holographic entanglement entropy

This thesis focuses on a particular entry in this holographic dictionary relating geometric entanglement entropy in a field theory to the area of boundary anchored minimal surfaces in its gravitational description known as the Ryu-Takayanagi (RT) formula [6, 7, 9, 8, 27, 28].

The entanglement entropy of a region A in a field theory in a particular state is given by the area of the minimal extremal area surface homologous[10] to A on the conformal boundary of the dual gravitational description of that state.

Let $\tilde{A}$ be an extremum of the area functional such that $\partial\tilde{A} = \partial A$, then

$$S(A) = \frac{|\tilde{A}|}{4G_N}, \tag{1.22}$$

where $|\tilde{A}|$ is the area of $\tilde{A}$ and G_N is Newton's constant. Figure 1.1 presents a few examples of such minimal surfaces for asymptotically AdS_3 spacetimes.

[10] Two submanifolds A and B of dimension k of a manifold M of dimension $d > k$ are homologous if $\partial A = \partial B$ and there exists a submanifold C such that $\partial C = A \cup B$. This essentially means that A is smoothly deformable into B.

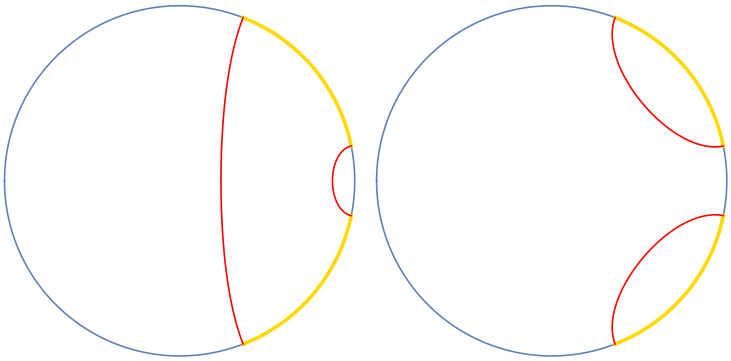

Figure 1.2: When the region A (in orange) is disconnected, there are multiple homologous extremal surfaces (in red). The extremal surface with the minimal area should be chosen.

If there are multiple extremal surfaces, the one with minimal area should be taken. If the gravitational state has a black hole, it may be necessary to include the area of an unconnected component of $\tilde{A}$ which wraps the horizon of the black hole so as to obey the homology constraint. In particular, there is no requirement for A or $\tilde{A}$ to be connected. See Figure 1.2 for an example where A is disconnected and Figure 1.3 for an example where $\tilde{A}$ is disconnected even though A is not.

For static geometries and regions defined on a fixed time slice of the field theory, the extremal surface is a minimal surface on the extension of that fixed time slice into the bulk of the dual geometry.

Regularisation

The entanglement entropy in field theories has a UV divergence as was discussed in Section 1.1.1. In holography this is reflected by the fact that the conformal boundary is at infinite distance, require any surface anchored there to have infinite area. In order to regularise the entanglement entropy, the surface is instead anchored to a distant cutoff surface. In this picture, the area law divergence typical of the entanglement entropies in field theories arises from the part of the minimal surface near the conformal boundary. In asymptotically AdS spaces, minimal surfaces quickly dive into the interior of the space and the divergence in their area comes from a throat near the boundary of the region (∂A) where they must be anchored to the

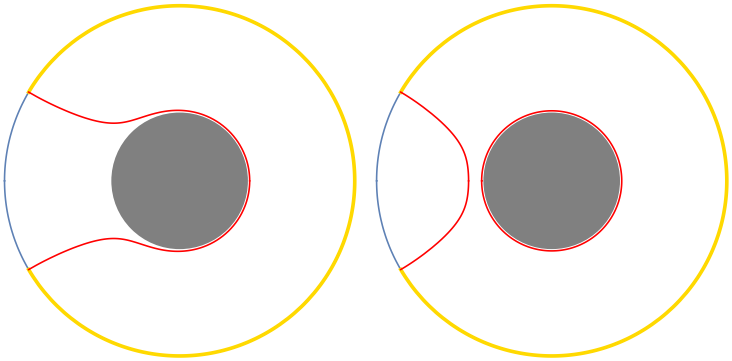

Figure 1.3: Two local minima of the area functional (in red) homologous to the same region (in orange) in an asymptotically AdS_3 BTZ black hole geometry corresponding to a thermal state of a CFT_2 (the conformal boundary is blue and the interior of the black hole horizon is grey). The extremal surface with the minimal area should be chosen.

conformal boundary.

Thermal states

In thermal states, for regions A much larger than the thermal scale, the entanglement entropy receives an extensive contribution proportional to the thermal entropy

$$S(A) \propto |A|s, \tag{1.23}$$

where $|A|$ is the volume of A and s is the entropy density in the thermal state.

The gravitational dual to a thermal state is generally a black hole where the thermal scale is tied to the size of the black hole. The extensive contribution to the entanglement entropy comes from the minimal surface dwelling near the horizon of the black hole as can be seen in Figure 1.1.

When A includes the entire boundary, the entanglement entropy is the thermodynamic entropy. In this case, the minimal surface homologous to the boundary cannot shrink to zero due to the presence of the black hole. Instead it wraps the horizon, reproducing the well known Bekenstein-Hawking entropy of the black

hole

$$S = \frac{\text{Area}}{4G_N}. \tag{1.24}$$

1.3 Noncommutative gauge theories

Noncommutative spaces arise naturally in string theory in the context of D-branes. Noncommutative spaces first manifest themselves in that the coordinates of a stack of D-branes are given by a set of noncommuting matrices rather than a list of numbers. In addition, the gauge field living on the worldvolume of a brane in the presence of a background NS-NS 2 form B field along the brane is a noncommutative field theory. In particular, the gauge theory on a D3-brane is Yang-Mills on a noncommutative plane. The gravity dual to this theory was found in [29, 30], which gives us the opportunity on one hand to learn about the application of the RT formula to new backgrounds[11] and on the other hand to study the entanglement entropy of this theory [31]. Part I of this thesis is dedicated to studying the entanglement entropy of noncommutative theories.

1.3.1 Summary of results for holographic entanglement entropy

In Chapter 2, the holographic RT formula is used to study entanglement entropies in a class of nonlocal theories related to field theories on noncommutative spaces. This will draw on my work with Joanna Karczmarek [31].

In a nonlocal theory, the behaviour of entanglement entropy could be expected to deviate from an area law and this is precisely what was found using holographic methods at strong coupling. In a simple nonlocal theory with a fixed scale of nonlocality a_L, a dipole deformation of $\mathcal{N} = 4$ SYM, the entanglement entropy is extensive (proportional to the volume of A), for regions A of size up to a_L. At length scales larger than a_L, it follows an area law, with an effective number of entangled degrees of freedom which is proportional to a_L. This is consistent with all the degrees of freedom within a region A of size a_L or smaller, and not only those

[11] This gravity dual has a number of unusual properties, including not being asymptotically AdS, a nontrivial dilaton profile and a nonzero B field.

living close to the boundary of A, having quantum correlations with the outside of A due to the nonlocal nature of the Hamiltonian. In contrast, in the noncommutative deformation of $\mathcal{N} = 4$ SYM, which is known to exhibit UV/IR mixing and whose nonlocality length scale grows with the UV cutoff, the entanglement entropy is extensive for all regions as long as their size is fixed as the UV cutoff is taken away.[12]

Since our theories differ from $\mathcal{N} = 4$ SYM in the UV, the holographic duals are not asymptotically AdS spaces. Their non-asymptotically AdS geometry has an interesting consequence. In previously studied examples of extensive behaviour of entanglement entropy (for example, in thermal states) this extensive behaviour was due to the minimal surface 'wrapping' a surface in the IR region of the dual, such as a black hole horizon (see for example [33]). Here, however, the extensivity arises from the fact that the minimal surfaces stays close to the cutoff surface: the volume law dependence of entanglement entropy is a UV phenomenon.

1.3.2 Summary of results for perturbative entanglement entropy

A natural question is whether the volume law behaviour found in the holographic analysis of entanglement entropies is generic to nonlocal theories or if it is confined to a strongly coupled, large N regime.

In Chapter 3, based on [34], the role of interactions in this question is investigated by considering field theories at small coupling and with one scalar degree of freedom and nonlocal interactions. The leading divergence in entanglement entropy of large regions to leading order in perturbation theory is not found to be proportional to the length scale of the nonlocality, hence no evidence of a volume law is found. Instead, the leading divergence in both theories has the same form as the standard local $\lambda\phi^4$ theory which follows an area law. This result indicates that, perturbatively these nonlocal interactions are not generating sufficient entanglement at distances of the nonlocality scale to change the leading divergence, at least to first order in the coupling.

[12] Entanglement entropy in the noncommutative theory was studied before in [32]. Here we extend and improve on those results.

1.4 The structure of holographic entanglement entropies

Part II investigates general features of the RT formula. This has the double goal of better understanding the two theories involved in the duality as well as clarifying the structure of the duality itself.

1.4.1 Constraints on geometry from entanglement

Entanglement entropy is a function on the subsets of a spacetime manifold. However not all such functions can arise as the entanglements entropies of some state. There are a number of constraints that the entanglement entropy of any state must obey. Similarly, not all such functions can arise as the areas of minimal surfaces in some geometry. Holographic entanglement entropy must satisfy both these sorts of constraints.

Studying these constraints and their translations through the gauge-gravity dictionary can provide new constraints on quantum gravity theories dual to quantum field theories. A strong form of gauge-gravity duality, where any quantum gravity theory with asymptotically *AdS* boundary conditions is dual to some field theory, would lead us to interpret any constraints following from the axioms of quantum mechanics as necessary conditions on any consistent theory of quantum gravity.

Constraints on entanglement entropies

The work in Chapter 4 concentrates on particular constraints on entanglement entropies following from the basic laws of quantum mechanics, which where discussed in Section 1.1.2. See [35] for more details on these constraints and additional references.

The RT formula gives a geometric interpretation of these entanglement inequalities in terms of the areas of minimal surfaces. The goal is to transform these constraints on the areas of surfaces into more useful geometric constraints.

Einstein Equations

This approach was used to derive that the holographic duals of states near the vacuum must obey the linearised Einstein equations near *AdS* [36, 37, 38].

Using techniques developed by Wald and Iyer for proving the first law of black

hole thermodynamics [39, 40], an integral of the linearised Einstein tensor for a perturbation over a region bounded by a minimal surface can be related to the change in the area and the energy associated to the asymptotic boost Killing vector.

Through the gauge-gravity dictionary these are related to the entanglement entropy and the expectation of the modular Hamiltonian. In the case of black hole thermodynamics a first law can be derived starting from the Einstein equations. In this case the logic can be reversed by using the first law of entanglement entropies in (1.16) for spherical boundary regions of all sizes to derive the linearised Einstein equations.

Energy conditions

Once we go beyond first order in perturbation theory, the field theory entanglement constraints no longer have the form of an equality, but rather of an inequality.

Inequalities that involve the Einstein tensor are referred to as energy or curvature conditions. Conditions of these form are usually assumed to hold for reasonable matter and are necessary to prove singularity theorems. Deriving such inequalities from the tenants of quantum mechanics would put them on more solid footing, so these provide a natural target.

Indeed some progress towards relating these constraints to such energy conditions has been made in low spacetime dimensions [41, 35, 42].

Chapter 4 shows that for $1+1$-dimensional spacetimes which have translational invariance, strong subadditivity can be related to an integrated null energy condition of the form

$$\int_\gamma ds T_{\mu\nu} u^\mu u^\nu \geq 0 \tag{1.25}$$

where γ is an arbitrary spatial geodesic and u^μ is a null vector generating a lightsheet of γ defined such that translation by u^μ produces an equal change in the spatial scale factor at all points.

In addition, a local version of the weak energy condition in the field theory directions of the dual geometry near the boundary follows from the positivity of the relative entropy. The near boundary expansion of $T_{\mu\nu}u^\mu u^\nu$ must be positive for any timelike vector u^μ with components only in the field theory directions, but not

in the holographic direction.

This chapter based on my work with Nima Lashkari, Philippe Sabella-Garnier and Mark Van Raamsdonk [35].

1.4.2 Expanding holographic entanglement entropies in terms of field theory one-point functions

In classical gravitational states, boundary conditions at the conformal boundary along with the equations of motion determine the geometry. Using the holographic duality this geometry allows us to compute whatever we wish about the state of a quantum theory with the boundary conditions at the conformal boundary as the only input. These are dual to the expectation value or one-point functions of operators in the quantum theory and the sources or coupling constants in its action. In other words, a holographic state, that is a state which is well approximated by a classical gravitational dual, is determined by its one-point functions. This can be contrasted to the fact that in a generic quantum state, knowledge of the expectation of an operator does not provide any information about the expectation value of the square of that operator.

Chapter 5 explores methods to compute the entanglement entropy in an expansion of one-point functions of operators in the field theory using both holographic and field theory methods. In particular, we developed an iterative method to express the entanglement entropy in a two-dimensional conformal field theory for states dual to gravity with no additional matter in terms of the one-point function of the stress tensor.

In [43], it was realised that the leading order contribution to entanglement entropy in this expansion can be understood in terms of the propagation of a scalar field in an auxiliary de Sitter space. We used our technique to compute the next order contribution and found that it could be understood by adding a simple interaction term to this scalar field.

This chapter is based on my work with Matt Beach, Jaehoon Lee and Mark Van Raamsdonk [44].

1.5 Outline

The following four chapters each contain my published work as described above and as detailed in the preface to this thesis. Each has its own introduction which introduces the concepts specific to that work and summarises the results of the rest of that publication. The final chapter is a conclusion which will summarise the original results contained in this thesis and discuss these results in the context of existing literature.

Part I

Entanglement Entropy in Noncommutative Field Theories

Chapter 2

Holographic Entanglement Entropies in Noncommutative Theories

2.1 Introduction

Geometric entanglement entropy as a tool to characterize physical properties of quantum field theories has recently received a large amount of attention. One attractive feature of geometric entanglement entropy as an observable is that it is defined in the same way in any quantum field theory: it is simply the von Neumann entropy, $-\mathrm{Tr}(\rho_A \log \rho_A)$, associated with the density matrix ρ_A describing degrees of freedom living inside a region A. ρ_A arises when the portion of total Hilbert space associated with degrees of freedom living outside of A is traced over. Universality of entanglement entropy is reflected in the Ryu-Takayanagi holographic formula [6]

$$S[A] = \frac{\mathrm{Vol_d}(\tilde{A})}{4G_N^{(d+2)}} \,. \tag{2.1}$$

Here, we place A, a d-dimensional spacial region, on a spacelike slice of the boundary of the (d+2)-dimensional spacetime dual to the quantum field theory of interest. $\tilde{A}$ is a minimal area surface in the bulk of the holographic dual spacetime homolo-

gous to A. $G_N^{(d+2)}$ is the (d+2)-dimensional Newton constant and the d-dimensional volume of $\tilde{A}$ is denoted with $\mathrm{Vol_d}(\tilde{A})$. [1]

The Ryu-Takayanagi formula (2.1) is applicable to holographic duals where the dilaton and the volume of the internal sphere are both constant. However, duals to the nonlocal theories we are interested in have neither, so the local gravitational constant $G_N^{(d+2)}$ varies. Thus we must use a generalized version of formula (2.1), given by [7]

$$S[A] = \frac{\mathrm{Vol}(\bar{A})}{4G_N^{(10)}}\,, \quad \text{with } \mathrm{Vol}(\bar{A}) = \int d^8\sigma e^{-2\phi}\sqrt{G^{(8)}_{\mathrm{ind}}}\,, \tag{2.2}$$

where $G_N^{(10)} = 8\pi^6(\alpha')^4 g_s^2$ is the (asymptotic) 10-dimensional Newton's constant and ϕ is the local value of the fluctuation in dilaton field (so that the local value of the 10-dimensional Newton's constant is $G_N^{(10)}e^{2\phi}$). Integration is now over a co-dimension two surface $\bar{A}$ that wraps the compact internal manifold of the holographic dual.

Because $\bar{A}$ wraps the internal manifold, its boundary is the direct product of the boundary of A, ∂A, and the internal manifold. To obtain entanglement entropy, $\bar{A}$ is chosen to to have minimal area (we will only work in static spacetimes). $G^{(8)}_{\mathrm{ind}}$ is the induced string frame metric on $\bar{A}$. By considering the standard relationship between local Newton's constants in different dimensions: $G_N^{(d+2),\mathrm{local}} = G_N^{(10)}e^{2\phi}/V_{8-d}$, together with $\mathrm{Vol}(\bar{A}) = V_{8-d}\ \mathrm{Vol_d}\tilde{A}$, (2.1) can be easily recovered from (2.2) for a scenario where the dilaton is a constant and the internal manifold has a constant volume V_{8-d} (in string metric). The more general formula (2.2) has been used to study, for example, tachyon condensation [46] and confinement-deconfinement transition [47]. We will refer to the 8-dimensional $\mathrm{Vol}(\bar{A})$ as the area of the minimal surface from now on.

Generically, geometric entanglement entropy has a UV divergence, so it needs to be regulated with a UV cutoff. Holographically, this is accomplished the usual way by placing the region A on a surface which is removed from the boundary of the holographic dual spacetime. Once the theory has been regulated with a

[1] For an accessible introduction and some recent developments to holographic entropy, see for example [8, 45].

cutoff, geometric entanglement entropy in the vacuum state can be thought to count effective degrees of freedom inside A that have quantum correlations with degrees of freedom outside of A. In other words, it measures the the range of quantum correlations generated in the ground state by the interactions in the Hamiltonian. For a local theory, degrees of freedom with correlations across the boundary of A must live near this boundary, which leads to the area law: entanglement entropy in local theories is generically proportional to the area of the boundary of A, $|\partial A|$. While the area law has not been proven for a general interacting field theory, it is expected to generically hold in local theories for the reason outlined above (see [18] for a review, focusing on lattice systems).

In a nonlocal theory, behaviour of entanglement entropy could be expected to deviate from the area law and this is precisely what we find using holographic methods at strong coupling. In a simple nonlocal theory with a fixed scale of nonlocality a_L, a dipole deformation of $\mathcal{N} = 4$ SYM, we find that entanglement entropy is extensive (proportional to the volume of A), for regions A of size up to a_L. At length scales higher than a_L, it follows an area law, with an effective number of entangled degrees of freedom which is proportional to a_L. This is consistent with all degrees of freedom within a region A of size a_L or smaller, and not only those living close to the boundary of A, having quantum correlations with the outside of A due to the nonlocal nature of the Hamiltonian. In contrast, in the noncommutative deformation of $\mathcal{N} = 4$ SYM, which is known to exhibit UV/IR mixing and whose nonlocality length scale grows with the UV cutoff, we find that entanglement entropy is extensive for all regions as long as their size is fixed as the UV cutoff is taken away to infinity.[2]

Recent work [48] links behaviour of entanglement entropy to the ability of a quantum system to 'scramble' information. Whether a given physical theory is capable of scrambling, and how fast it can scramble, has recently became of interest to the gravity community in the view of the so called fast scrambling conjecture [49]. It has been suggested that nonlocal theories might emulate the scrambling behaviour of stretched black hole horizons. While the results of [48] do not apply directly to quantum field theories, they are quite suggestive. Generally speaking,

[2]Entanglement entropy in the noncommutative theory was studied before in [32]. Here we extend and improve on those results.

they imply that local (lattice) theories, generally exhibiting area law for entanglement entropy at low energies, do not scramble information at these low energies, while theories with volume law entanglement entropy do. As we summarized above, we demonstrate here, in the two nonlocal theories we consider, that entanglement entropy follows a volume law in the vacuum state. There is no reason why entanglement entropy would cease to be extensive in an excited energy state; if anything, high energy states are more likely to have extensive entanglement entropy than low-lying states such as the vacuum state [50, 51]. Thus, the results of [48] would suggest that our nonlocal theories are capable of scrambling information. Combined with such results as those in [52], which shows that timescales for thermalization in nonlocal theories are accelerated compared to local theories, our work points towards these nonlocal theories at strong coupling being fast scramblers.

Since our theories differ from $\mathcal{N} = 4$ SYM in the UV, the holographic duals we use are not asymptotically AdS spaces. Their non-asymptotically AdS geometry has an interesting consequence. In previously studied examples of extensive behaviour of entanglement entropy (for example, in thermal states) this extensive behaviour was due to the minimal surface 'wrapping' a surface in the IR region of the dual, such as a black hole horizon (see for example [33]). Here, however, the extensivity arises from the fact that the minimal surfaces stays close to the cutoff surface: the volume law dependence of entanglement entropy is a UV phenomenon.

As we were finalizing this manustript, preprint [53] appeared, which also analizes entanglement entropy in the noncommutative SYM and which has some overlap with our work.

The reminder of the paper is organized as follows: in Section 2.2 we review nonlocal theories of interest and their gravity duals, in Section 2.3 we compute holographic entanglement entropy for a strip geometry, in Section 2.4 we compute holographic entanglement entropy in the noncommutative theory for a cylinder geometry, in Section 2.4 we briefly comment on mutual information in the noncommutative theory, and in Section 2.6 we offer further discussion of our results.

2.2 Theories considered and their gravity duals

We study the strong coupling limit of two different nonlocal deformations of $\mathcal{N} = 4$ SYM in 3+1 dimensions: a noncommutative deformation and a dipole deformation. Both of these can be realized as the effective low energy theory on D3-branes with a background NSNS B-field. To obtain the noncommutative deformation, both indices of the B-field must be in the worldvolume of the D3-brane, while to obtain the dipole theory, one of the indices must be in the worldvolume of the D3-brane while the other one must be in an orthogonal (spacial) direction.

Since both of these theories are UV deformations of the $\mathcal{N} = 4$ SYM, deep in the bulk their holographic duals reduce to pure AdS:

$$\frac{ds^2}{R^2} = u^2\left(-dt^2 + dx^2 + dy^2 + dz^2\right) + \frac{du^2}{u^2} + d\Omega_5^2 \tag{2.3}$$

with a constant dilaton:

$$e^{2\phi} = g_s^2 \ . \tag{2.4}$$

In our coordinates, the boundary of AdS space, corresponding to UV of the field theory, is at large u. It is in that region that the holographic duals in the next two sections will deviate from the above.

2.2.1 NCSYM

Noncommutative Yang-Mills theory is a generalization of ordinary Yang-Mills theory to a noncommutative spacetime, obtained by replacing the coordinates with a noncommutative algebra. We consider a simple set up where the x and y coordinates are replaced by the Heisenberg algebra, for which $[x,y] = i\theta$ and which corresponds to a noncommutative $x-y$ plane.

One way to define this noncommutative deformation of $\mathcal{N} = 4$ SYM is to replace all multiplication in the Lagrangian with a noncommutative star product:

$$(f\star g)(x,y) \ = e^{\frac{i}{2}\theta\left(\frac{\partial}{\partial\xi_1}\frac{\partial}{\partial\zeta_2} - \frac{\partial}{\partial\zeta_1}\frac{\partial}{\partial\xi_2}\right)} \ f(x+\xi_1, y+\zeta_1)g(x+\xi_2, y+\zeta_2) \ |_{\xi_1=\zeta_1=\xi_2=\zeta_2=0} \tag{2.5}$$

At low energy, this corresponds to deforming ordinary SYM theory by a gauge invariant operator of dimension six.

The holographic dual to this noncommutative SYM theory is given by the following bulk data [29, 30]

$$\begin{aligned}
\frac{ds^2}{R^2} &= u^2\left(-dt^2+f(u)\left(dx^2+dy^2\right)+dz^2\right)+\frac{du^2}{u^2}+d\Omega_5^2\,, \\
e^{2\phi} &= g_s^2\, f(u)\,, \\
B_{xy} &= -\frac{1-f(u)}{\theta} = -\frac{R^2}{\alpha'}\, a_\theta^2 u^4 f(u)\,, \\
f(u) &= \frac{1}{1+(a_\theta u)^4}\,,
\end{aligned} \tag{2.6}$$

where B_{xy} is the only nonzero component of the NS-NS form background. Note that x, y, z have units of length, while u has units of length inverse, or energy. $a_\theta = (\lambda)^{1/4}\sqrt{\theta}$ is the weak coupling length scale of noncommutativity $\sqrt{\theta}$ scaled by a power of the 't Hooft coupling λ and can be thought of as the length scale of noncommutativity at strong coupling.

In the infrared limit, $u \ll a_\theta^{-1}$, $f(u) \approx 1$ and the holographic dual appears to approach pure AdS space (2.3), while the UV region at large u is strongly deformed from pure AdS, so the holographic dual is not asymptotically AdS. Let ε denote the UV cutoff and $u_\varepsilon = \varepsilon^{-1}$ the corresponding energy cutoff. For $\varepsilon \gg a_\theta^{-1}$ ($u_\varepsilon \ll a_\theta^{-1}$), the deformed UV region of the dual spacetime is removed: noncommutativity has been renormalized away. However, when $u_\varepsilon > a_\theta^{-1}$, the non-AdS geometry near the boundary can influence the holographic computations of any field theory quantities, including those with large length scales. This opens the possibility of UV/IR mixing, defined as sensitivity of IR quantities to the exact value of the UV cutoff. Noncommutative theories are known to have UV/IR mixing [54]. The simplest way to understand the mechanism behind the UV/IR mixing in noncommutative theories is to consider fields with momentum p_y in the y-direction in (2.5): $f(x,y) = e^{-ip_y^f y}\hat{f}(x)$, $g(x,y) = e^{-ip_y^g y}\hat{g}(x)$. Then $f \star g(x,y) = e^{-i(p_y^g+p_y^f)y}\hat{f}(x-\theta p_y^g/2)\hat{g}(x+\theta p_y^f/2)$: the interaction in the x-direction is nonlocal on a length scale θp_y. We will see that this momentum (or energy) dependence of the scale of nonlocality is reflected in holographic entanglement entropy.

Finally, we need to understand the geometry of the boundary. The metric on the boundary of the gravitational spacetime (2.6) is singular since $f \to 0$ there.

However, this is not the metric applicable to the boundary field theory, as open string degrees of freedom see the so-called open string metric. This is the effective metric which enters open-string correlation functions in the presence of a NS-NS potential B, first derived in [55][3] and given by

$$G_{ij} = g_{ij} - \left(Bg^{-1}B\right)_{ij} , \tag{2.7}$$

where g_{ij} is the closed string metric. Substituting our holographic data at a fixed u, we obtain the open string metric, $G_{ij} = R^2u^2(\delta_{ij})$. Removing an AdS conformal factor, we see that the boundary field theory lives on a space with a conformally invariant metric $ds^2 = -dt^2 + dx^2 + dy^2 + dz^2$. This is the metric we will use to compute distances on the field theory side of the holographic correspondence.

2.2.2 Dipole theory

Another theory we will consider is the simplest dipole deformation of $\mathcal{N} = 4$ SYM [57, 58, 59]. A dipole theory is one in which multiplication has been replaced by the following noncommutative product:

$$(f\tilde{\star}g)(\vec{x}) = f\left(\vec{x} - \frac{\vec{L}_f}{2}\right) g\left(\vec{x} + \frac{\vec{L}_g}{2}\right) , \tag{2.8}$$

where $\vec{L}_f$ and $\vec{L}_g$ are the dipole vectors assigned to fields f and g respectively. At low energy, this corresponds to a deformation by a vector operator of dimension 5. To retain associativity of the new product, we must assign a dipole vector $\vec{L}_f + \vec{L}_g$ to $f\tilde{\star}g$. A simple way to achieve it is to associate with each field f a globally conserved charge Q_f and to let $\vec{L}_f = \vec{L}Q_f$. This can also be easily extended to multiple globally conserved charges. We will take $\vec{L} = L\hat{x}$ for some fixed length scale L, so that our theory is nonlocal only in the x-direction. As we saw in the previous section, noncommutative theory can be thought of as a dipole theory with the charges being momenta in a direction transverse to the dipole direction.[4]

[3] For an interpretation of the open string metric in the context of the AdS-CFT duality, see for example [56].

[4] This is not entirely accurate, as a field with transverse momentum p induces a dipole moment θp in all the fields it interacts with instead of in itself, but this detail will not be relevant to our

Dipole SYM is a simpler nonlocal theory than the NCSYM. Since the scale of the noncommutativity is fixed, the theory does not exhibit UV/IR mixing. We will see a clear signature of that in the entanglement entropy.

The holographic dual to a dipole deformation of $\mathscr{N}=4$ SYM theory where the scalar and fermion fields in $\mathscr{N}=4$ SYM are assigned dipole lengths based on global R-symmetry charges was found, using Melvin twists, in [25]. For the simplest case, where supersymmetry is broken completely and where all the scalar fields have the same dipole lengths, the holographic dual is given by the following bulk data:

$$\begin{aligned}
\frac{ds^2}{R^2} &= u^2\left(-dt^2+f(u)\left(dx^2\right)+dy^2+dz^2\right)+\frac{du^2}{u^2}+\text{metric on a deformed } S^5\ , \\
e^{2\phi} &= g_s^2\, f(u)\ , \\
B_{x\psi} &= -\frac{1-f(u)}{\tilde{L}} = -\frac{R^2}{\alpha'}a_L u^2 f(u)\ , \\
f(u) &= \frac{1}{1+(a_L u)^2}\ .
\end{aligned} \tag{2.9}$$

Similar to a_θ, $a_L=\lambda^{1/2}\tilde{L}$, $\tilde{L}=L/(2\pi)$ is the length scale of nonlocality at strong coupling. The usual S_5 of the gravity dual to a 3+1-dimensional theory is deformed in the following way: Express S^5 as S^1 fibration over $\mathbb{CP}^2$ (the Hopf fibration). Then the radius of the fiber acquires a u-dependent factor and is given by $Rf(u)$. The volume of the $\mathbb{CP}^2$ is constant and given by $R^4\pi^2/2$. Thus the compact manifold at radial position u has a volume given by $R^5\pi^3 f(u)$. ψ is the global angular 1-form of the Hopf fibration. For details, see [25].

As we did for the noncommutative theory in the previous section, we need to understand what metric to use for distances in the boundary dipole theory. Unfortunately, it does not seem possible to give an argument similar to the one in [55] to find an 'open string metric' for the D-branes whose low-energy theory gives us the dipole theory, since (in contrast to the noncommutative case) the dipole theory requires a nonzero NSNS field H and not just the nonzero potential B.[5] The

reasoning.

[5] A constant potential B which has only one of its indices in the worldvolume of a D-brane can be gauged away completely. It is therefore important that the other index is in a direction of a circle with varying radius, resulting in a nonzero H. In the holographic dual we consider, this circle is the

essence of the argument in [55] is that the only effect of the potential B is to change the boundary conditions for open string worldsheet theory. Thus, the boundary-boundary correlator is modified in a simple way that is equivalent to modifying the metric. To understand the open string metric for the dipole set up we need a different way to make the NSNS field B 'disappear'. We can accomplish this following [25] and using T-duality.

First, let's see what happens when we compactify the x direction in (2.6) on a circle of radius R_x and T-dualize using the prescription in [60]. The T-dual metric is

$$(Ru)^2\left(-dt^2+(dy-(\theta/\alpha')d\tilde{x})^2+dz^2\right)+\frac{1}{(Ru)^2}(d\tilde{x})^2+\frac{du^2}{u^2}+d\Omega_5^2\,, \qquad (2.10)$$

where $\tilde{x}$ is the T-dual coordinate to x. In the T-dual, B is zero. It has been traded for the twist around the $\tilde{x}$ circle: we identify $(\tilde{x},y)$ with $(\tilde{x}+2\pi\tilde{R}_x, y+2\pi\tilde{R}_x\theta)$, $R_x\tilde{R}_x\sim\alpha'$. Conformal invariance in the $t-y-z$ directions has been restored by T-duality, and we recover the open string metric (2.7) in those directions.[6] At the same time, the twist encodes the nonlocal structure of the theory. To see this recall that in the noncommutative theory, fields with momentum p_x in the x-direction appear to have dipole lengths θp_x. Taking x on a circle of radius R_x, $p=n/R_x$, with n an integer. When T-dualized, the corresponding open string mode has winding number n in the $\tilde{x}$ direction. Given the twist, the ends of this open string are separated by $\Delta y=2\pi\tilde{R}_x(\theta/\alpha')n$. Substituting $n=R_xp$ we get $\Delta y\sim\theta p$: the twist reproduces nonlocal behaviour of the noncommutative theory when the distances are measured in the conformally invariant (or open string) metric.

Returning to the dipole theory, we perform T-duality in the direction of the Hopf fiber to obtain

$$(Ru)^2\left(-dt^2+(dx-\tilde{L}d\tilde{\psi})^2+dy^2+dz^2\right)+\frac{(\alpha')^2}{R^2}(d\tilde{\psi})^2+\frac{du^2}{u^2}+d(\mathbb{CP}^2)\,. \quad (2.11)$$

Again, the NSNS potential $B_{\psi x}$ has been replaced by a twist. However, due to the

Hopf fiber.

[6] This is not a coincidence; the equation for the T-dual metric [60] and the equation for the open string metric (2.7) are functionally the same.

twist of the Hopf fibration, in the T-dual there is a new NSNS potential component, B_{xb} where b lies in the direction of the $\mathbb{CP}^2$, resulting in a nontrivial NSNS field H_{xbu}. Since ψ was a Dirichlet direction before T-duality, the interpretation is slightly different than it was in the noncommutative case. After T-duality, we have a twisted compactification identifying $(\tilde{\psi},x)$ with $(\tilde{\psi}+2\pi,x+2\pi\tilde{L})$. The proper distance between $(\tilde{\psi},x)$ and $(\tilde{\psi},x+2\pi\tilde{L})$ is therefore α'/R, which is small on the boundary in the large u limit. This is a sign of the nonlocality at the dipole length $L=2\pi\tilde{L}$. More relevant to us at this point is that, just like for the noncommutative theory, conformal invariance in the $t-x-y-z$ direction has been restored in the T-dual metric. It seems reasonable then to use the metric $-dt^2+dx^2+dy^2+dz^2$ to compute distances on in the boundary theory. For more details about this argument, as well as a string worldsheet argument about the origin of dipole theories, see [25, 61].

2.3 Entanglement entropy for the strip

We will start by studying entanglement entropy for degrees of freedom living on an infinitely long strip[7] $-l/2<x<l/2$, $-W/2<y,z<W/2$, $W\to\infty$. In this geometry, entanglement entropy follows the area law if it is independent of the strip width l. As we discussed in the Introduction, the relevant minimal surface is eight-dimensional; it wraps the compact (possibly deformed) sphere of the gravity dual and is homologous to the strip on the boundary in the non-compact dimensions. Its area is given by

$$\mathrm{Vol}(\bar{A})=\ \pi^3R^8W^2\int_{-l/2}^{l/2}dx\ (u(x))^3\ \sqrt{1+\frac{(u'(x))^2}{f(u)(u(x))^4}}\ , \tag{2.12}$$

where function $u(x)$ specifies the embedding of the bulk minimal area surface. The above formula for the area in terms of $u(x)$, with the appropriate form for $f(u)$, is applicable to all bulk metrics we are interested in: while the noncommutative theory dual has more directions warped by a factor $f(u)$ than the dipole one, in the dipole theory there is another factor of $f(u)$ accounting for the deformation of the

[7] In dimensions three and higher it would be perhaps more accurate to call this region a 'slab' rather than a 'strip'; nevertheless, we will use established terminology.

sphere on which the entangling surface is wrapped.

Following previous work, we can think of the problem of finding $u(x)$ corresponding to a minimal area surface as a dynamics problem in one dimension: x plays the role of time, $u(x)$ is the position and $u'(x)$ the velocity. Since the Lagrangian

$$\mathscr{L}(u,u') = u^3\sqrt{1+\frac{(u')^2}{f(u)u^4}} \tag{2.13}$$

does not depend explicitly on the 'time' x, there is a conserved Hamiltonian,

$$H = u'\frac{\partial\mathscr{L}(u,u')}{\partial u'} - \mathscr{L}(u,u') = -\frac{u^3}{\sqrt{1+\frac{(u')^2}{f(u)u^4}}}\ . \tag{2.14}$$

The Hamiltonian H is equal to $-u_*^3$, where u_* is the smallest value of $u(x)$ on the entangling surface. This point of deepest penetration of the minimal surface into the bulk occurs at $x=0$ by symmetry. $u'(x)$ vanishes there.

To implement the UV cutoff, the differential equation in (2.14) is to be solved with a boundary condition

$$u(x=\pm l/2) = u_\varepsilon = \frac{1}{\varepsilon}\ . \tag{2.15}$$

For some functions $f(u)$, (2.14) can be integrated explicitly. The answer is a hypergeometric function for $f(u)=1$ or $f(u)=1/(a_\theta u)^4$, and an elementary function for $f(u)=1/(a_L u)^2$. For $f(u)=1/(1+(a_L u)^2)$ or $f(u)=1/(1+(a_\theta u)^4)$, (2.14) can only be studied using series expansions in different limits.

To compute the area of the minimal surface, it is useful to solve (2.14) for $u'(x)$ as a function of u and substitute the result into (2.12). We obtain

$$\mathrm{Vol}(\bar{A}) = 2\pi^3 R^8 W^2\int_{u_*}^{u_\varepsilon}\frac{du}{u'}\,\frac{u^6}{(-H)} = 2\pi^3 R^8 W^2\int_{u_*}^{u_\varepsilon}\frac{duu^4}{u_*^3}\sqrt{\frac{u_*^6}{f(u)(u^6-u_*^6)}}\ . \tag{2.16}$$

To obtain the area of the minimal surface in terms of l from this equation, given u_ε, it is necessary to find the relationship between u_* and l.

2.3.1 Review of results for AdS space

For pure AdS, with $f(u) = 1$, we can remove the boundary of AdS all the way to infinity, $u_\varepsilon \to \infty$. Then, by integrating (2.14), we obtain a simple relationship between u_* and the width of the strip l:

$$l u_* = \frac{\Gamma(2/3)\Gamma(5/6)}{\sqrt{\pi}} \approx 0.8624 \, . \tag{2.17}$$

This relationship has a nice interpretation: holographic entanglement entropy for a structure of size l is given by the minimal surface that probes AdS bulk from the UV cutoff down to energy scales of order l^{-1}. Modes with wavelength longer than l do not contribute to the entanglement entropy.

To compute the leading order (for $u_\varepsilon \to \infty$) behaviour of the area of the minimal surface, we can we can use (2.16). Since u_* depends only on l and not on u_ε (i.e., it remains finite in the $u_\varepsilon \to \infty$ limit), the leading contribution to the area comes from large values of u. We can thus approximate

$$\mathrm{Vol}(\bar{A}) = 2\pi^3 R^8 W^2 \int^{u_\varepsilon} du u = \pi^3 R^8 \, \frac{W^2}{\varepsilon^2} \, . \tag{2.18}$$

A more precise result for the entanglement entropy density is obtained from a next-to-leading order computation. It gives a universal term which is finite and independent of the cutoff:

$$\frac{S}{W^2} = \frac{R^3}{4G_N^{(5)}} \left[\frac{1}{\varepsilon^2} - \frac{\left(2\Gamma\left(\frac{2}{3}\right)\Gamma\left(\frac{5}{6}\right)\right)^3}{\pi^{3/2}} \frac{1}{l^2} + (\text{terms that vanish for } \varepsilon \to 0) \right] . \tag{2.19}$$

In terms of field theory variables, we have

$$\frac{R^3}{4G_N^{(5)}} = \frac{N^2}{2\pi} \, , \tag{2.20}$$

so that the divergent part of the entanglement entropy is proportional to $N^2\varepsilon^{-2}$, with a numerical coefficient which is specific to strongly coupled $\mathcal{N} = 4$ SYM. The entanglement entropy is therefore of this generic form (applicable to 3+1 di-

mensions):

$$S = N_{\text{eff}} \frac{|\partial A|}{\varepsilon^2} = N_{\text{eff}} \frac{W^2}{\varepsilon^2} \tag{2.21}$$

with the number of effective on-shell degrees of freedom N_{eff} proportional to N^2.

Formula (2.21) supports the following simple picture of entanglement entropy in theory with a local UV fixed point: A quantum field theory in 3+1 dimensions with a UV cutoff ε^{-1} can be thought of as having on the order of one degree of freedom per cell of volume ε^3. The divergent part of the geometric entanglement entropy computed the vacuum state of such a theory is a measure of the effective number of degrees of freedom inside of a region A that have quantum correlations with degrees of freedom outside of A. In a local theory, only 'adjacent' degrees of freedom are coupled via the Hamiltonian and the simple intuition is that therefore quantum correlations between degrees of freedom inside of A and outside of A happen only across the boundary ∂A. Thus, the dominant part of the entanglement entropy comes from degrees of freedom which live within a distance ε of the boundary of A, with entanglement entropy proportional to the volume of this 'skin' region, equal to $\varepsilon|\partial A|$. Dividing this volume by the volume of one cell, ε^3, gives (2.21).

2.3.2 Dipole theory

Having briefly reviewed holographic entanglement entropy on a strip in undeformed SYM, we will now study it in the dipole theory.

In Figure 2.1, we show the relationship between l and u_* for the dipole theory. We see that it approaches the AdS result (2.17) for large strip widths l and that it deviates significantly from it for strips whose width is on the order of and smaller than a_L. For narrow strips, the entangling surface does not penetrate the bulk very deeply into the IR region. To study these, we assume that $u_* \gg a_L^{-1}$ and write $f(u) \approx (a_L u)^{-2}$. Here we get a pleasant surprise: the exact shape of the minimal surface can be obtained in terms of elementary functions

$$u(x) = \frac{u_*}{\cos(3x/a_L)^{1/3}} \quad \text{for } x/a_L \in [-\pi/6, \pi/6] \,. \tag{2.22}$$

The relationship between the penetration depth of the minimal surface and the

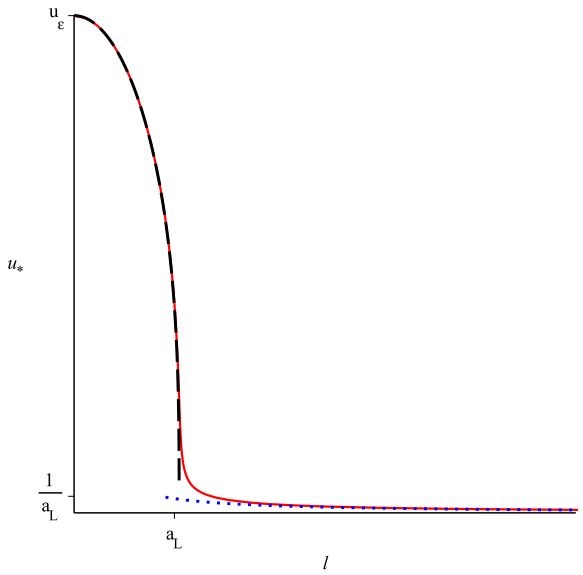

Figure 2.1: Point of deepest penetration u_* as a function of the strip width l for a minimal area surface in the gravity dual to the dipole theory (solid red line). The blue dotted line shows the result for pure AdS, given by (2.17), while the black dashed line shows the narrow strip approximation, (2.23). In this figure, $a_L u_\varepsilon = 30$.

width of the strip is

$$u_* = u_\varepsilon \left(\cos(3l/2a_L)\right)^{1/3} \ . \tag{2.23}$$

This equation is valid as long as $u_* \gg a_L^{-1}$, which, in the limit where u_ε is large, is true for all strip widths l up to $l = (\pi/3)a_L$. Notice that, in contrast to pure AdS, the point of deepest penetration u_* depends on the UV cutoff. Thus, if one works at the limit of infinite cutoff, these minimal area surfaces will be missed.

The area of the minimal surface under the approximation $f(u) \approx (a_L u)^{-2}$ is

$$\mathrm{Vol}(\bar{A}) = \pi^3 R^8 \left[\frac{W^2 a_L}{\varepsilon^3}\ \frac{2\sin(3l/2a_L)}{3}\right] \approx \pi^3 R^8\ \frac{W^2 l}{\varepsilon^3}\ , \tag{2.24}$$

where the final approximation is for a small strip width $l \ll a_L$. For narrow strips, entanglement entropy is extensive, proportional to the width of the strip. The first part of (2.24) gives the corrections to the volume scaling, controlled by the powers

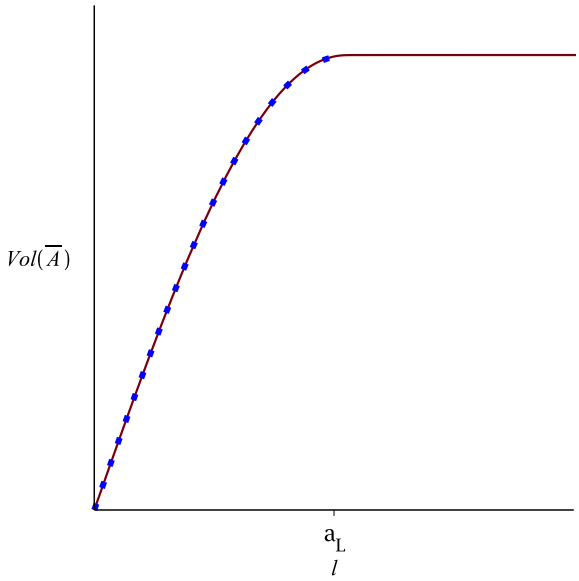

Figure 2.2: The area of the minimal surface as a function of the strip width l for for the dipole theory (solid red line). The blue dotted line shows result (2.24), valid for narrow strips $l < (\pi/3)a_L$. In this figure, $a_L u_\varepsilon = 30$.

of the ratio l/a_L.

For surfaces with large l (compared to a_L), we can use the same approximation as in (2.18), with $f(u) \approx (a_L u)^{-2}$:

$$\mathrm{Vol}(\bar{A}) = 2\pi^3 R^8 W^2 a_L \int^{u_\varepsilon} du u^2 = \pi^3 R^8 \, \frac{2W^2 a_L}{3\varepsilon^3} \tag{2.25}$$

We see that this area, which is independent of the width, is the same as the area obtained from (2.24) at the extremal value of l, $l = a_L\pi/3$. The situation is illustrated in Figure 2.2.

To summarize, we obtained the following result for the entanglement entropy density in the dipole theory:

$$\frac{S}{W^2} = \frac{N^2}{2\pi}\,\frac{2a_L}{3\varepsilon^3}\,G(l/a_L)\ , \quad \text{where } G(z) = \begin{cases} \sin(3z/2) & \text{for } z < \pi/3\ , \\ 1 & \text{for } z > \pi/3\ . \end{cases} \tag{2.26}$$

Entanglement entropy is extensive for very narrow strips, depends on the width of the strip in a nonlinear fashion for widths up to the nonlocality scale and smoothly goes over to a non-extensive (area law) behaviour for wide strips. For wide strips, while the entanglement entropy follows an area law, it has a different form than it would for a a generic local theory (given by (2.21)). To explain this, apply reasoning similar to that below (2.21) to a theory with a fixed scale of nonlocality a_L. By definition, the Hamiltonian of such a theory couples together degrees of freedom as far apart at a_L, thus, for a large region, the dominant part of geometric entanglement entropy should be proportional to the volume of a set of points no more than a_L away from the boundary of A. This volume, for a large enough region, can be approximated by $a_L|\partial A|$, leading to $S \propto a_L|\partial A|/\varepsilon^3$, which is exactly what we see in (2.26) for a strip with $l > (\pi/3)a_L$.

Applying our reasoning to the narrow strip, we see that, for $l < a_L$, all degrees of freedom inside the strip should are directly interacting with, and therefore entangled with, degrees of freedom outside of the strip. For a very narrow strip, degrees of freedom inside it will mostly be entangled with the degrees of freedom outside, and entanglement entropy should be proportional to l, which is exactly what we see. As the strip gets wider, some of the degrees of freedom inside the strip become entangled with each other, decreasing the entanglement with the outside and implying a sub-linear growth to the entanglement entropy as a function of l, again in agreement with (2.26).

The exact way in which S deviates from $S \propto l$ can be viewed as a way to probe the distribution of quantum correlations in the ground state of this nonlocal theory. It would be interesting to consider this further.

Finally, notice that above the nonlocality length scale a_L, the shape of the minimal surface is not greatly affected by the exact value of the cutoff; this is a sign that the dipole theory does not have UV/IR mixing. We will see a very different behaviour for the noncommutative theory.

2.3.3 NCSYM

For entanglement entropy of a strip in the noncommutative theory, the situation is more complicated. As is shown in Figure 2.3, there are as many as three extremal

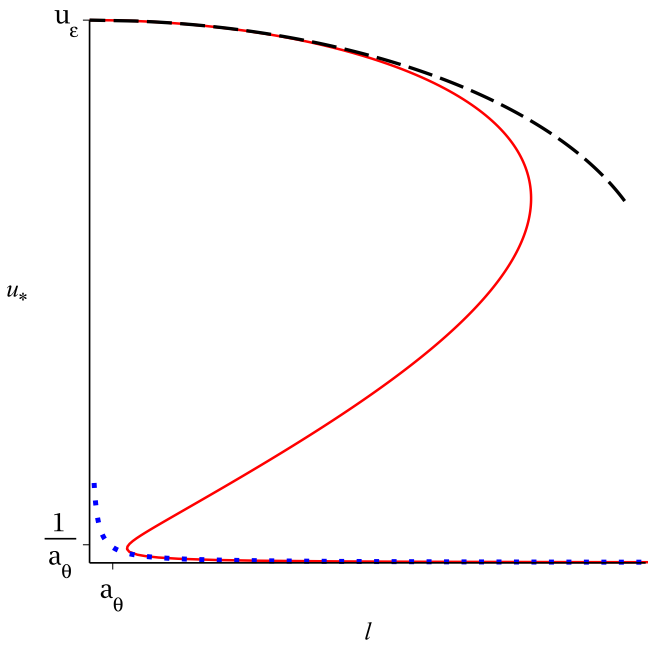

Figure 2.3: Point of deepest penetration u_* as a function of the strip width l for extremal area surfaces in the gravity dual to the noncommutative theory (solid red line). The blue dotted line shows the result for pure AdS, given by (2.17), while the black dashed line shows the result of (2.27). In this figure, $a_\theta u_\varepsilon = 30$.

area surfaces for a given width l of the strip. At large strip widths there is only one surface, for which the relationship between l and u_* approaches that of pure AdS, given by (2.17). At small widths, similarly to the dipole theory, there is a surface which stays close to the cutoff surface.[8] At intermediate l, there are three extremal surfaces, whose shape is shown in Figure 2.4. As we will see, the middle of the three surfaces is always unphysical (its area is never smaller than the other two). As the width is increased from zero, at some critical width l_c there is a phase transition as the area of the surface on the top-most branch becomes larger than the area of the surface on the bottom-most branch in Figure 2.3.

We start by studying top-most branch, which contains surfaces anchored on

[8] In [32], this surface was approximated by one placed exactly at the cutoff, at constant u.

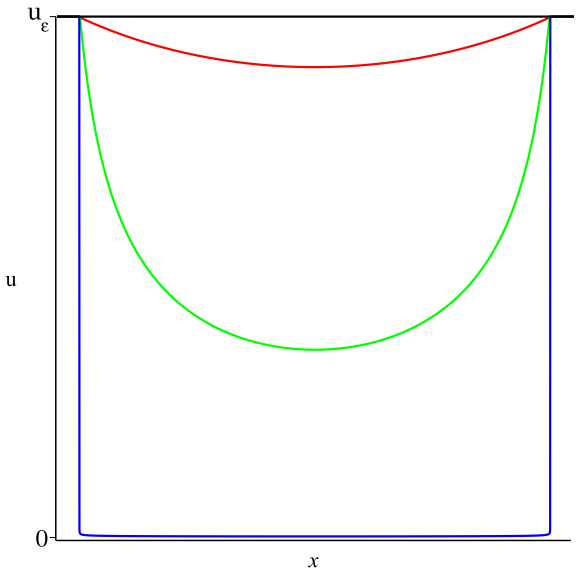

Figure 2.4: Shape of three extremal area surfaces, given as $u(x)$, all anchored on the same boundary strip.

narrow strips. To study these, we find $u(x)$ as a series expansion for small x. This allows us to write the relationship between l, u_* and u_ε for small l:

$$u_\varepsilon - u_* = \frac{3}{8}\frac{u_*^3}{1+(a_\theta u_*)^4} l^2 + \mathscr{O}((l/a_\theta)^4) \ . \tag{2.27}$$

The integral in (2.12) can also be expanded and evaluated for small l. Finally, substituting u_* from the expression above into the area integral, we can obtain the area for small l:

$$\mathrm{Vol}(\bar{A}) = \pi^3 R^8 W^2 \left[\frac{l}{\varepsilon^3} - \frac{3}{8}\frac{l^3}{a_\theta^4 \varepsilon (1+(\varepsilon/a_\theta)^4)} + \mathscr{O}((l/a_\theta)^4) \right] . \tag{2.28}$$

We have kept the sub-leading terms in ε for completeness — expression (2.28), as given, is correct even for large ε as long as l is small.

From (2.27) we see that as we increase u_ε keeping l fixed, $(u_\varepsilon - u_*) \propto l^2/u_*$, so that $u_\varepsilon - u_*$ approaches zero: the minimal surface approaches the boundary surface.

This result turns out to hold even for large (but fixed) strip width l in the large u_ε limit. In this limit, we approximate $f(u) \approx (a_\theta u)^4$. This allows us to obtain l and the area as a function of u_* and u_ε in terms of hypergeometric functions. We see that l/u_ε is a function of the ratio u_*/u_ε only. As u_ε approaches infinity with l fixed, this ratio goes to 1, showing that the entire minimal surface stays close to the boundary and that our approximation $f(u) \approx (a_\theta u)^4$ is self-consistent even for large l, as long as l is held fixed when the UV cutoff is removed. The following relationship holds under this approximation:

$$\int_{-l/2}^{l/2} dx\, \mathscr{L} = \frac{l u_*^3 + u_\varepsilon \sqrt{u_\varepsilon^6 - u_*^6}}{4} \,. \tag{2.29}$$

Thus, the leading order UV divergence of the area of the minimal surface at any fixed width l is

$$\text{Vol}(\bar{A}) = \pi^3 R^8 W^2 \frac{l}{\varepsilon^3} \,. \tag{2.30}$$

Having understood the top-most branch of the plot in Figure 2.3 , corresponding to surfaces that stay close to the boundary, we now move to the bottom-most one. These surfaces penetrate deeply into the bulk and their shape is not affected by the cutoff point. We can therefore use the same method as before for obtaining their area:

$$\text{Vol}(\bar{A}) = 2\pi^3 R^8 W^2 a_\theta^2 \int^{u_\varepsilon} u^3 du = \pi^3 R^8 \frac{W^2 a_\theta^2}{2\varepsilon^4} \,. \tag{2.31}$$

Since there are multiple extremal surfaces anchored on a strip, we need to find out which of them have the smallest area at a given l. At very small l there is only one surface (see Figure 2.3), thus, by continuity, for l less than some critical length l_c, the surface of the smallest area corresponds to the top-most branch of Figure 2.3. Its area is given by (2.30). At l_c there is a first order phase transition.[9] Above l_c, the surface with the smallest area is on the bottom-most branch of Figure 2.3 and its area is given by (2.31). To compute l_c, we set (2.30) and (2.31) equal and obtain that $l_c = a_\theta^2 u_\varepsilon/2$.

Since the critical length increases with u_ε, if we hold l fixed and take the limit

[9] This is similar to [62] and to [47], as well as to the recent paper [63]. Entanglement entropy is continuous across the transition, but its derivative is not.

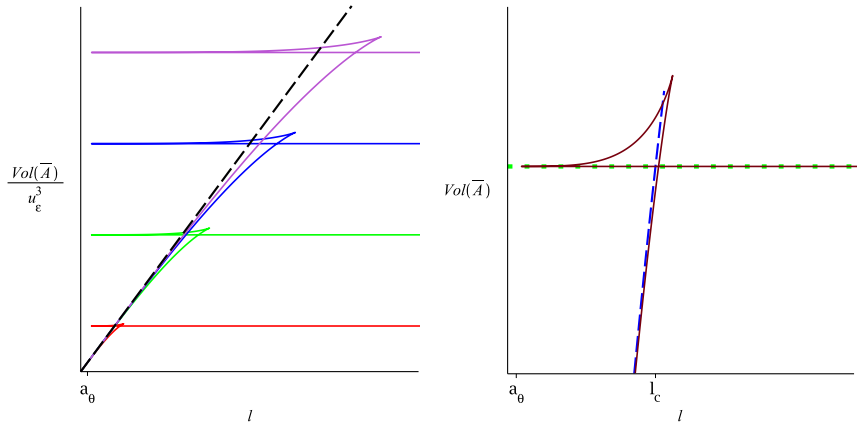

Figure 2.5: Area of the minimal surface as a function of strip width l for noncommutative theory. Top: Plots with $a_\theta u_\varepsilon = 10$, 30, 50 and 70 are shown. Area is scaled by a power of the cutoff to allow functions for different cutoffs to be plotted on the same set of axis. Dashed line corresponds to the leading term in (2.28), $\mathrm{Vol}(\bar{A})/u_\varepsilon^3 \propto l$. The range of validity of this approximate expression increases with increasing u_ε. Bottom: Detail of the fish-tail phase transition is shown. The green dotted line and the blue dashed line correspond to (2.31) and (2.28) respectively. $a_\theta u_\varepsilon = 30$.

$u_\varepsilon \to \infty$, l_c will diverge to infinity as well and (2.30) will hold for any l.

Our analysis implies that in the limit $\varepsilon \to 0$, the entanglement entropy density for a strip of a fixed length l is

$$\frac{S}{W^2} = \frac{N}{2\pi}\left[\frac{l}{\varepsilon^3} - \frac{3}{8}\frac{l^3}{a_\theta^4 \varepsilon} + \text{terms vanishing for } \varepsilon \to 0\right], \qquad (2.32)$$

which, to the leading order, is the same answer as for the dipole theory in the narrow strip limit ((2.26), $l \ll a_L$).

To understand the physics behind this result, we recall that in the noncommutative theory a mode with momentum p_y in the y-direction can be thought of as a dipole field with an effective dipole length θp_y in the x-direction. The high-momentum modes which dominate the divergent part of entanglement entropy all have large effective dipole moments. Therefore the entanglement entropy is that of a nonlocal theory with a large effective scale of nonlocality. This is precisely what

we see.

In the complementary limit, fixing a (large) UV cutoff first and then considering wide strips, $l > l_c$, (2.31) shows that entanglement entropy density is equal to

$$\frac{S}{W^2} = \frac{N^2}{2\pi}\,\frac{a_\theta^2}{2\varepsilon^4}\,. \tag{2.33}$$

We see that the area law applies and the number of degrees of freedom which are near enough to the boundary of the region to be entangled with the outside is proportional to a_θ^2/ε^2. This is equal to the scale of noncommutativity at the UV cutoff ($a_\theta^2 u_\varepsilon = a_\theta^2/\varepsilon$) divided by the cutoff length scale ε, consistent with our previous discussions.

In the next section, we will compute the entanglement entropy in the noncommutative theory for another geometry: a cylinder whose circular cross-section is in the two noncommutative directions x and y and which is extended infinitely in the commutative direction z. We will obtain a result for the entanglement entropy that is similar to the one in this section, while the geometry of the entangling surfaces will be very different.

2.4 Entanglement entropy for the cylinder in NCSYM

Consider a region on the boundary extended in the z direction ($-W/2 < z < W/2$, $W \to \infty$) and satisfying $x^2 + y^2 < l^2$ in the x and y directions. The area functional for a surface homologous to this cylindrical region, assuming rotational symmetry in the $x-y$ plane and translational symmetry in the z direction, is

$$\mathrm{Vol}(\bar{A}) = 2\pi^4 R^8 W \int_0^l dr\; r\; (u(r))^3\; \sqrt{1 + \frac{(u'(r))^2}{f(u)(u(r))^4}}\,, \tag{2.34}$$

where $r = \sqrt{x^2+y^2}$ and the surface is specified by a function $u(r)$.

Since r appears explicitly in the Lagrangian density, the equation of motion cannot be integrated explicitly even once. We will therefore have to rely more on numerical computation.

Figure 2.6 shows shapes of extremal surfaces anchored on a disk in the boundary noncommutative theory. As is easy to check analytically, all these surfaces

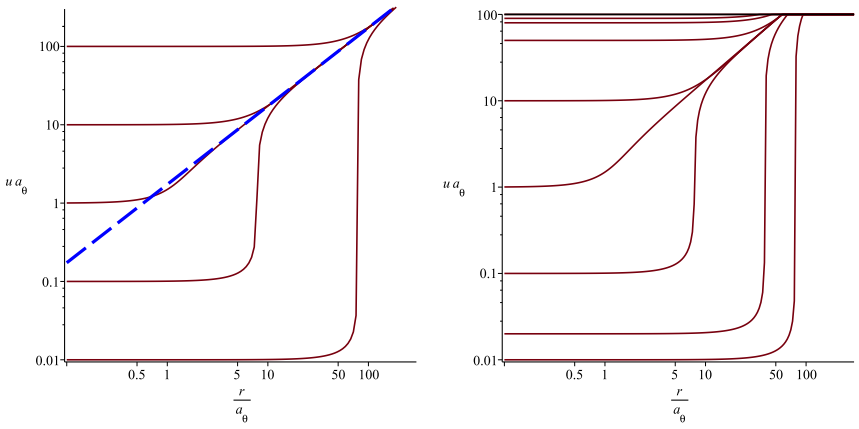

Figure 2.6: Extremal surfaces homologous to a cylinder in NCSYM, presented as $u(r)$. On the left, the straight dashed line is the asymptotic behaviour given by $a_\theta u = \sqrt{3}r/a_\theta$. On the right, surfaces with l sufficiently smaller or larger than $l_c = a_\theta^2 u_\varepsilon/\sqrt{3}$ to reach the cutoff before they had time to approach the this asymptote are shown as well.

asymptote at large r and u to a single 'cone' given by $a_\theta u = \sqrt{3}r/a_\theta$. A linear analysis about this asymptotic solution gives

$$a_\theta u(r) \approx \sqrt{3}r/a_\theta + t\cos\left(\frac{\sqrt{7}}{2}\ln(r/a_\theta) + \varphi\right) , \tag{2.35}$$

where t and φ are free parameters, with t small. In principle, a relationship between t and φ could be derived given that $u'(0) = 0$, but it cannot be obtained within perturbation theory. It is interesting and perhaps surprising that the fluctuations about the asymptote are oscillatory in r. This behaviour, which can be seen in Figure 2.6, agrees very well with more detailed numerical analysis.

From Figure 2.6 we see that surfaces with u_* relatively close to a_θ^{-1} approach the asymptote $u = \sqrt{3}r/a_\theta^2$ before reaching the cutoff, while those with large u_* ($a_\theta u_* \gg 1$) or small u_* ($a_\theta u_* \ll 1$) do not. At a fixed cutoff, then, we have three classes of surfaces: shallowly probing surfaces, $a_\theta u_* \gg 1$, with l smaller than and bounded away from $l_c := a_\theta^2 u_\varepsilon/\sqrt{3}$, deeply probing surfaces, $a_\theta u_* \ll 1$, with l larger than than and bounded away from l_c and the intermediate category, for which l is approximately equal to l_c. In the first and second category, there is a unique

extremal surface at a given radius l, while for radii close to l_c the situation is more complicated, due to the oscillatory nature of the near-asymptotic solutions shown in (2.35). Since the cutoff radius l_c increases with u_ε (similar to the behaviour in the strip geometry), the entanglement surface for a region with any radius l belongs to the first category for a sufficiently high UV cutoff.

First, let us consider the surfaces with small l/a_θ. These can be studied by expanding in l/a_θ. We get the following two results:

$$u_\varepsilon - u_* = \frac{3}{4}\frac{u_*^3}{1+(a_\theta u_*)^4} l^2 + \mathcal{O}((l/a_\theta)^4) \ , \tag{2.36}$$

$$\mathrm{Vol}(\bar{A}) = \ 2\pi^4 R^8 W \left[\frac{l^2}{2\varepsilon^3} \ - \ \frac{9}{32}\frac{l^4}{a_\theta^4 \varepsilon (1+(\varepsilon/a_\theta)^4)} + \mathcal{O}((l/a_\theta)^4) \right] \ . \tag{2.37}$$

The l/a_θ expansion for the area of the minimal surface has a structure which is similar to the one we obtained for the strip in the noncommutative theory: organizing the expansion in powers of l, the term of order l^n has as its leading ε dependence $1/\varepsilon^{5-n}$ (with n even). Assuming that this analytic structure is valid for finite l/a_θ, we obtain that in the limit $\varepsilon \to 0$, the entanglement entropy density for a cylinder at a fixed radius l is

$$\frac{S}{W} = \frac{N}{2\pi} \left[\frac{\pi l^2}{\varepsilon^3} \ - \ \frac{9}{32}\frac{l^4}{a_\theta^4 \varepsilon} + \text{terms vanishing for } \varepsilon \to 0 \right] \ . \tag{2.38}$$

Qualitatively, this is the same answer as we obtained for the strip: entanglement entropy is extensive, proportional to the volume of the considered region. Notice that neither expression has a non-zero universal (independent of ε part).

At finite (and large) cutoff, we can consider large radius cylinders. For l sufficiently larger than l_c we see from Figure 2.6 that $u_* a_\theta \ll 1$ and the entangling surface seems close in shape to that in pure AdS (as it approaches the boundary at approximately the right angle, based on numerical evidence). Thus, $u_* \propto l^{-1}$ and

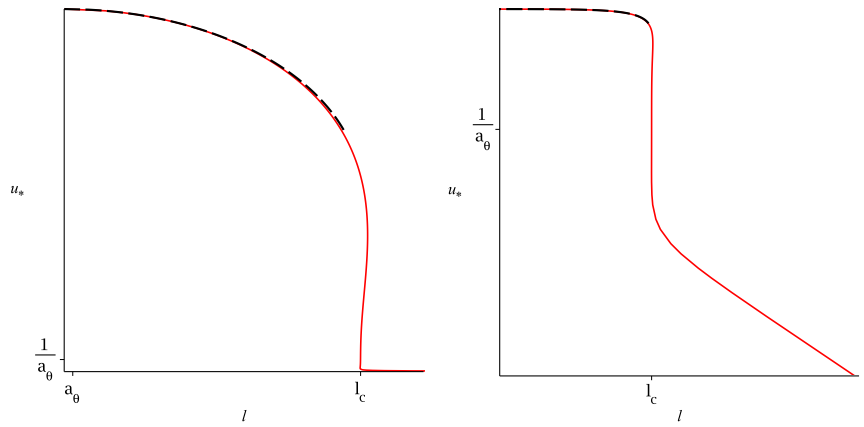

Figure 2.7: Point of deepest penetration u_* as a function of the cylinder's radius l for the minimal surface homologous to a cylinder in the noncommutative theory. The black dashed line corresponds to (2.36). Linear scale on the left, log-log scale on the right; $a_\theta u_\varepsilon = 30$ for both plots.

the area is approximately

$$\mathrm{Vol}(\bar{A}) = 2\pi^4 R^8 W a_\theta^2 \int dr\, r\, u^3\, u'(r) = 2\pi^4 R^8 W a_\theta^2 l \int^{u_\varepsilon} du u^3 = \pi^3 R^8 \frac{2\pi l W a_\theta^2}{4\varepsilon^4}\,, \tag{2.39}$$

where we have used $f(u) \approx (a_\theta u)^{-4}$ and approximated $r \approx l$ in the region near the boundary. Resulting entanglement entropy has the same interpretation as the one in (2.33), with the area of the strip's boundary, W^2 replaced by the area of the boundary of the cylinder, $2\pi l W$.

Having understood the minimal surface in the large l and small l limits, we now turn to l near the cutoff radius $l_c = a_\theta^2 u_\varepsilon/\sqrt{3}$, which corresponds to $u_* a_\theta$ close to 1. Figure 2.7 shows the dependence of u_* on l over the entire range for a finite cutoff. We notice that near l_c, there are multiple values of u_* at a given l: just like in the case of the strip, there is a range of radii l for which there exist multiple extremal surfaces anchored on the same cylinder. This is related the oscillating nature of the asymptotic solution (2.35). Since taking a large cutoff limit removes the radius l_c, at which phase transition take place, to infinity, we will not attempt a detailed study of the properties of the phase transition, which is complicated by the oscillatory nature of the minimal surfaces near the critical radius.

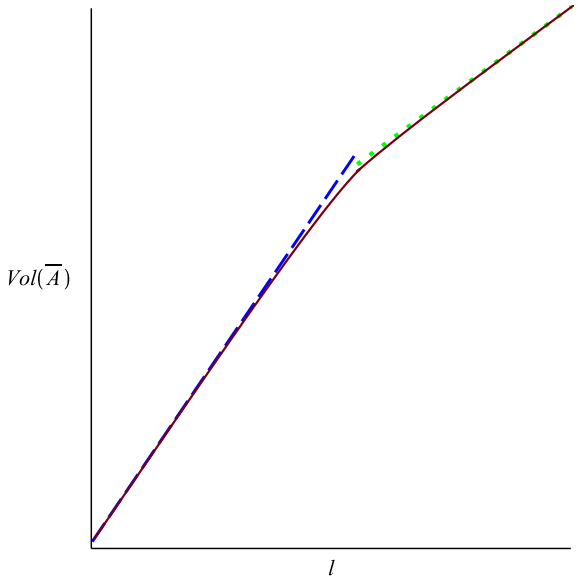

Figure 2.8: Area of the minimal surface homologous to a cylinder, as a function of the cylinder's radius l, with both axis shown in logarithmic scale. $a_\theta u_\varepsilon = 30$. The green dotted line and the blue dashed line correspond to (2.39) and (2.37) respectively.

It is interesting to notice that, apart from the details of the phase transition, the entanglement entropy for the cylinder has the same qualitative behaviour as it does for the strip, ever though the geometry of the minimal surfaces is very different.

2.5 Mutual information in NCSYM

To strengthen our discussion of UV/IR mixing in noncommutative SYM theory, it would be interesting to study the behaviour of an observable that (in the commutative theory) is finite in the large UV cutoff limit. One such observable is mutual information.

Consider two disjoint regions A and B. Mutual information is defined by $I(A,B) := S(A) + S(B) - S(A \cup B)$. Subadditivity implies that mutual information is a non-negative quantity. For local theories, holographic mutual information is UV finite, since contributions from the near-boundary parts of the minimal surfaces cancels. It is known to exhibit a phase transition [64]: if the regions A and

B have width l and the distance between them is x, $I(A,B)$ is nonzero for x less than some x_c and zero for x greater than x_c, with x_c/l of order 1. The origin of this phase transition is shown in Figure 1.2: for large x/l, the minimal area surface has the the topology shown on the right of Figure 1.2, while for small x/l, it has the topology shown on the left of Figure 1.2. Behaviour of mutual information and the existence or disappearance of this phase transition can be used to find characteristic length scales, see for example [65] and [66]. For NCSYM we find that the mutual information phase transition is absent for length scales less than l_c. The fact that l_c depends on the UV cutoff is then a signature of the UV/IR mixing.

To study the details of this signature, let regions A and B be strips of width l_A and l_B respectively, separated by a distance x. Then, if l_A, l_B and x are held fixed as the cutoff u_ε is taken to infinity, entanglement entropies associated with strips of width x, l_A, l_B and $l_A + l_B + x$ are all extensive. Therefore, $S(l_A) + S(l_B) < S(l_A + l_B + x) + S(x)$, i.e. the surface on the right in Figure 1.2 has a smaller area than that on the left in Figure 1.2. This implies that $I(A,B) = 0$ for any x and there is no phase transition. On the other hand, if l_A and l_B are both larger than l_c, then $S(l_A) \approx S(l_B) \approx S(l_A + l_B + x)$ because to leading order the entanglement entropies do not depend on the width of the strip. Mutual information is positive (and divergent, since entanglement entropy in the noncommutative theory does not have a UV-finite piece) as long as x is small enough and undergoes a phase transition as x is increased just like it does for a local field theory.

It would be interesting to study the behaviour of mutual information near the phase transition in detail. We leave this to future work.

2.6 Final comments

A key ingredient in our analysis was keeping the cutoff finite, if large. Only when the entangling region A is placed on a cutoff surface at finite $u = u_\varepsilon$ can the correct minimal area minimal surfaces be found. This is especially true in the noncommutative theory, where UV/IR mixing implies that infrared physics is affected by the precise value of the cutoff.

We have already discussed the origins of the dependence of the entanglement entropy on the size (volume or area) of the region A, on the cutoff length ε and on

the intrinsic length scales a_L and a_θ built into our nonlocal theories. The numerical coefficients we obtain are of physical significance: In the volume law regime, the coefficient measures whether degrees of freedom inside of A are are entangled with the outside of A or with each other. Therefore, this coefficient controls the maximum size of the region over which the theory thermalizes [48]. A similar statement can be made about the coefficient in the area law regime.

While the open string metric gives distances in the nonlocal boundary field theory, it is the closed string metric that determines the causal structure of the theory. In a local field theory, knowledge of the density matrix ρ_A in the region A is enough to compute all observables within the domain of dependence of A. While we don't know exactly which portion of the total holographic dual spacetime is dual to ρ_A itself [67, 68, 69, 70], the answer must involve the bulk (closed string) metric and its causal structure. Applying this argument to our nonlocal theories, we see that it is the bulk metric that determines the extent of the holographic dual to the density matrix ρ_A. For example, this holographic dual might be bounded by the minimal surface. Then, the intersection between the AdS boundary and the lightsheets originating from the minimal surface might be interpreted as the boundary of the "domain of dependence" of the region A in a nonlocal theory. We would expect that knowledge of the density matrix ρ_A would be sufficient to determine all observables within this "domain of dependence". This new "domain of dependence" is determined causally not by the open string metric but by the bulk closed string metric at a fixed cutoff. This closed string metric is not isotropic, in fact, it has a very large "speed of light" in the nonlocal directions, compared with the open string metric. Field theory computations show that nonlocal field theories have large propagation speeds , see for example the behaviour discussed in [54], or the observations that the propagation speed in the noncommutative theory is effectively infinite [71, 72]. As a result, in a nonlocal theory the "domain of dependence" should have a very small time-like extent. This is consistent with it being bound by lightsheets which originate on a minimal surface which does penetrate the bulk very far, a feature we have observed.

A related feature of our minimal surfaces is that they are not necessarily orthogonal to the boundary at a finite cutoff. Therefore, for example, the two proposals given in [9] for a covariant version of holographic entanglement entropy are

not necessarily equivalent, raising an interesting question about time-dependent nonlocal theories. Similarly, arguments for strong subadditivity of covariant holographic entanglement entropy in time dependent spacetimes, in [73], do not apply either (however, the simple argument for static spacetimes, in [74], does apply, and therefore the entanglement entropies computed in this paper do satisfy strong subadditivity).

Since our computations were done using holography, they are reliable in the strong coupling limit. It would be interesting to see whether the same results apply at weak coupling, with the appropriate nonlocal scale, a_θ or a_L, replaced by its weak coupling counterpart, $\sqrt{\theta}$ or L respectively. This might not necessarily be the case: for example, the enhancement to the rate of dissipation provided by noncommutativity at strong coupling is not seen at weak coupling [52]. The analysis in [52] points towards strong coupling being necessary for scrambling in noncommutative theory, and, if the results in [48] can be extended to this situation, strong coupling being necessary for extensive entanglement entropy. It would be interesting to settle this question by a direct computation of geometric entanglement entropy in a weakly coupled noncommutative theory. Unfortunatelly, it will not be possible to learn anything from free noncommutative theories as these are equivalent to their commutative counterparts.

A simple example of a nonlocal field theory with volume scaling of its entanglement entropy was given in [75]. In that work, it was proposed that volume scaling was a necessary feature of entanglement entropy in a hypothetical field theory dual to flat space. In contrast to this hypothetical theory, our nonlocal theories do not have vanishing correlation functions.

Finally, it would be interesting to study other extremal surfaces in holographic duals to nonlocal theories, following the work for local theories [76], as well as to extend our results to finite temperature.

Chapter 3

Perturbative Entanglement Entropies in Noncommutative Theories

3.1 Introduction

Local field theories generally exhibit what is know as an area law behaviour, where the leading divergence in the entanglement entropy of a spatial region is proportional to the area of the boundary of that region. That is, $S \sim |\partial A|\Lambda^{d-2}$, where S is the entanglement entropy, $|\partial A|$ the area of the boundary of the region and Λ is the momentum scale of the UV regulator of the theory, for example the inverse of a lattice spacing.[1] However, recent holographic studies of strongly coupled nonlocal theories have found a volume law behaviour instead [32, 75, 53, 31, 77]. That is, for a nonlocality scale l, $S \sim |A|\Lambda^{d-1}$ for regions much smaller than l and $S \sim l|\partial A|\Lambda^{d-1}$ for regions much larger than l [31], as discussed in Chapter 2. Note that entanglement entropy of large regions is sufficient to differentiate this type of volume law from an area law, as the entanglement entropy is proportional to the length scale of the nonlocality times an additional factor of the UV regulator. To

[1] See for example [18] for a review of area laws in entanglement entropy.

summarise,

$$\text{area law}: \qquad S \sim |\partial A|\Lambda^{d-2}, \tag{3.1}$$

$$\text{volume law}: \qquad S \sim |A|\Lambda^{d-1}, \qquad \text{(small regions)} \tag{3.2}$$

$$S \sim l|\partial A|\Lambda^{d-1}. \qquad \text{(large regions)} \tag{3.3}$$

These results can be understood intuitively by assuming that all the degrees of freedom within the range of the nonlocality are equally entangled with each other. Then, for regions much smaller than l, all the degrees of freedom inside the region, not only those near the boundary, are entangled with degrees of freedom outside. For regions much larger than l, all the degrees of freedom within a distance l of the boundary are entangled with those outside. In both cases, the number of degrees of freedom strongly entangled across the boundary is proportional to Λ^{d-1} rather than the Λ^{d-2} expected from an area law.

A natural question is whether this behaviour is generic to nonlocal theories or if it is confined to a strongly coupled, large N regime. One approach is to study entanglement entropy for a free scalar field on the fuzzy sphere [78, 79, 80, 81]. This turns out to be proportional to the area[2] for small polar caps [80, 81]. However, two issues arise which question whether this should be characterised as a volume law. First, the dependence of the entanglement entropy on the UV regulator does not match the volume law described above. Second, the entanglement entropy does not scale like the number of degrees of freedom contained in the polar cap, as the degrees of freedom are not uniformly distributed across the sphere. Instead it scales as the number of degrees of freedom near the boundary [78, 79]. Another limitation of this theory is that the nonlocality scale is tied to the size of the sphere so it is not possible to study regions much larger than the nonlocality scale.

Another approach is to study a free field theory on a lattice with a nonlocal kinetic term, in which case a volume law was found [82].

This paper investigates the role of interactions in this question by considering two theories with nonlocal interactions: scalar $\lambda\phi^4$ theory on the noncommutative plane and $\lambda\phi^4$ theory with a dipole type nonlocal modification with fixed nonlo-

[2]The fuzzy sphere is a two-dimensional surface, thus $|A|$ is an area and $|\partial A|$ is a circumference.

cality scale. The leading divergence in entanglement entropy of large regions is calculated to leading order in perturbation theory and is not found to be proportional to the length scale of the nonlocality, hence no evidence of a volume law is found. Instead, the leading divergence in both theories has the same form as the standard local $\lambda\phi^4$ theory which follows an area law. This result indicates that, perturbatively these nonlocal interactions are not generating sufficient entanglement at distances of the nonlocality scale to change the leading divergence, at least to first order in the coupling.

The free theory with $\lambda = 0$ for both of these nonlocal theories is equivalent to the regular commutative $\lambda\phi^4$ theory. There is no modification of the entanglement entropy at this order. Perturbation theory can be used to study the nonlocal theories at small λ.

The entanglement entropy is calculated using the replica trick and the formula $S = -\partial_n \left[\ln Z_n - n \ln Z_1\right]_{n=1}$, where Z_n is the partition function of the field theory defined on an n-sheeted space [83, 84, 85]. This partition function can be reduced to computing vacuum bubble diagrams and the $O(\lambda)$ contribution in perturbation theory comes from bubble diagrams with one vertex and two loops. Consistent with the results of previous investigations of perturbative noncommutative theories [54], the planar diagrams in the nonlocal theories give the standard commutative result, which is $S \sim G_1(0) \int dx \partial_{n=1} G_n(x) \sim A_\perp \Lambda^2 \ln(\Lambda/m)$, where $A_\perp$ is the (infinite) area of the boundary of our region, Λ our UV regulator, m our IR regulator and G_n is the Green's function on the n-sheeted space used in the replica trick [85]. This contribution follows an area law, as $S \propto A_\perp \Lambda^2$ up to logarithmic corrections.

The nonlocality only affects the nonplanar diagram. This diagram contributes a term of the form $S \sim G_1(0,\Delta x) \int dx \partial_{n=1} G_n(x, x+\Delta x) \sim \frac{A_\perp}{(\Delta x)^2} \ln f(\Lambda, m, \Delta x)$, where now Δx corresponds to a translation from the nonlocality.

In the dipole theory, Δx is proportional to the fixed dipole length. Thus the nonplanar diagram has only a logarithmic IR divergence and is subleading compared to the planar diagrams. In the noncommutative theory the translation along the noncommuative plane is proportional to the momentum in the other noncommutative direction, so this contribution must be integrated over this momentum. If we don't impose an IR regulator, the momentum controlling the translation is allowed to vanish and $G(0,\Delta x) \to G_1(0) \sim \Lambda^2$. This gives a contribution that is of

the same order as the planar diagrams. However, if we impose an IR regulator, Δx has a minimal value and this divergence can be reinterpreted as an IR divergence. This is familiar from the UV/IR connection described for example in [54].

Our results for the $O(\lambda)$ contribution to the entanglement entropy, S_1, are

$$\text{real scalar :} \qquad S_1 = 2\lambda S_{\text{planar}} + \lambda S_{\text{nonplanar}} \tag{3.4}$$

$$\text{complex scalar :} \qquad S_1 = (2\lambda_0 + \lambda_1) S_{\text{planar}} + \lambda_1 S_{\text{nonplanar}}, \tag{3.5}$$

where S_{planar} and $S_{\text{nonplanar}}$ denote the contributions from planar and nonplanar diagrams respectively.

The leading divergences from these diagrams in each of the theories considered are

$$S_{\text{planar}} = -\frac{A_\perp \Lambda^2}{2^{10} 3^2 \pi^3} \ln \frac{\Lambda^2}{4m^2} \tag{3.6}$$

$$\text{Commutative theory :} \qquad S_{\text{nonplanar}} = S_{\text{planar}} \tag{3.7}$$

$$\text{Noncommutative plane :} \qquad S_{\text{nonplanar}} = -\frac{A_\perp \Lambda^2}{2^9 3^2 \pi^3} \frac{-\ln\left(\frac{\Theta^2 m^2 \Lambda^2}{4}\right)}{1 - \frac{\Theta^2 m^2 \Lambda^2}{4}} + \text{subleading} \tag{3.8}$$

$$\text{Dipole theory :} \qquad S_{\text{nonplanar}} \text{ is subleading,} \tag{3.9}$$

where Λ is our UV regulator, m is our IR regulator, $A_\perp$ is the area of the boundary, Θ is the noncommutativity parameter of the plane and a is the nonlocality scale of the dipole theory. The details of the expansion in $\frac{m}{\Lambda}$ used to extract these leading divergences are discussed in Section 3.5.2.

In both cases, the contribution from these nonplanar diagrams does not have the right form to be interpreted as the sign of a volume law in the entanglement entropy and we must conclude that these nonlocal theories at least to first order in perturbation theory obey an area law. This can be contrasted with the strong coupling result which found clear signs of the volume law even for large regions [31]. Thus, the volume law must either only appear at higher orders in perturbation theory or it must require strong coupling. Consistent with our analysis, previous investigations of perturbative dynamics of the noncommutative theory [54] have

shown that noncommutativity does not introduce any new perturbative UV divergences that cannot be reinterpreted as IR divergences. Thus, is it hard to see how the higher degree of divergence required for a volume law can arise in perturbation theory. We are lead to the conclusion that entanglement on distances of the nonlocality scale and volume laws require strong coupling and are not accessible to perturbation theory.

The remainder of the paper is organised as follows: Section 3.2 describes the theories we study, Section 3.3 explains how the entanglement entropy can be computed perturbatively in these theories, Section 3.4 shows that the results for the free theory are unchanged in these nonlocal theories, Section 3.5.1 computes the first order correction in the coupling to the entanglement entropy in a real scalar ϕ^4 theory for a warm-up and for later reference. Section 3.5.2 extends the calculation to the real scalar on the noncommutative plane. Section 3.5.3 reproduces the results for the previous two sections in the case of the complex scalar. Section 3.5.4 computes the result for the complex scalar in the dipole theory. Finally, Section 3.6 concludes with a discussion of these results.

3.2 Theories

The theories used in this paper are scalar field theories on $\mathbb{R}^{1,3}$ where products of fields are replaced with a possibly noncommutative product denoted $\star$. Three examples of this product will be used: the regular commutative one, the Moyal product associated with the noncommutative plane and the dipole product with a fixed nonlocality scale. See [86] for a review of noncommutative field theory. The Euclidean action is

$$\mathscr{S}_E = \int d^d x \left[-\frac{1}{2}\partial\phi \star \partial\phi(x) + \frac{1}{2}m^2\phi\star\phi(x) + \frac{\lambda}{4!}\phi\star\phi\star\phi\star\phi(x) \right]. \tag{3.10}$$

The entanglement entropy in these three theories is calculated to leading order in the coupling λ. The mass is present to serve as an IR regulator and will be taken to be small in the end.

First, the standard commutative case, where $(f\star g)(x) = f(x)g(x)$, is reviewed and presented in our notation in Sections 3.4 through 3.5.1. The entanglement

entropy for this theory was studied in [85] and the approach contained therein will be followed for each of the theories we consider.

Second, in Section 3.5.2, the entanglement entropy of a field theory defined on the noncommutative plane, where

$$(f\star g)(x)=\exp\left(\frac{i}{2}\Theta^{\mu\nu}\frac{\partial}{\partial\xi^{\mu}}\frac{\partial}{\partial\zeta^{\nu}}\right)f(x+\xi)g(x+\zeta)|_{\xi=\zeta=0}, \tag{3.11}$$

is studied. The noncommutativity is parametrised by the antisymmetric tensor Θ. This theory has been studied perturbatively in [54]. In this case especially, the mass should be thought of as an IR regulator and taken to zero at the end of the calculation in order to see full effects of the UV/IR mixing present in this theory. We specialise to the case commonly referred to as the noncommutative plane where $\Theta^{\mu\nu}=\Theta\left(\delta^{1\mu}\delta^{2\nu}-\delta^{2\mu}\delta^{1\nu}\right)$ for simplicity.

Finally, the entanglement entropy of the a simpler nonlocal theory with a fixed nonlocality scale along a particular axis, known as a dipole theory, is studied. For this product, a vector called a dipole must be assigned to every field. The noncommutative product is

$$(f\star g)(x^{\mu})=f(x^{\mu}+\frac{1}{2}L^{\mu}(g))g(x^{\mu}-\frac{1}{2}L^{\mu}(f)), \tag{3.12}$$

where $L^{\mu}(f)$ is the dipole assigned to the field f.

These dipoles must obey various rules set out in [61]. In particular, the dipole of the $\star$-product of two field must be the sum of their dipoles. As well, the dipole of the complex conjugate of a field must be minus the dipole of the original field. This means that a real field must have a zero dipole and that a complex scalar must be used rather than the real scalar field theory discussed so far. The action for a complex scalar is

$$\mathscr{S}_E=\int d^dx\left[-\partial\phi^{\dagger}\star\partial\phi(x)+m^2\phi^{\dagger}\star\phi(x)+\frac{\lambda_0}{4}\phi^{\dagger}\star\phi\star\phi^{\dagger}\star\phi(x)+\frac{\lambda_1}{4}\phi^{\dagger}\star\phi\star\phi\star\phi^{\dagger}(x)\right]. \tag{3.13}$$

where there two ϕ^4 terms which are inequivalent due to our noncommutative prod-

uct [61].[3]

The result from the real scalar theory will be extended to this complex scalar theory in Section 3.5.3, then the dipole theory will be studied in Section 3.5.4.

Setting $L^\mu(\phi) = a\delta^{\mu 1}$, the terms in the action can be written in a more explicit form:

$$\begin{aligned}
\int dx(\phi^\dagger \star \phi)(x) &= \int dx \phi^\dagger(x+\frac{1}{2}a)\phi(x+\frac{1}{2}a) = \int dx \phi^\dagger(x)\phi(x), \\
\int dx(\phi^\dagger \star \phi)\star(\phi^\dagger \star \phi)(x) &= \int dx \phi^\dagger(x)\phi(x)\phi^\dagger(x)\phi(x), \\
\int dx(\phi^\dagger \star \phi)\star(\phi \star \phi^\dagger)(x) &= \int dx \phi^\dagger(x+\frac{1}{2}a)\phi(x+\frac{1}{2}a)\phi(x-\frac{1}{2}a)\phi^\dagger(x-\frac{1}{2}a),
\end{aligned} \tag{3.14}$$

where only the dependence on the first coordinate, labelled x, is highlighted as the other coordinates are unaffected by this deformation.

In fact, renormalisability requires that we include in the action terms of the form

$$\lambda_n \int dx(\phi^\dagger \phi)(x+\frac{1}{2}na)(\phi^\dagger \phi)(x-\frac{1}{2}na) \tag{3.15}$$

for all n [61]. However, the contributions from these terms can be obtained by simply substituting $a \to na$ into the results for $n = 1$ and summing over n. The results in Section 3.5.4 are such that this sum is guaranteed to converge as long as the λ_n don't grow too quickly. As the inclusion of these terms would not affect our conclusions, we will not consider them separately.

3.3 Entanglement entropy

The standard technique of the replica trick is used to compute the entanglement entropy [83]. This technique was used in a perturbative context in [85], whose approach is followed here.

Starting with ρ_A, the reduced density matrix of the ground state of the theory

[3] These noncommutative products are constructed to ensure that integrals of products of fields are invariant under cyclic permutations.

in question for a region A, the idea is to evaluate

$$S = -\operatorname{Tr}(\rho_A \ln \rho_A) = -\frac{\partial}{\partial n} \ln \operatorname{Tr}(\rho_A^n)|_{n=1}, \tag{3.16}$$

by calculating $\operatorname{Tr} \rho_A^n$ for arbitrary n and analytically continuing. In this paper we will concentrate on the simplest case where A is the half plane ($A = \{(x_1, x_2, x_3) \in \mathbb{R}^3 | x_1 > 0\}$).

The main result that will be needed can be lifted directly from [83, 85]:

$$\ln \operatorname{Tr}(\rho_A^n) = \ln Z_n - n \ln Z_1, \tag{3.17}$$

where Z_n is the partition function of the theory on an n-sheeted surface with a cut along the region A that connects the sheets. However, some details of this n-sheeted space will be needed in the argument to follow, so the rest of this section will define it more carefully.

3.3.1 *n*-sheeted surfaces

The density matrix can be written as a path integral, (at finite inverse temperature of β)

$$\langle \phi_2 | \rho | \phi_1 \rangle = (Z_1)^{-1} \int \mathscr{D}\phi_{\phi(x,0)=\phi_1}^{\phi(x,\beta)=\phi_2} e^{-\mathscr{S}_E}, \tag{3.18}$$

where Z_1 is a normalisation factor to ensure that $\operatorname{Tr} \rho = 1$. Then the reduced density matrix for a region A is obtained by periodically identifying the field in the Euclidean time direction along $\bar{A}$, the complement of A, while leaving the boundary condition along A untouched. To look at the ground state, β must be sent to infinity. We do this while keeping the cut along A near the origin.

Then,

$$\operatorname{Tr}(\rho_A^n) = (Z_1)^{-n} \left[\int \mathscr{D}\phi_{\phi(x\in A,0^+)=\phi_1}^{\phi(x\in A,0^-)=\phi_2} e^{-\mathscr{S}_E} \right] \left[\int \mathscr{D}\phi_{\phi(x\in A,0^+)=\phi_2}^{\phi(x\in A,0^-)=\phi_3} e^{-\mathscr{S}_E} \right] \cdots \left[\int \mathscr{D}\phi_{\phi(x\in A,0^+)=\phi_n}^{\phi(x\in A,0^-)=\phi_1} e^{-\mathscr{S}_E} \right]. \tag{3.19}$$

This identification of boundary conditions can be replaced by defining the field

theory on an n-sheeted surface with a cut along A that takes you from one sheet to the next. Calling this n-sheeted surface $\left(\mathbb{R}^d \setminus A\right)^n$, the projection onto the sheet $\pi : \left(\mathbb{R}^d \setminus A\right)^n \to \mathbb{R}^d \setminus A$ and the indicator function telling you if you are on the k^{th} sheet $\chi_k : \left(\mathbb{R}^d \setminus A\right)^n \to \mathbb{Z}_1$, this means that $\Phi : \left(\mathbb{R}^d \setminus A\right)^n \to \mathbb{R}$ can be defined as $\Phi(x) = \sum_{k=1}^{N} \phi_k(\pi(x))\chi_k(x)$, so that

$$\text{Tr}\,(\rho_A^n) = (Z_1)^{-n} \left[\int \mathscr{D}\Phi e^{-\mathscr{S}_E}\right], \tag{3.20}$$

where $\mathscr{S}_E$ for Φ has the same form as that for each ϕ, since the action for each sheet is additive.

With our simple region A, a half-plane, polar coordinates can be defined in the x-τ plane of $\mathbb{R}^d \setminus A$. Then the glueing required to create this n-sheeted surface is simply to identify $\theta = 2\pi$ on one sheet to $\theta = 0$ on the next. Thus polar coordinates can be defined on $\left(\mathbb{R}^d \setminus A\right)^n$ where $\theta \in [0, 2\pi n)$, such that each interval of length 2π corresponds to a sheet, *i.e.* $\pi(r,\theta,y,z) = (r, \theta \bmod 2\pi, y, z)$ and $\chi_k(r,\theta,y,z) = \chi_{[2\pi(k-1),2\pi k)}(\theta)$.

This gives us the result from [83, 85] cited above, as $Z_n = \int \mathscr{D}\Phi e^{-\mathscr{S}_E}$. This path integral over Φ is the path integral over the n-sheeted surface.

3.4 Free theory

The first step is to understand the free theories where $\lambda = 0$. The action for the free noncommutative and dipole theories is the same for that of the commutative theory, since the star product of 2 fields is the same as the regular product up to a total derivative [54].

For the noncommutative theory,

$$\begin{aligned}\int d^4x (f \star g)(x) &= \int d^4x \sum_{n=0}^{\infty} \frac{i^n}{2^n}\, \Theta^{\mu_1\nu_1} \ldots \Theta^{\mu_n\nu_n}\, \partial_{\mu_1} \ldots \partial_{\mu_n} f(x)\, \partial_{\nu_1} \ldots \partial_{\nu_n} g(x) \\ &= \int d^4x \left[f(x)g(x) + \partial_{\mu_1} \sum_{n=1}^{\infty}\, \Theta^{\mu_1\nu_1} \ldots \Theta^{\mu_n\nu_n}\, \partial_{\mu_2} \ldots \partial_{\mu_n} f(x)\, \partial_{\nu_1} \ldots \partial_{\nu_n} g(x) \right],\end{aligned} \tag{3.21}$$

so that the quadratic term in the action is the same as for the commutative case up

to a total derivative. As there are no boundaries, the only place this total derivative could make for a finite contribution is at the conical singularity introduced at the origin when considering the n-sheeted path integral.

Around the origin this term contributes (note that the singularity is at the origin of the x-τ plane and is not localised in the y-z directions),

$$\lim_{r\to 0} A_\perp \sum_{n=1}^{\infty} \int r d\theta \; \Theta^{r\nu_1}\Theta^{\mu_2\nu_2}\ldots\Theta^{\mu_n\nu_n}\; \partial_{\mu_2}\ldots\partial_{\mu_n}\phi \; \partial_{\nu_1}\ldots\partial_{\nu_n}\phi \sim \lim_{r\to 0}\sum_n r\partial^n\phi\partial^{n+1}\phi, \tag{3.22}$$

where $A_\perp$ is the area of the y-z plane. As long as $\partial^n\phi \; \partial^{n+1}\phi$ is regular at the origin this term will not contribute to the action. This means that ϕ needs to be C^∞ at the origin, which is just the regular boundary condition imposed in the commutative case.

For the dipole theory, direct calculation of the $\star$-product of two fields can be seen to reduce to the commutative result in (3.14).

Thus the free theory is the same for all three theories.

3.4.1 Green's functions

Since the free theories are the same, they have the same Green's functions. This Green's function is straightforward in the polar coordinates introduced in Section 3.3.1. Since the action for Φ living on the n-sheeted surface is the same as the action for ϕ living on any particular sheet, the local equation that the Green's function must obey will be the same. The only difference is that θ must be periodic with period $2\pi n$ rather than the usual period of 2π. The Green's function for the field living on the n-sheeted surface is, from [85],

$$G_n(x,x') = \frac{1}{2\pi n}\int \frac{d^{d_\perp}p^\perp}{(2\pi)^{d_\perp}} \sum_{k=0}^{\infty} a_k \int_0^\infty dqq \frac{J_{k/n}(qr)J_{k/n}(qr')}{q^2+p_\perp^2+m^2}\cos(k(\theta-\theta')/n)e^{ip_\perp(x_\perp-x'_\perp)}, \tag{3.23}$$

where $a_0 = 1$, $a_{k\neq 0} = 2$, $p_\perp = (p_y, p_z)$ and $x_\perp = (x_2, x_3)$. $\perp$ refers to the directions orthogonal to the cut introduced by the replica trick.

The Euler-Maclaurin formula,

$$\sum_{k=0}^{\infty} a_k F(k) = 2\left[\int_0^{\infty} dk F(k)\right] - \frac{1}{6}F'(0) - 2\sum_{j>1}\frac{B_{2j}}{(2j)!}F^{(2j-1)}(0), \tag{3.24}$$

can be applied to this Green's function to replace the sum over k,

$$\begin{aligned} G_n(x,x') = &\int_0^{\infty}\frac{dk}{\pi}\int\frac{d^{d_\perp}p^\perp}{(2\pi)^{d_\perp}}\int_0^{\infty}dqq\frac{J_k(qr)J_k(qr')}{q^2+p_\perp^2+m^2}\cos(k(\theta-\theta'))e^{ip_\perp(x_\perp-x'_\perp)} \\ &-\frac{1}{12\pi n^2}\int\frac{d^{d_\perp}p^\perp}{(2\pi)^{d_\perp}}\int_0^{\infty}dqq\frac{\partial_\nu[J_\nu(qr)J_\nu(qr')]_{\nu=0}}{q^2+p_\perp^2+m^2}e^{ip_\perp(x_\perp-x'_\perp)} \\ &-\sum_{j>1}\frac{B_{2j}}{\pi n^{2j}(2j)!}\int\frac{d^{d_\perp}p^\perp}{(2\pi)^{d_\perp}}\int_0^{\infty}dqq\frac{(\partial_\nu)^{2j-1}[J_\nu(qr)J_\nu(qr')\cos(\nu(\theta-\theta'))]_{\nu=0}}{q^2+p_\perp^2+m^2}e^{ip_\perp(x_\perp-x'_\perp)}. \end{aligned} \tag{3.25}$$

It will be useful to define $G_n(x,x';p)$ as

$$G_n(x,x';p_y) = \frac{1}{2\pi n}\int\frac{dp_z}{2\pi}\sum_{k=0}^{\infty}a_k\int_0^{\infty}dqq\frac{J_{k/n}(qr)J_{k/n}(qr')}{q^2+p_y^2+p_z^2+m^2}\cos(k(\theta-\theta')/n)e^{ip_z(x_3-x'_3)+ip_y(x_2-x'_2)} \tag{3.26}$$

such that

$$G_n(x,x') = \int\frac{dp_y}{2\pi}G_n(x,x';p_y) \tag{3.27}$$

$$\frac{\partial}{\partial x_2}G_n(x,x';p) = -\frac{\partial}{\partial x'_2}G_n(x,x';p) = ipG_n(x,x';p). \tag{3.28}$$

It is also useful to define $f_n(x,x')$ and $f_n(x,x';p)$ as

$$\begin{aligned} f_n(x,x') &= G_n(x,x') - G_1(x,x') \\ &= \frac{n^2-1}{12\pi n^2}\int\frac{d^{d_\perp}p^\perp}{(2\pi)^{d_\perp}}\int_0^{\infty}dqq\frac{\partial_\nu[J_\nu(qr)J_\nu(qr')]_{\nu=0}}{q^2+p_\perp^2+m^2}e^{ip_\perp(x_\perp-x'_\perp)} + (j>1) \end{aligned} \tag{3.29}$$

$$f_n(x,x';p) = G_n(x,x';p) - G_1(x,x';p), \tag{3.30}$$

where G_1 is the Green's function on the 1-sheeted surface, that is just the regular Green's function.

Single sheeted limit

This Green's function for the n-sheeted space must reduce to the regular Green's function in the limit where $n \to 1$. Starting with our expression for the Green's function in (3.23), defining $\varphi = \theta - \theta'$ for convenience and setting $n = 1$,

$$G_1(x,x') = \frac{1}{2\pi}\int \frac{d^{d_\perp}p^\perp}{(2\pi)^{d_\perp}} \sum_{k=0}^{\infty} a_k \int_0^\infty dq q \frac{J_k(qr)J_k(qr')}{q^2+p_\perp^2+m^2}\cos(k\varphi)e^{ip_\perp(x_\perp - x'_\perp)}. \quad (3.31)$$

(10.9.E2) in the DLMF [87] provides a useful integral representation of the Bessel functions, which can be rewritten as, $J_n(z) = \int_{-\pi}^{\pi}\frac{d\gamma}{2\pi}e^{i(z\sin\gamma - n\gamma)}$. Using this representation and the fact that $J_{-k}(z) = (-1)^k J_k(z)$, [4]

$$\begin{aligned}\sum_{k=0}^{\infty} a_k J_k(qr)J_k(qr')\cos(k\varphi) &= \sum_{k=-\infty}^{\infty}\int_{-\pi}^{\pi}\frac{d\gamma d\kappa}{(2\pi)^2}e^{iq(r\sin\gamma + r'\sin\kappa) - ik(\gamma+\kappa)}e^{ik\varphi} \\ &= \int_{-\pi}^{\pi}\frac{d\gamma}{2\pi}e^{iq[r\sin\gamma + r'\sin(\varphi-\gamma)]}. \end{aligned} \quad (3.32)$$

Defining our position axes on the x_0-x_1 plane such that $\vec{x} = (0,r)$ implies that $\vec{x}' = (-r'\sin\varphi, r'\cos\varphi)$. Then defining $\vec{q} = (q\cos\gamma, q\sin\gamma)$,

$$\vec{q}\cdot(\vec{x}-\vec{x}') = q\left[r\sin\gamma + r'\sin(\varphi-\gamma)\right] \quad (3.33)$$

$$\sum_{k=0}^{\infty} a_k J_k(qr)J_k(qr')\cos(k\varphi) = \int_{-\pi}^{\pi}\frac{d\gamma}{2\pi}e^{i\vec{q}\cdot(\vec{x}-\vec{x}')} \quad (3.34)$$

Finally, defining $p = (\vec{q}, p_\perp)$,

$$G_1(x,x') = \int \frac{d^d p}{(2\pi)^d}\frac{e^{ip(x-x')}}{p^2+m^2}, \quad (3.35)$$

which is the usual Euclidean Green's function.

3.4.2 Entanglement entropy in the free theory

The entanglement entropy when $\lambda = 0$ must be identical in the three theories as it was shown above that the quadratic terms in the action are the same. This can

[4] (10.4.E1) in [87]

be seen more explicitly by using the approach from [85]. Starting from $S_A = -\partial_n \left[\ln Z_n - n \ln Z_1\right]_{n=1}$, the part of the entanglement entropy which depends on the mass can be related to the Green's function by

$$\frac{\partial}{\partial m^2} \ln Z_n = -\frac{1}{2} \int_n d^d x \langle \Phi^2(x) \rangle_n. \tag{3.36}$$

In the commutative case, $\langle \Phi^2(x) \rangle_n = G_n(x,x)$. In the non-commutative case,

$$\begin{aligned}
\langle \Phi \star \Phi(x) \rangle_n &= \left(\exp\left[\frac{i}{2} \Theta \left(\frac{\partial}{\partial \xi_1} \frac{\partial}{\partial \zeta_2} - \frac{\partial}{\partial \xi_2} \frac{\partial}{\partial \zeta_1} \right) \right] \langle \Phi(x+\xi) \Phi(x+\zeta) \rangle_n \right)_{\xi=\zeta=0} \\
&= \left(\exp\left[\frac{i}{2} \Theta \left(\frac{\partial}{\partial \xi_1} \frac{\partial}{\partial \zeta_2} - \frac{\partial}{\partial \xi_2} \frac{\partial}{\partial \zeta_1} \right) \right] G_n(x+\xi, x+\zeta) \right)_{\xi=\zeta=0} \\
&= \int \frac{dp_y}{2\pi} \left(\exp\left[\frac{1}{2} \Theta p_y \left(\frac{\partial}{\partial \xi_1} + \frac{\partial}{\partial \zeta_1} \right) \right] G_n(x+\xi, x+\zeta; p_y) \right)_{\xi=\zeta=0} \\
&= \int \frac{dp_y}{2\pi} G_n(x + \frac{1}{2} \Theta p_y \hat{\imath}, x + \frac{1}{2} \Theta p_y \hat{\imath}; p_y).
\end{aligned} \tag{3.37}$$

That the $\star$-product turns out to just translate the argument of the Green's function is an important theme of the calculation in this paper.

The only difference for a complex scalar is that the mass term in the action is proportional to $\Phi^\dagger \star \Phi$ instead of $\Phi \star \Phi$, however the expectation value of this leads to the same Green's function and the same result follows.

The dipole theory is identical except that translations by Θ times the momentum in the y-direction are replaced by translations by a.

Thus, still for the non-commutative case,

$$\begin{aligned}
\frac{\partial}{\partial m^2} \ln Z_n &= -\frac{1}{2} \int_n d^d x \langle \Phi \star \Phi(x) \rangle_n \\
&= -\frac{1}{2} \int_n d^d x \int \frac{dp}{2\pi} G_n(x + \frac{1}{2} \Theta p \hat{\imath}, x + \frac{1}{2} \Theta p \hat{\imath}; p) \\
&= -\frac{1}{2} \int_n d^d x \int \frac{dp}{2\pi} G_n(x,x;p) = -\frac{1}{2} \int_n d^d x G_n(x,x),
\end{aligned} \tag{3.38}$$

recovering explicitly the result from the commutative case by shifting the integration variable.

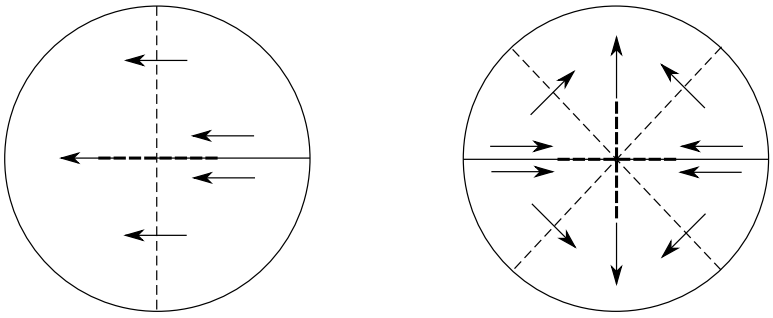

Figure 3.1: Translations on each of the sheets of the n-sheeted surface (on the left) give a well defined map on the whole surface (shown for $n = 2$ in the polar coordinates described in Section 3.3.1 on the right), except for a measure zero set near the singularity at the origin.

However, this shift of the integration variable on the n-sheeted surface bears further investigation. It is sketched in Figure 3.1.

This shift is well defined except for the region which gets translated into or out of the origin. However, this region has measure zero and cannot affect the result of the integral. As long as only a countable number of such shifts are done, these points can be omitted from the integral without changing the result. Finally, the integral over the whole n-sheeted surface can be written as a sum over the sheets and the Jacobian of this shift on each sheet is 1, so the Jacobian of the whole shift does not introduce any new factors into the integral. Thus shifting the variable of integration on this n-sheeted surface is allowed with no Jacobian, just as for the plane.

3.5 First order in perturbation theory

3.5.1 Commutative theory

We will start by computing the first order correction to the entanglement entropy for the commutative ϕ^4 theory. This was done previously in [85], but will be repeated here with more explicit regulators that will allow a direct comparison to the

nonlocal cases. From [85],

$$\begin{aligned}\ln Z_n &= \ln \int \mathscr{D}\phi e^{-S_E[\phi]} \\ &= \ln Z_{n,0} - \frac{\lambda}{4!}\int_n d^4x \langle \Phi^4(x)\rangle_0 + ... \\ &= \ln Z_{n,0} - \frac{3\lambda}{4!}\int_n d^4x \left[G_n(x,x)\right]^2 + ...,\end{aligned} \tag{3.39}$$

where $\int_n$ denotes integration over the n-sheeted surface and $\ln Z_{n,k}$ is the k^{th} order term in a λ expansion of $\ln Z_n$. Generally, adding subscript will denote the order of a term in a λ expansion, e.g. $X = X_0 + X_1 + X_2 + \ldots$

The entanglement entropy can be calculated using (3.16) and (3.17),

$$\begin{aligned}\ln\ \mathrm{Tr}\ (\rho_A^n)_1 &= \ln Z_{n,1} - n \ln Z_{1,1} \\ &= -\frac{3\lambda}{4!}\int_n d^4x \left[G_n(x,x)\right]^2 + \frac{3n\lambda}{4!}\int d^4x \left[G_1(x,x)\right]^2 \\ &= -\frac{3\lambda}{4!}\int_n d^4x \left[2G_1(x,x) f_n(x,x) + f_n^2(x,x)\right].\end{aligned} \tag{3.40}$$

Recalling from (3.29),

$$f_n(x,x') = \frac{n^2-1}{12\pi n^2}\int \frac{d^{d_\perp}p^\perp}{(2\pi)^{d_\perp}}\int_0^\infty dqq \frac{\partial_\nu [J_\nu(qr)J_\nu(qr')]_{\nu=0}}{q^2+p_\perp^2+m^2} e^{ip_\perp(x_\perp - x'_\perp)} + (j>1). \tag{3.41}$$

The $j > 1$ terms don't contribute [83], so they will be dropped in what follows. This is the same on each sheet, so the integral over the n-sheeted surface is n times in integral on one sheet. Finally, $f_1(x,x') = 0$, so $\partial_n f_n^2(x,x')|_{n=1} = 0$ and

$$S_1 = -\partial_n \left[\ln\ \mathrm{Tr}\ (\rho_A^n)_1\right]_{n=1} = \frac{6\lambda}{4!}\int d^4x G_1(x,x)\partial_n \left[n f_n(x,x)\right]_{n=1} \tag{3.42}$$

$$S_1 = \frac{12\lambda A_\perp}{12\pi\cdot 4!}\int r dr d\phi \int \frac{d^4k dp_y dp_z}{(2\pi)^6}\frac{1}{k^2+m^2}\int_0^\infty dqq \frac{\partial_\nu [J_\nu(qr)J_\nu(qr)]_{\nu=0}}{q^2+p_y^2+p_z^2+m^2}. \tag{3.43}$$

Schwinger parameters are introduced to allow the denominators to be combined, using

$$\frac{1}{A} = \int_0^\infty d\alpha e^{-A\alpha}. \tag{3.44}$$

This allows us to regulate the UV divergence in S_1 by introducing a factor of $e^{-\frac{1}{\alpha\Lambda^2}}$, as was done in previous perturbative studies of noncommutative theories [54]. This regulator is convenient in the noncommutative case and is used here so that the results can be compared. Using (25) from p.146 in volume I of [88],

$$\int_0^\infty dt e^{-pt-\frac{a}{4t}} = \sqrt{\frac{a}{p}} K_1(\sqrt{ap}), \tag{3.45}$$

the effect of this regulator is

$$\begin{aligned}\int_0^\infty d\alpha e^{-\alpha p^2 - \frac{1}{\alpha\Lambda^2}} = \frac{2}{\Lambda p} K_1\left(\frac{2p}{\Lambda}\right) &\xrightarrow{\frac{p}{\Lambda}\to\infty} \sqrt{\frac{2}{\Lambda p^3}} e^{-\frac{2p}{\Lambda}}, \\ &\xrightarrow{\frac{p}{\Lambda}\to 0} \frac{1}{p^2}.\end{aligned} \tag{3.46}$$

Thus it regulates the UV and leaves the IR unaffected. This can be seen simply from the fact that $e^{-\frac{1}{\alpha\Lambda^2}}$ vanishes for $\alpha \ll \Lambda^{-2}$ and goes to one for $\alpha \gg \Lambda^{-2}$. A mass m regulates the IR by contributing a factor of $e^{-\alpha m^2}$, which has the opposite behaviour.

Introducing these Schwinger parameters and regulating,

$$S_1 = \frac{\lambda A_\perp}{3\cdot 2^3}\int dr \frac{d^4k dp_y dp_z}{(2\pi)^6} dq \int_0^\infty d\alpha d\beta q r e^{-\alpha k^2 - \beta\left[q^2+p_y^2+p_z^2\right] - \alpha m^2 - \frac{1}{\alpha\Lambda^2} - \beta m^2 - \frac{1}{\beta\Lambda^2}} \partial_\nu [J_\nu(qr) J_\nu(qr)]_{\nu=0}. \tag{3.47}$$

All the momenta integrals except q are Gaussian,

$$S_1 = \frac{\lambda A_\perp}{3\cdot 2^9\pi^3}\int dr dq \int_0^\infty d\alpha d\beta \frac{qr}{\alpha^2\beta} e^{-\beta q^2 - \alpha m^2 - \frac{1}{\alpha\Lambda^2} - \beta m^2 - \frac{1}{\beta\Lambda^2}} \partial_\nu [J_\nu(qr) J_\nu(qr)]_{\nu=0}. \tag{3.48}$$

Using (10.22.E67) from the Digital Library of Mathematical Functions (DLMF)

[87],

$$\int_0^\infty te^{-p^2t^2}J_\nu(at)J_\nu(bt)dt = \frac{1}{2p^2}e^{-\frac{(a^2+b^2)}{4p^2}}I_\nu\left(\frac{ab}{2p^2}\right), \tag{3.49}$$

the q integral can be evaluated. This along with the fact that $\partial_\nu I_\nu(z)|_{\nu=0} = -K_0(z)$[5] gives

$$S_1 = -\frac{\lambda A_\perp}{3\cdot 2^{10}\pi^3}\int dr\int_0^\infty d\alpha d\beta\frac{r}{\alpha^2\beta^2}e^{-\frac{r^2}{2\beta}-\alpha m^2-\frac{1}{\alpha\Lambda^2}-\beta m^2-\frac{1}{\beta\Lambda^2}}K_0\left(\frac{r^2}{2\beta}\right). \tag{3.50}$$

(21) on p. 131 of [88],

$$\int_0^\infty dte^{-at}K_0(ty) = \frac{\arccos(\frac{a}{y})}{\sqrt{y^2-a^2}} \xrightarrow{\frac{a}{y}\to 1} \frac{1}{y}, \tag{3.51}$$

after substituting $r^2 \to t$ and setting $a = y = \frac{1}{2\beta}$, gives

$$S_1 = -\frac{\lambda A_\perp}{3\cdot 2^{10}\pi^3}\left(\int_0^\infty\frac{d\alpha}{\alpha^2}e^{-\alpha m^2-\frac{1}{\alpha\Lambda^2}}\right)\left(\int_0^\infty\frac{d\beta}{\beta}e^{-\beta m^2-\frac{1}{\beta\Lambda^2}}\right). \tag{3.52}$$

Looking at the α integral first,

$$\begin{aligned}\int_0^\infty\frac{d\alpha}{\alpha^2}e^{-\alpha m^2-\frac{1}{\alpha\Lambda^2}} =& \int_0^\infty d\alpha e^{-\frac{m^2}{\alpha}-\frac{\alpha}{\Lambda^2}} \\ =& 2m\Lambda K_1\left(\frac{2m}{\Lambda}\right) \xrightarrow{\frac{m}{\Lambda}\to 0} \Lambda^2\end{aligned} \tag{3.53}$$

by substituting $\alpha \to \frac{1}{\alpha}$ in the first line and using (3.45) as well as in the second. This recovers the Λ^2 divergence seen previously in this case [85].

Using (29) from Volume 1, p. 146 of [88]

$$\int_0^\infty t^{\nu-1}e^{-pt-\frac{a}{4t}}dt = 2\left(\frac{a}{4p}\right)^{\frac{\nu}{2}}K_\nu(\sqrt{ap}) \tag{3.54}$$

[5] (10.38.E4) in the DLMF [87].

the β integral gives,

$$\int_0^\infty \frac{d\beta}{\beta} e^{-\beta m^2 - \frac{1}{\beta\Lambda^2}} = 2K_0\left(\frac{2m}{\Lambda}\right) \xrightarrow{\frac{m}{\Lambda}\to 0} -2\ln\frac{2m}{\Lambda} = \ln\frac{\Lambda^2}{4m^2}, \tag{3.55}$$

as $K_0(z) \to -\ln z$ as $z \to 0$. This reproduced the logarithmic divergence seen previously in this case [85] and makes explicit its form in our regularisation scheme.

Combining, the first order in λ correction to the entanglement entropy in the commutative theory is

$$S_{1,\text{Comm.}} = -3\lambda \frac{A_\perp \Lambda^2}{3^2 \cdot 2^{10}\pi^3} \ln\frac{\Lambda^2}{4m^2}. \tag{3.56}$$

This is proportional to the area of the boundary of A, that is $A_\perp$, and the leading divergence is of order Λ^2, so this result fits with the area law picture discussed in the introduction.

3.5.2 Noncommutative theory

Next we will compute the first order correction to the entanglement entropy for the noncommutative ϕ^4 theory. Similarly to the commutative theory,

$$\begin{aligned} \ln Z_n &= \ln \int \mathscr{D}\phi e^{-S_E[\phi]} \\ &= \ln Z_{n,0} - \frac{\lambda}{4!}\int_n d^4x \langle \Phi\star\Phi\star\Phi\star\Phi(x)\rangle_0 + \ldots \end{aligned} \tag{3.57}$$

Using the associativity of the $\star$-product, this can be written as

$$\begin{aligned} \int_n d^4x \langle \Phi\star\Phi\star\Phi\star\Phi(x)\rangle_0 = \int_n d^4x \Bigg(&\exp\left[\frac{i}{2}\Theta\left(\frac{\partial}{\partial\xi_1}\frac{\partial}{\partial\zeta_2} - \frac{\partial}{\partial\xi_2}\frac{\partial}{\partial\zeta_1}\right)\right]\Bigg)_{\xi=\zeta=0} \\ &\left(\exp\left[\frac{i}{2}\Theta\left(\frac{\partial}{\partial\eta_1}\frac{\partial}{\partial\varsigma_2} - \frac{\partial}{\partial\eta_2}\frac{\partial}{\partial\varsigma_1}\right)\right]\right)_{\eta=\varsigma=0} \\ &\left(\exp\left[\frac{i}{2}\Theta\left(\frac{\partial}{\partial\gamma_1}\frac{\partial}{\partial\kappa_2} - \frac{\partial}{\partial\gamma_2}\frac{\partial}{\partial\kappa_1}\right)\right]\right)_{\gamma=\kappa=0} \\ &\langle\Phi(x+\xi+\eta)\Phi(x+\xi+\varsigma)\Phi(x+\zeta+\gamma)\Phi(x+\zeta+\kappa)\rangle. \end{aligned} \tag{3.58}$$

The usual Wick's Theorem can be applied to calculate the four-point function,

$$\langle\Phi(w)\Phi(x)\Phi(y)\Phi(z)\rangle = G_n(w,x)G_n(y,z)+G_n(w,y)G_n(x,z)+G_n(w,z)G_n(x,y). \tag{3.59}$$

The key point is that while the conical singularity breaks the translational invariance in the x_0-x_1 plane, it is preserved in the x_2-direction. Thus the star product reduces to a translation in the x_1-direction by an amount determined by the momentum in the x_2-direction. Defining $G_n(w,z) = \int \frac{dp_y}{2\pi} G_n(w,z;p_y)$ as in (3.26),

$$\begin{aligned}\exp\left(\frac{i}{2}\Theta\frac{\partial}{\partial w_1}\frac{\partial}{\partial z_2}\right)G_n(w,z) &= \int\frac{dp_y}{2\pi}\exp\left(\frac{1}{2}p_y\Theta\frac{\partial}{\partial w_1}\right)G_n(w,z;p_y)\\ &= \int\frac{dp_y}{2\pi}G_n(w+\frac{1}{2}p_y\Theta\hat{\imath},z;p_y),\end{aligned} \tag{3.60}$$

this can be used to evaluate the 4-point function,

$$\begin{aligned}&\int_n d^4x <\Phi\star\Phi\star\Phi\star\Phi(x)>_0 \\ &\quad= \int_n d^4x\int\frac{dk_y dp_y}{(2\pi)^2}\Big[G_n(x+\frac{1}{2}\Theta k_y\hat{\imath},x+\frac{1}{2}\Theta k_y\hat{\imath};k_y)G_n(x+\frac{1}{2}\Theta p_y\hat{\imath},x+\frac{1}{2}\Theta p_y\hat{\imath};p_y)\\ &\qquad+G_n(x+\frac{1}{2}\Theta k_y\hat{\imath},x+\frac{1}{2}\Theta(k_y+2p_y)\hat{\imath};k_y)G_n(x+\frac{1}{2}\Theta(2k_y+p_y)\hat{\imath},x+\frac{1}{2}\Theta p_y\hat{\imath};p_y)\\ &\qquad+G_n(x+\frac{1}{2}\Theta k_y\hat{\imath},x+\frac{1}{2}\Theta k_y\hat{\imath};k_y)G_n(x+\frac{1}{2}\Theta(2k_y+p_y)\hat{\imath},x+\frac{1}{2}\Theta(2k_y+p_y)\hat{\imath};p_y)\Big].\end{aligned} \tag{3.61}$$

Then, by shifting the spatial integral,

$$\begin{aligned}&= \int_n d^4x\int\frac{dk_y dp_y}{(2\pi)^2}\Big[G_n(x,x;k_y)G_n(x+\frac{1}{2}\Theta(p_y-k_y)\hat{\imath},x+\frac{1}{2}\Theta(p_y-k_y)\hat{\imath};p_y)\\ &\quad+G_n(x-\frac{1}{2}\Theta p_y\hat{\imath},x+\frac{1}{2}\Theta p_y\hat{\imath};k_y)G_n(x+\frac{1}{2}\Theta k_y\hat{\imath},x-\frac{1}{2}\Theta k_y\hat{\imath};p_y)\\ &\quad+G_n(x,x;k_y)G_n(x+\frac{1}{2}\Theta(k_y+p_y)\hat{\imath},x+\frac{1}{2}\Theta(k_y+p_y)\hat{\imath};p_y)\Big].\end{aligned} \tag{3.62}$$

In [54] it is seen that the effects of the non-commutativity manifest themselves in the diagrams where lines cross each other. This is also present here, as Figure 3.2 shows that it is only the second term that involves lines crossing. The other

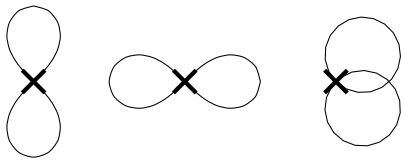

Figure 3.2: Vacuum bubble diagrams at leading order in a real scalar $\lambda\phi^4$ theory. The only vacuum bubble where lines cross is the second one. This is the only one which is affected by the non-commutativity, as discussed in [54].

two terms are two self-coincident Green's functions – the same result as was found in the commutative case in Section 3.5.1 and [85]. The second term, which corresponds to the nonplanar diagram, is the only one which is different than what was found in the commutative case.

The entanglement entropy can be calculated using (3.16),

$$\begin{aligned} S_1 =& -\partial_n \left[\ln Z_{n,1} - n \ln Z_{1,1}\right]_{n=1} \qquad (3.63)\\ =& \frac{2\lambda}{4!}\partial_n \left(\int d^4x \left[2G_1(x,x) n f_n(x,x) + \int \frac{dk_y dp_y}{(2\pi)^2} G_1(x, x+\Theta p_y \hat{\imath}; k_y) n f_n(x, x-\Theta k_y \hat{\imath}; p_y) \right] \right)_{n=1} \end{aligned}$$

where the fact that the spatial integral can be shifted, that the momenta can be renamed, that $G_1(x,x;p_y) = G_1(x+a,x+a;p_y)$, that $f_n(x,x',p_y) = f_n(x,x';-p_y)$ as long as $x_2 = x_2'$ and that $f_1 = 0$ so that the terms with f_n^2 can be ignored have all been used. The $j > 1$ terms in f_n have also been dropped again, which allows us here to write the integral over the n-sheeted surface as n times the integral over a sheet. In the commutative case, it was clear that these $j > 1$ terms do not contribute [83]. In Appendix A it is argued that the leading divergence must be entirely contained in the $j = 1$ term even in this noncommutative theory.

New contribution from the nonplanar diagram

The first term in (3.63) is the contribution from the two planar diagrams. These give the same result as in the commutative case, namely $\frac{\lambda A_\perp \Lambda^2}{2^{10}3^2\pi^3} \ln \frac{\Lambda^2}{4m^2}$ from each diagram. However, the nonplanar diagram gives a new contribution to the entanglement entropy from the non-commutativity. The contribution from this nonplanar

diagram will be denoted $S_{\text{nonplanar}}$,

$$\begin{aligned} S_{\text{nonplanar}} =& \frac{2\lambda}{4!}\int d^4x \int \frac{dk_y dp_y}{(2\pi)^2} G_1(x,x+\Theta p_y \hat{\imath};k_y)\partial_n \left[n f_n(x,x-\Theta k_y \hat{\imath};p_y)\right]_{n=1} \\ =& \frac{4\lambda A_\perp}{12\pi\cdot 4!}\int r dr d\phi \int \frac{d^4k dp_y dp_z}{(2\pi)^6}\frac{e^{i\Theta k_x p_y}}{k^2+m^2}\int_0^\infty dq q \frac{\partial_\nu [J_\nu(qr)J_\nu(qr')]_{\nu=0}}{q^2+p_y^2+p_z^2+m^2}, \end{aligned} \tag{3.64}$$

where $r'^2 = (\vec{r}-\Theta k_y \hat{\imath})^2 = r^2+(\Theta k_y)^2 - 2\Theta r k_y \cos\phi$ and $A_\perp$ is the area of the x_2-x_3 plane that bounds the region for which the entanglement entropy is being calculated.

The next step is to introduce Schwinger parameters and to regulate this integral in the same manner as the integrals for other perturbative calculations in this noncommutative theory were regulated in [54], as discussed in Section 3.5.1,

$$\begin{aligned} S_{\text{nonplanar}} = \frac{\lambda A_\perp}{2^3 3^2 \pi}\int r dr d\phi \frac{d^4k dp_y dp_z}{(2\pi)^6} dq \int_0^\infty d\alpha d\beta q r e^{-\alpha k^2 - \beta\left[q^2+p_y^2+p_z^2\right] - \frac{1}{\alpha\Lambda^2} - \alpha m^2 - \frac{1}{\beta\Lambda^2} - \beta m^2} \\ e^{i\Theta k_x p_y}\partial_\nu [J_\nu(qr)J_\nu(qr')]_{\nu=0}. \end{aligned} \tag{3.65}$$

The p_y, p_z and k except for k_y integrals are all Gaussian (recall that r' is a function of k_y),

$$\begin{aligned} S_{\text{nonplanar}} =& \frac{\lambda A_\perp}{2^8 3^2 \pi^{\frac{9}{2}}}\int r dr d\phi dk_y dq \int_0^\infty d\alpha d\beta \frac{qr}{\alpha\sqrt{\beta}\sqrt{4\alpha\beta+\Theta^2}} \\ & e^{-\alpha k_y^2 - \beta q^2 - \frac{1}{\alpha\Lambda^2} - \alpha m^2 - \frac{1}{\beta\Lambda^2} - \beta m^2}\partial_\nu [J_\nu(qr)J_\nu(qr')]_{\nu=0}. \end{aligned} \tag{3.66}$$

In order to make explicit some of the symmetry between r and r', ρ and φ can be defined such that $r = \rho\sin\varphi$ and $k_y = \frac{\rho}{\Theta}\cos\varphi$, with $\rho \in [0,\infty)$ and $\varphi \in [0,\pi]$. Then defining $g(\phi,\varphi) = \sqrt{1+\sin 2\varphi\cos\phi}$, gives $r' = \rho\, g(\phi,\varphi)$ in these variables.

Performing this change of variables,

$$S_{\text{nonplanar}} = \frac{\lambda A_{\perp}}{2^8 3^2 \pi^{\frac{9}{2}} \Theta} \partial_{\nu}|_{\nu=0} \int d\rho d\varphi d\phi dq d\alpha d\beta \frac{q\rho^2 \sin\varphi}{\alpha\sqrt{\beta}\sqrt{4\alpha\beta+\Theta^2}} \\ e^{-\frac{\alpha}{\Theta^2}\rho^2\cos^2\varphi - \beta q^2 - \frac{1}{\alpha\Lambda^2} - \alpha m^2 - \frac{1}{\beta\Lambda^2} - \beta m^2} J_{\nu}(q\rho\sin\varphi) J_{\nu}(q\rho g(\phi,\varphi)). \tag{3.67}$$

From the DLMF (10.22.E67) [87],

$$\int_0^{\infty} t e^{-p^2 t^2} J_{\nu}(at) J_{\nu}(bt) = \frac{1}{2p^2} e^{-\frac{(a^2+b^2)}{4p^2}} I_{\nu}\left(\frac{ab}{2p^2}\right) \tag{3.68}$$

so that,

$$S_{\text{nonplanar}} = \frac{\lambda A_{\perp}}{2^9 3^2 \pi^{\frac{9}{2}} \Theta} \partial_{\nu}|_{\nu=0} \int d\rho d\varphi d\phi d\alpha d\beta \frac{\rho^2 \sin\varphi}{\alpha\beta^{\frac{3}{2}}\sqrt{4\alpha\beta+\Theta^2}} \\ e^{-\frac{\alpha}{\Theta^2}\rho^2\cos^2\varphi - \rho^2\frac{\sin^2\varphi + g^2(\varphi,\phi)}{4\beta} - \frac{1}{\alpha\Lambda^2} - \alpha m^2 - \frac{1}{\beta\Lambda^2} - \beta m^2} I_{\nu}\left(\frac{\rho^2}{2\beta} g(\phi,\varphi)\sin\varphi\right). \tag{3.69}$$

Now ρ and α can be rescaled to simplify this expression as $\rho \to 2\sqrt{\beta}\rho$ and $\alpha \to \frac{\Theta^2}{4\beta}\alpha$,

$$S_{\text{nonplanar}} = \frac{\lambda A_{\perp}}{2^6 3^2 \pi^{\frac{9}{2}} \Theta^2} \partial_{\nu}|_{\nu=0} \int d\rho d\varphi d\phi d\alpha \frac{\rho^2 \sin\varphi}{\alpha\sqrt{\alpha+1}} \left(\int_0^{\infty} d\beta e^{-\beta\left(m^2 + \frac{4}{\Theta^2\Lambda^2\alpha}\right) - \frac{1}{\beta}\left(\frac{1}{\Lambda^2} + \frac{\Theta^2 m^2 \alpha}{4}\right)} \right) \\ e^{-\alpha\rho^2\cos^2\varphi - \rho^2\left[\sin^2\varphi + g^2(\phi,\varphi)\right]} I_{\nu}\left(2\rho^2 g(\phi,\varphi)\sin\varphi\right). \tag{3.70}$$

(25) from p.146 in volume I of [88],

$$\int_0^{\infty} dt e^{-pt - \frac{a}{4t}} = \sqrt{\frac{a}{p}} K_1(\sqrt{ap}), \tag{3.71}$$

allows the β integral to be evaluated,

$$\int_0^\infty d\beta e^{-\beta\left(m^2+\frac{4}{\Theta^2\Lambda^2\alpha}\right)-\frac{1}{\beta}\left(\frac{1}{\Lambda^2}+\frac{\Theta^2m^2\alpha}{4}\right)} = \sqrt{\frac{\frac{4}{\Lambda^2}+\Theta^2m^2\alpha}{m^2+\frac{4}{\Theta^2\Lambda^2\alpha}}}K_1\left(\sqrt{\left(\frac{4}{\Lambda^2}+\Theta^2m^2\alpha\right)\left(m^2+\frac{4}{\Theta^2\Lambda^2\alpha}\right)}\right),$$
$$= \Theta\sqrt{\alpha}K_1\left(\frac{4}{\Theta\Lambda^2\sqrt{\alpha}}+\Theta m^2\sqrt{\alpha}\right). \qquad (3.72)$$

Using the identity $\partial_\nu|_{\nu=0}I_\nu(z) = -K_0(z)$,

$$S_{\text{nonplanar}} = -\frac{\lambda A_\perp}{2^6 3^2\pi^{\frac{9}{2}}\Theta}\int d\rho d\varphi d\phi d\alpha \frac{\rho^2\sin\varphi}{\sqrt{\alpha}\sqrt{\alpha+1}}e^{-\rho^2\left[\alpha\cos^2\varphi+\sin^2\varphi+g^2(\phi,\varphi)\right]}$$
$$K_0\left(2\rho^2 g(\phi,\varphi)\sin\varphi\right)K_1\left(\frac{4}{\Theta\Lambda^2\sqrt{\alpha}}+\Theta m^2\sqrt{\alpha}\right). \qquad (3.73)$$

Taking a large Λ limit of this expression and expanding $K_1(x) \approx \frac{1}{x}$ for $x \to 0$ allows us to extract an overall quadratic divergence. However, more progress can still be made by evaluating the ρ integral.

Using in order (23) from p. 131 of [88] and (15.9.E19) of [87],

$$\int_0^\infty d\rho\rho^2 e^{-A\rho^2}K_0(B\rho^2) = \int_0^\infty dx\sqrt{x}e^{-Ax}K_0(Bx)$$
$$= \frac{1}{2}\sqrt{\pi}\frac{[\Gamma(\frac{3}{2})]^2}{\Gamma(2)(A+B)^{\frac{3}{2}}}{}_2F_1\left(\frac{3}{2},\frac{1}{2};2;\frac{A-B}{A+B}\right) \qquad (3.74)$$
$$= \frac{\pi^{\frac{3}{2}}}{8\sqrt{2}B^{\frac{3}{2}}}\frac{1}{\sqrt{\left(\frac{A}{B}\right)^2-1}}P^1_{-\frac{1}{2}}\left(\frac{A}{B}\right),$$

where $P^1_{-\frac{1}{2}}(x)$ is the appropriate branch of the associated Legendre function with non-integer degree.

Defining $z = \frac{\alpha\cos^2\varphi+\sin^2\varphi+g^2(\varphi,\phi)}{2g(\phi,\varphi)\sin\varphi}$ and recalling that $g(\phi,\varphi) = \sqrt{1+\sin 2\varphi\cos\phi}$,

$$S_{\text{nonplanar}} = -\frac{\lambda A_\perp}{2^{11}3^2\pi^3\Theta}\int_0^\infty d\alpha \frac{G(\alpha)}{\sqrt{\alpha}\sqrt{\alpha+1}} K_1\left(\frac{4}{\Theta\Lambda^2\sqrt{\alpha}} + \Theta m^2\sqrt{\alpha}\right) \text{ and} \tag{3.75}$$

$$G(\alpha) = \int_0^\pi d\varphi \int_0^{2\pi} d\phi \frac{1}{[g(\phi,\varphi)]^{\frac{3}{2}}\sqrt{\sin\varphi}} \frac{P^1_{-\frac{1}{2}}(z)}{\sqrt{z^2-1}}, \tag{3.76}$$

where $G(\alpha)$ is dimensionless and finite for $\alpha \in (0,\infty)$.

At this point, the asymptotic behaviour of $G(\alpha)$ can be analysed numerically, as no analytic formula for this integral was found in the tables consulted. However, while analysing this asymptotic behaviour, we found that $G(\alpha) = \frac{16}{\sqrt{\alpha+1}}$ gives an exact match up to high numerical accuracy across the many orders of magnitude that were checked.[6]

Using this result for $G(\alpha)$,

$$S_{\text{nonplanar}} = -\frac{\lambda A_\perp}{2^7 3^2\pi^3\Theta}\int_0^\infty \frac{d\alpha}{\sqrt{\alpha}}\frac{1}{\alpha+1} K_1\left(\frac{4}{\Theta\Lambda^2\sqrt{\alpha}} + \Theta m^2\sqrt{\alpha}\right). \tag{3.77}$$

Note that this result is invariant under $\Theta\Lambda^2 \leftrightarrow \Theta m^2$, another sign of the UV/IR connection in non-commutative theories.

This integral has two regulators, Λ and m. The only other dimensionful parameter is Θ, so the only dimensionless products of these regulators are $\frac{m}{\Lambda}$ and $\Theta m\Lambda$. As is familiar from the UV/IR mixing in this theory, the limits $\Lambda\to\infty$ and $m\to 0$ do not commute. This can be resolved by taking $\frac{m}{\Lambda}\to 0$ while fixing $\Theta m\Lambda$. Then taking the limit $m\to 0$ or $\Lambda\to\infty$ first corresponds to the limits $\Theta m\Lambda\to 0$ or $\Theta m\Lambda\to\infty$ respectively. [7]

[6] The only potential divergences in the integral for $S_{\text{nonplanar}}$ come from the regions of small and large α. If the reader is uncomfortable with this numeric argument, this functional form for $G(\alpha)$ could also be thought of more conservatively as a function with the right asymptotic behaviour to reproduce the correct divergences in this integral.

[7] This discussion applies even if we want to think of m as a physical mass, as the ratio $\frac{m}{\Lambda}$ will still vanish if m is fixed while $\Lambda\to\infty$. This case corresponds to $\Theta m\Lambda\to\infty$.

Introducing $\gamma = \sqrt{\alpha}$,

$$\begin{aligned} S_{\text{nonplanar}} &= -\frac{\lambda A_\perp}{2^6 3^2 \pi^3 \Theta} \int_0^\infty d\gamma \frac{1}{\gamma^2+1} K_1\left(\frac{2m}{\Lambda}\left[\frac{2}{\Theta m \Lambda \gamma} + \frac{\Theta m \Lambda \gamma}{2}\right]\right) \\ &\xrightarrow{\frac{m}{\Lambda}\to 0} -\frac{\lambda A_\perp \Lambda}{2^8 3^2 \pi^3 \Theta m} \int_0^\infty d\gamma \frac{1}{\gamma^2+1} \frac{1}{\frac{2}{\Theta m \Lambda \gamma} + \frac{\Theta m \Lambda \gamma}{2}} \\ &= -\frac{\lambda A_\perp \Lambda^2}{2^9 3^2 \pi^3} \frac{-\ln\left(\frac{\Theta^2 m^2 \Lambda^2}{4}\right)}{1-\frac{\Theta^2 m^2 \Lambda^2}{4}} = -\frac{\lambda A_\perp}{2^7 3^2 \pi^3 \Theta^2 m^2} \frac{-\ln\left(\frac{4}{\Theta^2 m^2 \Lambda^2}\right)}{1-\frac{4}{\Theta^2 m^2 \Lambda^2}}, \end{aligned} \tag{3.78}$$

where the last line uses (2) from Volume 2 p.216 of [88].

This result illustrates the UV/IR connection in non-commutative theories. If the IR regulator is removed first ($\Theta m \Lambda \ll 1$), $S_{\text{nonplanar}} \sim A_\perp \Lambda^2$ – a quadratic UV divergence. However if the UV regulator is removed first ($\Theta m \Lambda \gg 1$), $S_{\text{nonplanar}} \sim \frac{A_\perp}{\Theta^2 m^2}$, allowing the same divergence to be interpreted as an IR divergence. In addition, whether $\frac{\Theta^2 m^2 \Lambda^2}{4}$ is taken to be large or small there is a logarithmic divergence as is found in the commutative case. However, here there is the additional option of keeping both regulators, that is keeping $\frac{1}{2}\Theta m \Lambda$ finite, which eliminates the logarithmic divergence seen in the commutative case.[8] In particular, there is a natural choice of IR regulator[9], $m = \frac{2}{\Theta \Lambda}$ where

$$S_{\text{nonplanar}} = -\frac{\lambda A_\perp}{2^7 3^2 \pi^3 \Theta^2 m^2} = -\frac{\lambda A_\perp \Lambda^2}{2^9 3^2 \pi^3}. \tag{3.79}$$

From a mathematical point of view, this UV/IR connection can be seen to originate from the translation of the arguments of the Green's function. In the commutative theory, $S_{\text{nonplanar}} \sim \int_n dx G_n(x,x) f_n(x,x)$ where as in the noncommutative theory, the non-planar diagram made a contribution of the form $S_{\text{nonplanar}} \sim \int_n dx G_n(x, x+\Theta p) f_n(x, x+\Theta p)$. If an IR regulator is imposed, this momentum cannot vanish and regulates the integral. This can be seen more clearly in the dipole theory (analysed in Section 3.5.4) where the fixed translation regulates the UV divergence of the integral.

[8] Note that if a $\Theta \to 0$ limit is taken, this option is no longer available and the commutative result is recovered, although the exact form of the logarithmic divergence depends on how the Θ limit is taken.

[9] See Section 6 of [54]

It is important to note that contributions from the $j > 1$ terms in (3.25) were dropped at the start of this section and are not present in (3.78) or elsewhere in these results. However, as is discussed in Appendix A, these do not affect the leading divergence in $S_{\text{nonplanar}}$ or the conclusion that there is no volume law.

In contrast to strong coupling results, which saw signs of a volume law for the entanglement entropy even with large regions, this perturbative calculation is only sees an area law. The leading divergence in $S_{\text{nonplanar}}$ is quadratic and proportional to the area of the boundary of the region, $A_\perp$, in line with the area law discussed in the introduction.

3.5.3 Complex scalar

The difference when considering a complex scalar is the Wick contraction in (3.39) and (3.59) for the commutative and the noncommutative theory respectively. For the real scalar

$$\lambda \langle \phi(w)\phi(x)\phi(y)\phi(z)\rangle = \lambda \left(G_n(w,x)G_n(y,z) + G_n(w,y)G_n(x,z) + G_n(w,z)G_n(x,y)\right), \tag{3.80}$$

whereas for the complex scalar this must be replaced with

$$\begin{aligned} &\lambda_0 \langle \phi^\dagger(w)\phi(x)\phi^\dagger(y)\phi(z)\rangle + \lambda_1 \langle \phi^\dagger(w)\phi(x)\phi(y)\phi^\dagger(z)\rangle \\ &= \lambda_0 \left(G_n(w,x)G_n(y,z) + G_n(w,z)G_n(x,y)\right) + \lambda_1 \left(G_n(w,x)G_n(z,y) + G_n(w,y)G_n(z,x)\right). \end{aligned} \tag{3.81}$$

In the commutative theory, the fields in the 4-point function are all inserted at the same point, that is $w = x = y = z$. Taking into account the difference in the normalisation of the ϕ^4 term in the action, the only change is to replace an overall factor of $\frac{3\lambda}{4!}$ by $\frac{2(\lambda_0+\lambda_1)}{4}$. This has no effect on the intermediate steps of the calculation and can just be carried through straight to the final result:

$$S_{1,\text{Comm.}} \to -\frac{(\lambda_0+\lambda_1)A_\perp \Lambda^2}{3\cdot 2^8 \pi^3} \ln \frac{\Lambda^2}{4m^2}. \tag{3.82}$$

For the noncommutative theory, it is a simple matter of writing out the $\star$-products explicitly and following through similar transformations of the integra-

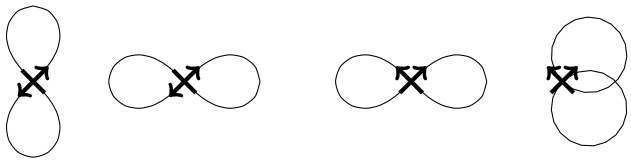

Figure 3.3: Vacuum bubble diagrams at leading order in the noncommutative complex scalar $\lambda\phi^4$ theory. The two on the left come from the $\lambda_0\phi^\dagger\star\phi\star\phi^\dagger\star\phi$ term in the action whereas the two on the right from the $\lambda_1\phi^\dagger\star\phi\star\phi\star\phi^\dagger$ term.

tion variables as in the previous section. This procedure gives $2\lambda_0+\lambda_1$ times the commutative result plus λ_1 times the result for the nonplanar diagram already encountered for the real scalar. This result can be obtained directly by looking at the 4 diagrams in Figure 3.3 and realising that only the term proportional to λ_1 gives a nonplanar diagram.

Thus the result for the noncommutative theory with a complex scalar is

$$S_{1,\mathrm{NC}} \to (2\lambda_0+\lambda_1)\frac{A_\perp\Lambda^2}{3\cdot 2^9\pi^3}\ln\frac{\Lambda^2}{4m^2} - \lambda_1\frac{A_\perp\Lambda^2}{3\cdot 2^8\pi^3}\frac{-\ln\left(\frac{\Theta^2m^2\Lambda^2}{4}\right)}{1-\frac{\Theta^2m^2\Lambda^2}{4}} \tag{3.83}$$

3.5.4 Dipole theory

For the dipole theory, the explicit form of the interaction terms was written out in (3.14). Thus,

$$\begin{aligned}\ln Z_n &= \ln\int\mathscr{D}\phi\, e^{-S_E[\phi]} \qquad (3.84)\\ &= \ln Z_{n,0} - \int_n d^4x\left\langle\frac{\lambda_0}{4}\Phi^\dagger(x)\Phi(x)\Phi^\dagger(x)\Phi(x)+\frac{\lambda_1}{4}\Phi^\dagger(x+\frac{1}{2}a)\Phi(x+\frac{1}{2}a)\Phi(x-\frac{1}{2}a)\Phi^\dagger(x-\frac{1}{2}a)\right\rangle_0+\ldots\end{aligned}$$

Applying Wick's Theorem, using the facts that $G_1(x,x)=G_1(x+a,x+a)$ and

$f_n(x+a,x) = f_n(x,x+a)$ (when ignoring the $j > 1$ terms) and shifting the integral,

$$\begin{aligned}\ln Z_{n,1} =& -\frac{1}{4}\int_n d^4x\,[2\lambda_0 G_n(x,x)G_n(x,x) \qquad (3.85)\\ &+\lambda_1\left(G_n(x+\frac{1}{2}a,x+\frac{1}{2}a)G_n(x-\frac{1}{2}a,x-\frac{1}{2}a)+G_n(x+\frac{1}{2}a,x-\frac{1}{2}a)G_n(x-\frac{1}{2}a,x+\frac{1}{2}a)\right)\Big]\\ S_1 =& -\partial_n\left[\ln Z_{n,1} - n\ln Z_{1,1}\right]_{n=1} \qquad (3.86)\\ =&\frac{2}{4}\partial_n\left(\int d^4x\left[(2\lambda_0+\lambda_1)G_1(x,x)nf_n(x,x)+\lambda_1 G_1(x,x+a)nf_n(x,x-a)\right]\right)_{n=1}.\end{aligned}$$

Again this is as expected from the diagrammatic approach. Only the single nonplanar diagram gives a new contribution and the 3 planar diagrams give contributions identical to those in the commutative theory.

Focusing on the contribution from the nonplanar diagram, the explicit forms of G_1 and f_n give

$$S_{\text{nonplanar}} = \frac{4\lambda A_\perp}{12\pi\cdot 4}\int r dr d\phi \int \frac{d^4k dp_y dp_z}{(2\pi)^6}\frac{e^{ik_x a}}{k^2+m^2}\int_0^\infty dqq\frac{\partial_\nu[J_\nu(qr)J_\nu(qr')]_{\nu=0}}{q^2+p_y^2+p_z^2+m^2}, \tag{3.87}$$

where now $r'^2 = (\vec{r}-a\hat{\imath})^2 = r^2+a^2-2ra\cos\phi$.

Introducing Schwinger parameters and regulating,

$$\begin{aligned}S_{\text{nonplanar}} = \frac{\lambda A_\perp}{2^2 3\pi}\int dr d\phi \frac{d^4k dp_y dp_z}{(2\pi)^6}dq\int_0^\infty d\alpha d\beta qre^{-\alpha k^2-\beta\left[q^2+p_y^2+p_z^2\right]-\frac{1}{\alpha\Lambda^2}-\alpha m^2-\frac{1}{\beta\Lambda^2}-\beta m^2}\\ e^{ik_x a}\partial_\nu[J_\nu(qr)J_\nu(qr')]_{\nu=0}.\end{aligned} \tag{3.88}$$

In this case, all the momenta integrals except q are Gaussian,

$$S_{\text{nonplanar}} = \frac{\lambda A_\perp}{2^8 3\pi^4}\int dr d\phi dq d\alpha d\beta \frac{qr}{\alpha^2\beta}e^{-\frac{a^2}{4\alpha}-\frac{1}{\alpha\Lambda^2}-\alpha m^2-\beta q^2-\frac{1}{\beta\Lambda^2}-\beta m^2}\partial_\nu[J_\nu(qr)J_\nu(qr')]_{\nu=0}. \tag{3.89}$$

The α integral can be factored out to give, using (3.45),

$$\int_0^\infty d\alpha \frac{e^{-\frac{1}{\alpha}\left(\frac{a^2}{4}+\frac{1}{\Lambda^2}\right)-\alpha m^2}}{\alpha^2} = \int_0^\infty d\alpha e^{-\alpha\left(\frac{a^2}{4}+\frac{1}{\Lambda^2}\right)-\frac{m^2}{\alpha}} = \frac{2m}{\sqrt{\frac{a^2}{4}+\frac{1}{\Lambda^2}}} K_1\left(2m\sqrt{\frac{a^2}{4}+\frac{1}{\Lambda^2}}\right)$$
$$\xrightarrow{\Lambda\to\infty} \frac{4m}{a} K_1(ma) \tag{3.90}$$
$$\xrightarrow{m\to 0} \frac{4}{a^2}$$

This factor came from evaluating $G_1(0, a\hat{\imath})$ which goes as $\sim \frac{1}{a^2}$ as expected. The fixed nonlocality scale has regulated the UV divergence in this case. In the dipole theory the distance of the translation is fixed, as opposed to the non-commutative case where the translation is proportional to the momentum in the y-direction which can vanish in the IR.

Using (3.49),

$$S_{\text{nonplanar}} = -\frac{\lambda A_\perp}{2^7 3\pi^4 a^2} \int_0^\infty d\beta \left[\int_0^\infty dr \int_0^{2\pi} d\phi \frac{r}{\beta^2} e^{-\frac{r^2+r'^2}{4\beta}} K_0\left(\frac{rr'}{2\beta}\right)\right] e^{-\frac{1}{\beta\Lambda^2}-\beta m^2}. \tag{3.91}$$

Rescaling $r \to ar$ and $\beta \to a^2\beta$ to make them dimensionless ($r' \to a\sqrt{r^2+1-2r\cos\phi}$ under this) and defining $H(\beta)$ as the part of the previous equation enclosed in brackets,

$$S_{\text{nonplanar}} = -\frac{\lambda A_\perp}{2^7 3\pi^4 a^2} \int_0^\infty d\beta H(\beta) e^{-\frac{1}{\beta a^2\Lambda^2}-\beta a^2 m^2}. \tag{3.92}$$

$H(\beta)$ is dimensionless and finite for $\beta \in (0,\infty)$. The integrand is exponentially suppressed for small β and numerical evaluation of the r and ϕ integrals confirm that $H(\beta) \xrightarrow{\beta\to 0} 0$. The other potential source of a divergence is at large β and numerical integration finds that $H(\beta) \xrightarrow{\beta\to\infty} \frac{2\pi}{\beta}$ leading to a logarithmic divergence at large β that must be regulated by $e^{-\beta a^2 m^2}$,

$$\int^\infty \frac{d\beta}{\beta} e^{-\beta a^2 m^2} = -\ln(a^2 m^2) + O(m^0), \tag{3.93}$$

to leading order in the small m limit.

Thus $S_{\text{nonplanar}}$ has only an IR divergence in the dipole theory. The leading divergence in the $j = 1$ term is

$$S_{\text{nonplanar}} = -\frac{\lambda A_{\perp}}{3 \cdot 2^6 \pi^3 a^2} \left[-\ln(a^2 m^2) \right], \tag{3.94}$$

however there will be contributions to this order from the $j > 1$ terms which were dropped. The the conclusion of this analysis is that the nonplanar diagram does not contribute to the leading divergence of entanglement entropy at this order as it is subleading to the contribution from the planar diagram.

The nonlocality introduced in the dipole theory does not affect the area law, as the total entanglement entropy at this order in perturbation theory is dominated by the planar diagrams which matched the result from the commutative theory. Even the subleading terms we have analysed do not follow any sort of volume law as they are not proportional to the lengthscale of the nonlocality. The only effect of the nonlocality is to regulate the UV divergence otherwise present. Similar behaviour was observed in [54], where one of the ways that the nonlocality manifested itself was by softening divergences in nonplanar diagrams.

3.6 Final remarks

In this paper we computed the first perturbative correction to the entanglement entropy in two nonlocal theories, a ϕ^4 theory defined on the noncommutative plane and a dipole theory.

The contribution to the entanglement entropy in each of these theories at first order in coupling comes from vacuum bubble diagrams. The planar diagrams give the same contribution in all three theories. However, the nonplanar diagram is affected by the modified $\star$-product. Never the less, these diagrams do not modify the area law observed in the commutative theory. Thus, at this order in perturbation theory and for the region considered at least, all these theories follow an area law with no sign of a volume law, as opposed to the strongly coupled case where the signature of the volume law could be seen even for large regions.

In the commutative theory it has been shown that the modification to the en-

tanglement entropy at first order in perturbation theory can be absorbed into the renormalisation of the mass [85]. It would be interesting to see if a similar interpretation can be made in the case of the theories considered here.

Finally, a comment about the commutative limit. Since the quantities dealt with in the paper are not UV finite, this is not a straightforward issue. The general pattern is that the nonlocality has served as an additional regulator that softens certain divergences. Thus, if the nonlocality is removed, these divergences reappear and the commutative limit applied to the final results is not smooth.

Part II

The Structure of Holographic Entanglement Entropy

Chapter 4

Inviolable Energy Conditions

4.1 Introduction

The AdS/CFT correspondence provides a remarkable connection between quantum gravitational theories and non-gravitational quantum systems [4, 5]. There are believed to be many examples of the correspondence; indeed, it may be that any consistent quantum gravity theory for asymptotically AdS spacetimes can be used to define a CFT on the boundary spacetime. In this paper, we focus on examples with a classical limit described by Einstein's equations coupled to matter. We seek to derive results that are universally true for all such theories, by translating to gravitational language results that are universally true in all quantum field theories. Specifically, we will translate some basic constraints on the structure of entanglement in quantum systems to derive some fundamental constraints on spacetime geometry that must hold in all consistent theories of Einstein gravity coupled to matter.

Our main tool will be the Ryu-Takayanagi formula (and its covariant generalization due to Hubeny, Rangamani, and Takayanagi)[6, 9].[1] This relates entanglement entropy for spatial regions A in the field theory to the areas of extremal surfaces ∂A in the dual geometry with the same boundary as A (see Section 4.2 for

[1] A recent proof was given in [27].

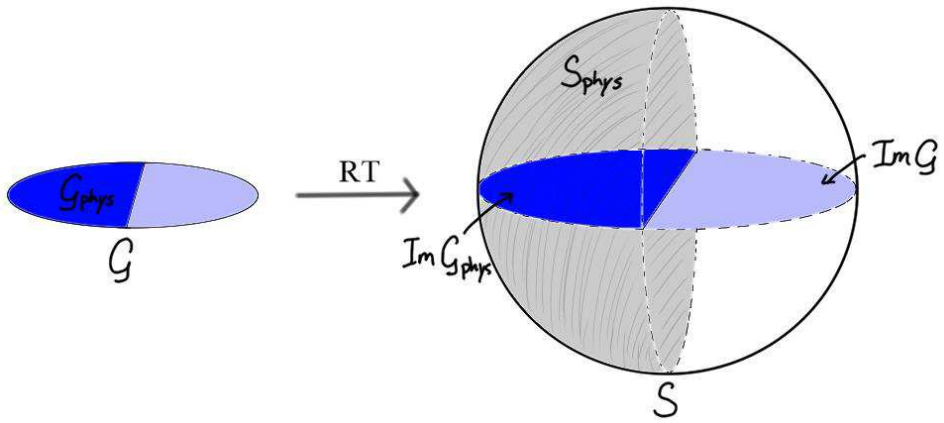

Figure 4.1: Ryu-Takayanagi formula as a map from the space $\mathscr{G}$ of geometries with boundary B to the space $\mathscr{S}$ of mappings from subsets of B to real numbers. Mappings in region $\mathscr{S}_{phys}$ (shaded) correspond to physically allowed entanglement entropies. Geometries in region $\mathscr{G}_{phys}$ map into $\mathscr{S}_{phys}$ while the remaining geometries are unphysical in any consistent theory for which the Ryu-Takayanagi formula holds (plausibly equal to the set of gravity theories with Einstein gravity coupled to matter in the classical limit).

a review). Generally speaking, we can understand this as a mapping

$$RT : \mathscr{G} \to \mathscr{S}$$

from the set $\mathscr{G}$ of asymptotically AdS spacetimes with boundary geometry B to the set $\mathscr{S}$ of maps S from subsets of B to real numbers.[2]

This mapping is depicted in Figure 4.1. Physically allowed entanglement structures must obey constraints, such as strong subadditivity and positivity/monotonicity of relative entropy, so only a subset $\mathscr{S}_{phys}$ of maps represented by $\mathscr{S}$ can represent physically allowed entanglement structures. If a geometry $M \in \mathscr{G}$ maps to a point outside this subset, we can conclude that such a geometry is not allowed, in any theory for which the Ryu-Takayanagi formula is valid (which we believe to be

[2]To avoid divergent quantities, we could define the map S associated with a geometry M such that for subset B of the boundary of M, $S_M(B)$ is the difference between the area of the extremal surface $\tilde{B}_M$ and the corresponding extremal surface $\tilde{B}_{AdS}$ in pure AdS.

all consistent gravity theories whose classical limit is Einstein gravity coupled to matter). Another interesting point is that the space of geometries with boundary B is much smaller than the space of functions on subsets of B, so the image of $\mathscr{G}$ in $\mathscr{S}$ will be a measure zero subset $\mathscr{S}_G$. This implies that the entanglement structures for quantum field theory states with gravity duals are extremely constrained.

This picture suggests several interesting directions for research:

- Characterize the geometries $\mathscr{G}_{phys}$ that map to physically allowed entanglement entropies $\mathscr{S}_{phys}$. While some of these geometries may be ruled out by additional constraints not related to entanglement, we can say that any geometry not in $\mathscr{G}_{phys}$ cannot represent a physical spacetime.

- Characterize the constraints on entanglement structure implied by the existence of a holographic dual i.e. understand the subset $\mathscr{S}_G$. Examples include the monogamy of mutual information [89], but there should be much stronger constraints through which the entanglement entropies for most regions are determined in terms of the entanglement entropies for a small subset of regions.

- Better understand the inverse mapping from $\mathscr{S}_{phys}$ to $\mathscr{G}_{phys}$ to be able to explicitly reconstruct geometries from entanglement entropies.

In this paper, we focus on the first direction, though we will have some comments on the second direction in Section 4.6. Many recent papers discuss the third direction, including [90, 91, 92].

Constraining geometry from entanglement

The question of which geometries give rise to allowed entanglement structures was considered at the level of first order perturbations to pure AdS in [36, 37, 38] (see also [93, 94]). Such perturbations correspond to small perturbations of the CFT vacuum state. For these first order CFT perturbations, the entanglement entropy for ball-shaped regions is determined in terms of the expectation value of the stress-energy tensor[3] via the "first law of entanglement," which we review in Section 4.2

[3]The stress tensor is determined in terms of the entanglement entropy for infinitesimal ball shaped regions, so we can think of the entanglement first law as a constraint determining the entanglement

below. As shown in [36, 37] the gravitational version of this constraint is exactly the linearized Einstein equation. For a discussion of constraints at the second-order in the metric perturbation, see [95, 96].

In this paper, we begin to unravel the implications of entanglement constraints on geometries away from this perturbative limit. One might ask whether it is possible to obtain the full non-linear Einstein equations in this way. However, at the classical level, the entanglement quantities tell us only about the dual geometry, so the entanglement constraints will be constraints on the geometries themselves, without reference to any bulk stress-energy tensor. Further, the specific constraints we consider (strong subadditivity of entanglement entropy, and the positivity and monotonicity of relative entropy) take the form of inequalities, so we should expect that the nonlinear constraints also take the form of geometrical inequalities ruling out some geometries as unphysical. This is a natural outcome: since the results must apply to all consistent theories, we cannot expect specific non-linear equations to emerge, but there should be restrictions that apply to the whole class of allowed theories.

In interpreting these geometrical constraints, it is useful to translate them into constraints on the stress-energy tensor *assuming* that Einstein's equations hold. This is a very plausible assumption. Indeed, it is possible to argue [38] indirectly using the linearized results that Einstein's equations must be obtained.[4] Any geometry provides a solution to Einstein's equations for some stress tensor. Thus, given a geometry that violates the entanglement constraints, we can conclude that no consistent theory of gravity can produce the associated stress tensor. Expressed in this way, the constraints from entanglement inequalities can be thought of as certain "energy conditions."

We will see that some of the conditions we obtain are closely related to some of the standard energy conditions used in classical general relativity. However,

entropies for arbitrary ball-shaped regions from the entanglement entropies for infinitesimal balls.

[4] In [38], it was shown that by considering quantum corrections to the Ryu-Takayanagi formula, the expectation value of the bulk stress-energy tensor comes in as a source for the linearized Einstein equations. Assuming that the source is a generally a local operator, this is enough to see that it must be the stress-energy tensor. It has been argued that the linearized equations together with the stress-energy tensor as a source imply the full non-linear Einstein equations if one demands conservation of the stress-energy tensor in the full theory.

we emphasize that while these standard conditions (such as the weak and null-energy conditions) are simply plausible assumptions on the properties of matter, the conditions we derive follow from fundamental principles of quantum mechanics (assuming the Ryu-Takayanagi formula holds) and cannot be violated.

Summary of results

In this paper, we take a few modest steps towards understanding the general constraints on non-linear gravity due to entanglement inequalities, investigating these constraints in the case of highly symmetric spacetimes. Specifically, we determine constraints on static, translationally invariant spacetimes in 2+1 dimensions, and static, spherically-symmetric spacetimes in general dimensions. We find the following main results:

- For spacetimes dual to the vacuum states of 1+1 dimensional Lorentz-invariant field theories flowing between two CFT fixed points, the constraints due to strong-subadditivity are satisfied if and only if the spacetime satisfies a set of averaged null energy conditions

$$\int_\gamma ds T_{\mu\nu} u^\mu u^\nu \geq 0$$

  where γ is an arbitrary spatial geodesic and u^μ is a null vector generating a light-sheet of γ defined such that translation by u^μ produces an equal change in the spatial scale factor at all points (Section 4.3).

- For static translation-invariant spacetimes dual to excited states of 1+1 dimensional CFTs, we show that the monotonicity of relative entropy implies that the minimum scale factor reached by an RT surface for spatial interval is always less than the scale factor reached by the corresponding RT surface in the geometry for the thermal state with the same stress-energy tensor (Section 4.4).

- For these spacetimes, we find that asymptotically, the positivity of relative entropy is exactly equivalent to the statement that observers near the boundary moving at arbitrary velocities in the field theory direction cannot observe negative energy. That is, we get a subset of the weak energy condition

$T_{\mu\nu}u^\mu u^\nu \geq 0$ where u^μ is an arbitrary timelike vector with no component in the radial direction.

- For static spherically symmetric asymptotically AdS spacetimes, the positivity of relative entropy implies that the area of a surface bisecting the spacetime symmetrically is bounded by the mass of the spacetime. For four-dimensional gravity, the specific result is (Section 4.5)

$$\Delta A \leq 2\pi G_N M \ell_{AdS} \, .$$

We offer a few concluding remarks in Section 4.6.

Previous connections between energy conditions and entanglement inequalities appeared in [97, 98, 73, 99] who noted that the null energy condition is sufficient to prove certain entanglement inequalities holographically. The use of relative entropy in holography was pioneered in [100] and applied to derive gravitational constraints at the perturbative level in [95, 96].

Note: While this manuscript was in preparation, the paper [41] appeared, which overlaps with the results in Section 4.4.2.

4.2 Background

4.2.1 Entanglement inequalities

In this section, we review various entanglement inequalities that should place constraints on possible dual spacetimes via the holographic entanglement entropy formula.[5]

Strong subadditivity

To begin, we recall that the entanglement entropy $S(A)$ for a subsystem A of a quantum system is defined as $S(A) = -\mathrm{tr}(\rho_A \log(\rho_A))$, where ρ_A is the reduced density matrix for the subsystem.

[5] See, for example [14], for a more complete discussion of entanglement inequalities.

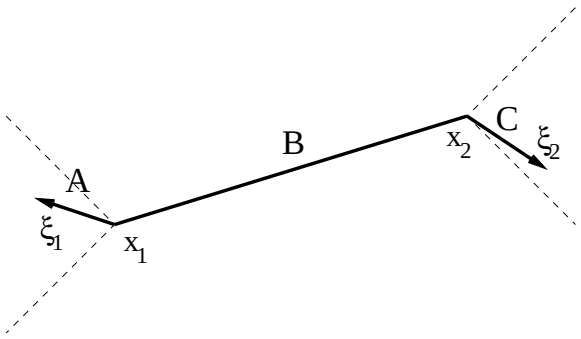

Figure 4.2: Spacelike intervals for strong subadditivity.

The strong subadditivity of entanglement entropy states that for any three disjoint subsystems A, B, and C,

$$S(A\cup B)+S(B\cup C)\geq S(B)+S(A\cup B\cup C). \tag{4.1}$$

Considering only spatial regions of a constant-time slice in a time-invariant state corresponding to a static dual geometry, this constraint places no constraints on the dual geometry, as shown in [74]. However, in the time-dependent cases, or for regions of a time-slice that do not respect the symmetry, this inequality gives non-trivial constraints, as we will see below.

For our analysis below, we will be interested in applying the constraints of strong subadditivity in the case of 1+1 dimensional field theories. Entanglement entropy is the same for any spacelike regions with the same domain of dependence, so for any connected spacelike region A, entanglement entropy is a function of the two endpoints of the region. We write $S(x_1,x_2)$ to denote the entanglement entropy of the interval $[x_1,x_2]$ (or any spacelike region with the same domain of dependence). We focus on the case where A, B, and C in (4.1) are adjacent spacelike intervals, as shown in Figure 4.2.

We note first that the full set of strong subadditivity constraints for adjacent intervals follow from the constraints in the case where the intervals A and C are infinitesimal. For suppose the strong-subadditivity constraint is true for regions A, B, and C with the proper length of A and C less than L_{max}. Then we can show that the constraint holds for intervals with A and C less than $2L_{max}$, and so forth. For

example, if A, B, C_1 and C_2 are adjacent intervals with C_1 and C_2 having proper length less than L_{max}, we have

$$\begin{aligned} S(A\cup B)+S(B\cup C_1) &\geq S(A\cup B\cup C_1)+S(B) \\ S(A\cup B\cup C_1)+S(B\cup C_1\cup C_2) &\geq S(A\cup B\cup C_1\cup C_2)+S(B\cup C_1) \end{aligned}$$

Adding these, we find

$$S(A\cup B)+S(B\cup\{C_1\cup C_2\})\geq S(A\cup B\cup\{C_1\cup C_2\})+S(B)\,.$$

In this way, we can combine two strong subadditivity constraints for which the rightmost interval has length smaller than L_{max} to obtain a constraint where the rightmost interval is any interval with length less than $2L_{max}$.[6]

Now, consider the strong subadditivity constraint where B is the interval $[x_1,x_2]$ while A and C are the intervals $[x_1+\varepsilon\xi_1,x_1]$ and $[x_2,x_2+\delta\xi_2]$, as shown in Figure 4.2. In this case, the constraint (4.1) gives

$$\begin{aligned} & S([x_1+\varepsilon\xi_1,x_1]\cup[x_1,x_2])+S([x_1,x_2]\cup[x_2+\delta\xi_2]) \\ &\qquad\qquad \geq S([x_1+\varepsilon\xi_1,x_1]\cup[x_1,x_2]\cup[x_2+\delta\xi_2])+S([x_1,x_2]) \\ \Longrightarrow\quad & S(x_1+\varepsilon\xi_1,x_2)+S(x_1,x_2+\delta\xi_2)-S(x_1+\varepsilon\xi_1,x_2+\delta\xi_2)-S(x_1,x_2)\geq 0 \end{aligned}$$

Expanding to first order in both δ and ε, this gives

$$\xi_1^\alpha\xi_2^\beta\partial_\alpha^1\partial_\beta^2 S(x_1,x_2)\leq 0\,.$$

Since this constraint is linear in the spacelike vectors ξ_1 and ξ_2, it is sufficient to require that the constraint be satisfied in the lightlike limit of ξ_1 and ξ_2, i.e. when ξ_1 and ξ_2 lie along the dotted lines in Figure 4.2. Thus, a minimal set of strong subadditivity constraints that imply all constraints for connected regions is

$$\partial_+^1\partial_+^2 S(x_1,x_2)\leq 0\qquad \partial_+^1\partial_-^2 S(x_1,x_2)\leq 0\qquad \partial_-^1\partial_+^2 S(x_1,x_2)\leq 0\qquad \partial_-^1\partial_-^2 S(x_1,x_2)\leq 0\,.$$

[6]Essentially the same argument works in general dimensions to show that the full set of strong subadditivity constraints are implied by considering the constraint (4.1) where B is an arbitrary region and where A and C are taken to be infinitesimal.

In the special case of states invariant under spacetime translations, the entanglement entropy for an interval can only depend on the difference between the endpoints so $S(x_1,x_2) = S(x_2 - x_1)$. In this case, the basic constraints may be written as[7]

$$\partial_+\partial_+ S(x) \leq 0 \qquad \partial_-\partial_- S(x) \leq 0 \qquad \partial_+\partial_- S(x) \leq 0 \qquad \partial_-\partial_+ S(x) \leq 0;. \quad (4.2)$$

Only the latter two constraints here are saturated for the vacuum state, so we expect these will provide more useful constraints.

Finally, in the case of a Lorentz-invariant state, the entanglement entropy can depend only on the proper length of the interval, so is described by a single function $S(R)$. In this case, the constraints reduce to

$$\frac{d^2S}{dR^2} \pm \frac{1}{R}\frac{dS}{dR} \leq 0\,, \quad (4.3)$$

where the first two constraints in (4.2) give the $-$ sign and the latter two give the $+$ sign. In particular, the constraint with the $+$ sign (which is saturated for vacuum states) is equivalent to

$$c'(R) \leq 0 \qquad\qquad c(R) \equiv R\frac{dS}{dR}\,.$$

This was shown by Casini and Huerta [101] in their proof of the c-theorem using strong-subadditivity.

Positivity and Monotonicity of Relative Entropy

A very general class of constraints on the entanglement structure of a quantum system are related to *relative entropy*. This gives a measure of distinguishability of a density matrix ρ to a reference state σ, defined as

$$S(\rho||\sigma) = \mathrm{tr}(\rho\log\rho) - \mathrm{tr}(\rho\log\sigma)\,.$$

[7] Similar constraints were noted in [42], which appeared while the current version of this paper was in preparation.

Relative entropy is always positive, increasing from zero for identical states ρ and σ to infinity for orthogonal states. Furthermore, for reduced density matrices ρ_A and σ_A obtained by a partial trace operation from ρ and σ, we have

$$S(\rho_A \| \sigma_A) \leq S(\rho \| \sigma). \tag{4.4}$$

This decrease in ρ under restriction to a subsystem is known as the monotonicity of relative entropy, or the data processing inequality [14].

It is useful to define the modular Hamiltonian associated with the reference state as $H_\sigma = -\log(\sigma)$, in analogy with thermodynamics. Using this, and the definition $S(\rho) = -\mathrm{tr}(\rho \log(\rho))$ for entanglement entropy, we can rewrite the expression for relative entropy as

$$\begin{aligned} S(\rho||\sigma) &= \mathrm{tr}(\rho\log\rho) - \mathrm{tr}(\sigma\log\sigma) + \mathrm{tr}(\sigma\log\sigma) - \mathrm{tr}(\rho\log\sigma) \\ &= \langle -\log\sigma\rangle_\rho - \langle -\log\sigma\rangle_\sigma - S(\rho) + S(\sigma) \\ &= \Delta\langle H_\sigma\rangle - \Delta S. \end{aligned} \tag{4.5}$$

For nearby states, $\rho - \sigma = \varepsilon X$ with $\varepsilon \ll 1$ and X an arbitrary traceless Hermitian operator, one can expand relative entropy in powers of ε. To the first order in ε relative entropy vanishes. This is typically referred to as the first law of entanglement since it implies $\delta\langle H_\sigma\rangle = \delta S$. The expression at second order in ε is known as *Fisher information*, and is discussed in detail in Section 4.3.

The rewriting in (4.5) becomes useful in cases where we can compute the modular Hamiltonian H_σ. Generally this is possible when the reference state is thermal with respect to some Hamiltonian. For example, the density matrix for a half-space in the vacuum state of a Lorentz-invariant field theory on Minkowski space is thermal with respect to the Rindler Hamiltonian (boost generator), so we have $H_{mod} = c\int d^d x x T_{00}$. The cases we consider below can all be obtained by conformal transformations from this example [102, 100].

For a ball shaped region in the vacuum state of a CFT on $R^{d,1}$, we have [100]

$$H_B = 2\pi \int_{|x|<R} d^d x \frac{R^2 - |x|^2}{2R} T_{00}^{\mathrm{CFT}} \,. \tag{4.6}$$

For a ball-shaped region in the vacuum state of a CFT on a sphere, we have

$$H_B = 2\pi \int_B d^d x \frac{\cos(\theta) - \cos(\theta_0)}{\sin(\theta_0)} T_{00} \ . \tag{4.7}$$

In the special case of 1+1 dimensional CFTs the modular Hamiltonian can also be calculated for thermal states. For a spatial interval $[-R, R]$ in an unboosted thermal state with temperature $T = \beta^{-1}$, the modular Hamiltonian is

$$H_B = \frac{2\beta}{\sinh\left(\frac{2\pi R}{\beta}\right)} \int_{-R}^{R} dx \sinh\left(\frac{\pi(R-x)}{\beta}\right) \sinh\left(\frac{\pi(R+x)}{\beta}\right) T_{00}(x) \ , \tag{4.8}$$

We can also obtain the expression for the modular Hamiltonian of an interval in a boosted thermal state. This is derived in Appendix B.

Optimal relative entropy constraints for a family of reference states

In various situations, we may have a family of reference states σ_α depending on parameters α_i (e.g. temperature), and we would like to find the strongest relative entropy constraint coming from this family. We will assume that the modular Hamiltonians for these reference states take the form of an integral over linear combination of local operators with α-dependent coefficients,

$$H_\alpha = \int d^d x f_n(x, \alpha) \mathscr{O}_n(x) \ . \tag{4.9}$$

According to the entanglement first law, under first order variation of the reference state σ_α, the entanglement entropy of this state changes as

$$\delta S_\alpha = \int d^d x f_n(x, \alpha) \delta \langle \mathscr{O}_n(x) \rangle_\alpha \ .$$

Here the right side corresponds to the variation in the expectation value of the modular Hamiltonian for the reference state under a variation of the state (while keeping the modular Hamiltonian fixed). Using this result and the definition (4.5), we have

$$\delta S(\rho || \sigma^\alpha) \quad = \quad \delta \left\{ \langle H_\beta \rangle_\rho - \langle H_\beta \rangle_{\sigma^\beta} - S(\rho) + S(\sigma^\beta) \right\}$$

$$= \int d^d x \delta f_n(x,\alpha) \left[\langle \mathscr{O}_n(x) \rangle_\rho - \langle \mathscr{O}_n(x) \rangle_{\sigma_\alpha} \right] . \tag{4.10}$$

Thus, the relative entropy will be extremized with respect to parameters α_i if we can choose a reference state such that

$$\int d^d x \frac{\partial f_n(x,\alpha)}{\partial \alpha_i} \left[\langle \mathscr{O}_n(x) \rangle_\rho - \langle \mathscr{O}_n(x) \rangle_{\sigma_\alpha} \right] = 0 . \tag{4.11}$$

In the special case where the initial state and reference states are translation invariant, this becomes

$$\frac{\partial I_n(\alpha)}{\partial \alpha_i} \left[\langle \mathscr{O}_n \rangle_\rho - \langle \mathscr{O}_n \rangle_{\sigma_\alpha} \right] = 0 , \tag{4.12}$$

where

$$I_n(\alpha) = \int d^d x f_n(x,\alpha) .$$

so we see that an extremum will be obtained if we can choose a reference state with the same expectation value as our state for each of the operators,

$$\langle \mathscr{O}_n \rangle_\rho = \langle \mathscr{O}_n \rangle_{\sigma_\alpha} \tag{4.13}$$

The same state will also be provide an extremum for the monotonicity constraint, since if R parameterizes a region whose size increases with R,

$$\frac{d}{d\alpha_i} \frac{d}{dR} S(\rho||\sigma^\alpha) = \frac{\partial^2 I_n(\alpha,R)}{\partial R \partial \alpha_i} \left[\langle \mathscr{O}_n \rangle_\rho - \langle \mathscr{O}_n \rangle_{\sigma_\alpha} \right] = 0 .$$

Thus the reference state σ^{α^*} whose operator expectation values match the state ρ will also give the minimum $dS(\rho||\sigma^\alpha)/dR$ (and thus the strongest monotonicity constraint), assuming that the extremum is a minimum.[8]

The matching of operator expectation values and the form (4.9) of the Hamiltonian implies that $\Delta\langle H_{\alpha^*} \rangle = 0$, so in this case, the constraint from positivity and

[8] In practice, we should also check whether other extrema exist, and check the boundary of the parameter space. However, since the relative entropy provides a measure of how close our state is to the reference state, it is plausible that the relative entropy is minimized by matching the expectation values of operators. For the cases below, we have explicitly checked that this is the case using the explicit form of the modular Hamiltonian.

monotonicity of relative entropy are simply that[9]

$$S(\rho_R) - S(\sigma_R^{\alpha^*}) \leq 0 \qquad\qquad \frac{d}{dR}(S(\rho_A) - S(\sigma_A^{\alpha^*})) \leq 0. \tag{4.14}$$

4.2.2 Holographic formulae for entanglement entropy

In this paper, we consider general theories of gravity dual to holographic QFTs such that the leading order (in the $1/N$ expansion) entanglement entropy for spatial regions of the field theory is computed by the Ryu-Takayanagi formula [6], or its covariant generalization [9]. This states that the entanglement entropy of a region A is given by

$$S(A) = \frac{\text{Area}(\tilde{A})}{4G_N} ,$$

where $\tilde{A}$ is the extremal surface in the dual geometry with $\partial\tilde{A} = \partial A$ (i.e. such that A and ∂A have the same boundary). The surface $\tilde{A}$ is also required to be homologous to A, and in cases where multiple extremal surfaces exist, it is the extremal surface with least area.

The Ryu-Takayanagi formula receives quantum corrections from the entanglement entropy of bulk quantum fields, but we consider only the classical limit in this paper. We note also that for theories of gravity with higher powers of curvature or higher derivatives, the entropy is computed using a more complicated functional than area. However, we restrict attention in this paper to theories for which the gravitational sector is Einstein gravity.

4.2.3 Energy conditions

To end this section, we briefly review a few of the standard energy conditions discussed in the gravitational literature. These are statements about the stress-energy tensor that are taken to be plausibly true, but which are generally not derived from any underlying quantum theory.[10] The *weak energy condition* states that the energy density in any frame of reference must be non-negative. Specifically, if u^μ

[9] A similar simplification of relative entropy was noted in [103] when considering the problem of finding entropy-maximizing states consistent with local data.

[10] See [104] for a recent argument for the null-energy condition based on perturbative string theory.

is a timelike vector, then

$$T_{\mu\nu}u^\mu u^\nu \geq 0\,.$$

The *null energy condition* takes the same form, but with u is taken to be a null vector. This is implied by the weak energy condition.

Various authors have also considered averaged energy conditions, in which the conditions are only required to hold when averaged over some geodesic or spatial region. This is the type of contraint that we will find below.

4.3 Constraints on spacetimes dual to Lorentz-invariant 1+1D field theories

In this section, we consider Lorentz-invariant holographic two-dimensional field theories that flow from some CFT in the UV to another CFT in the IR. For such theories, the vacuum state is dual to a spacetime of the form[11]

$$ds^2 = \frac{F^2(r)}{r^2}dr^2 + r^2(-dt^2+dx^2)\,, \tag{4.15}$$

where $F(r)$ approaches constants both at $r=0$ and at $r=\infty$ (giving AdS geometries corresponding to the IR and UV fixed points).[12] We would like to understand the constraints on the function $F(r)$ that arise from entanglement inequalities in the CFT. Specifically, we consider the constraints arising from strong subadditivity.

For any spacelike interval, Lorentz-invariance implies that the entanglement entropy depends only on the proper length of the interval, so entanglement entropy for connected regions is captured by a single function $S(R)$. As we reviewed in Section 4.2, Casini and Huerta have shown [101] starting from strong subadditivity that the function $c(R) = dS/d(\ln(R)) = RdS/dR$ obeys $c'(R) \leq 0$. The function $c(R)$ therefore decreases monotonically for increasing R, which leads immediately to the Zamolodchikov c-theorem, since $c(R)$ reduces to the UV and IR central charge for small and large R respectively.

The holographic version of the statement $c'(R) \leq 0$ was obtained previously

[11] In special cases, there may be additional compact directions in the dual spacetime. In these cases, we consider the KK-modes of the metric and other fields as part of the matter sector.

[12] This choice of coordinates assumes that the spatial scale factor is monotonic in the radial direction. At the end of this section, we comment on the case where this doesn't hold.

in [97], but we review the calculation here since we will be generalizing this in the next section. Using the Ryu-Takayanagi formula, the entanglement entropy for an interval of length R in the geometry (4.15) is obtained by the minimum of the action

$$S = \int d\lambda \sqrt{\frac{F^2(r)}{r^2}\left(\frac{dr}{d\lambda}\right)^2 + r^2\left(\frac{dx}{d\lambda}\right)^2} \tag{4.16}$$

with boundary conditions $(r(\lambda_i), x(\lambda_i)) = (r_{max}, 0)$ and $(r(\lambda_f), x(\lambda_f)) = (r_{max}, R)$, where r_{max} is a regulator that we will take to infinity. In Appendix C, we derive a general formula for the variation of the entanglement entropy under a variation in the endpoints of the interval for translation-invariant geometries. For the case of variations in the size of spatial interval, the result (derived previously in [97]) is that $\frac{dS}{dR}$ equals the minimum spatial scale factor reached by the RT surface. Thus, for our choice of coordinates,

$$\frac{dS}{dR} = r_0 \qquad\qquad c(R) = r_0 R\,. \tag{4.17}$$

To find an explicit relation between r_0 and R (and check that r_0 has a well-defined limit as we remove the regulator), we note that the equation for curves $x(r)$ extremizing the action (4.16) is

$$\frac{d}{dr}\left(\frac{r^2\frac{dx}{dr}}{\sqrt{\frac{F(r)^2}{r^2} + r^2\left(\frac{dx}{dr}\right)^2}}\right) = 0\,.$$

In terms of the r_0, the value of r where dr/dx vanishes, we have

$$\left(\frac{dx}{dr}\right)^2 = \frac{F^2(r)}{r^4\left(\frac{r^2}{r_0^2} - 1\right)}\,. \tag{4.18}$$

Thus, we obtain

$$\begin{aligned} R &= 2\int_{r_0}^{\infty} dr \frac{F(r)}{r^2}\frac{1}{\sqrt{\frac{r^2}{r_0^2} - 1}} \\ &= 2\int_1^{\infty} dx \frac{F(r_0 x)}{r_0 x^2\sqrt{x^2-1}}. \end{aligned} \tag{4.19}$$

We can now translate the strong-subadditivity condition $c'(R) \leq 0$ to a convenient bulk expression. Starting from the relation (4.17), we have that

$$\frac{d}{dR}c(R) = \frac{dr_0}{dR}\frac{d}{dr_0}(Rr_0) = \frac{d^2S}{dR^2}\int_1^\infty dx \frac{F'(rx)}{x\sqrt{x^2-1}} \tag{4.20}$$

Strong subadditivity implies that[13]

$$\frac{dr_0}{dR} = \frac{d^2S}{dR^2} \leq 0\,, \tag{4.21}$$

so we have finally that $\frac{d}{dR}c(R) \leq 0$ is equivalent to the condition on $F(r)$ that

$$\int_{r_0}^\infty dr \frac{F'(r)}{r\sqrt{\frac{r^2}{r_0^2}-1}} \geq 0 \tag{4.22}$$

for every r_0. This result was derived originally in [97].

4.3.1 An averaged null energy condition

We will now show that the condition (4.22) can be interpreted as a particular averaged null energy condition in this geometry.

We start by considering the light sheet emanating from the curve B, pointing in the forward direction in time with light rays going towards the boundary. We can define a null vector field on B directly along this lightsheet by the conditions that $u \cdot u = 0$, $u \cdot \partial_\lambda x_B = 0$ and $u^\mu \partial_\mu r = 1$. Here, the scale factor r can be defined as $r = \sqrt{\xi \cdot \xi}$, where ξ is the Killing vector corresponding to spatial translations along the field theory direction. In our coordinates, we have

$$(u^t, u^r, u^x) = \left(\frac{F(r)}{rr_0}, -1, \pm\frac{F(r)\sqrt{r^2-r_0^2}}{r_0 r^2}\right)\,.$$

[13] To see this, apply the strong subadditivity constraint (4.1) to the case where B is an interval of length R and A and C are intervals of length δR to the left and right. Then strong subadditivity implies that $2S(R+\delta R) - S(R) - S(R+2\delta R) \geq 0$ which gives $S''(R) \leq 0$ in the limit $\delta R \to 0$. Holographically, this implies that Ryu-Takayanagi surfaces for larger intervals must penetrate deeper into the bulk.

Physically, this null vector field is normalized so that translation by the vector field produces the same (additive) change in the scale factor everywhere.

Defining $T_{\mu\nu}$ to be the stress tensor giving rise to the geometry (4.15) via Einstein's equations, we find that

$$T_{\mu\nu}u^\mu u^\nu \propto \frac{F'(r)}{rF(r)} ,$$

where we have used that the Einstein tensor in our geometry is

$$\begin{aligned} G_{rr} &= \frac{1}{r^2} \\ G_{tt} = -G_{xx} &= \frac{r^3}{F(r)^3}F'(r) - \frac{r^2}{F(r)^2} . \end{aligned}$$

From (4.15) and (4.18) the distance element along an RT curve B with minimal radial coordinate r_0 is given by

$$ds = \frac{drF(r)}{r_0\sqrt{\frac{r^2}{r_0^2}-1}}$$

It follows that the condition (4.22) is equivalent to the condition that for every RT curve B

$$\int_B T_{\mu\nu}u^\mu u^\nu ds \geq 0. \tag{4.23}$$

Thus, the positivity of Casini and Huerta's entanglement c-function is equivalent in holographic theories (at the classical level) to this averaged null-energy condition.[14] This is clearly implied by the null energy condition, but is a weaker condition, since it is possible for $T_{\mu\nu}u^\mu u^\nu \leq 0$ to be negative locally while all the integrals are positive.

We can give an alternative statement of the energy condition in terms of a globally defined null vector field $\hat{u}$, defined by replacing the condition $u\cdot\partial_\lambda x_B = 0$ with $u\cdot\xi = 0$, where ξ is the spatial Killing vector. In our coordinates, $(\hat{u}^t,\hat{u}^r,\hat{u}^x) = (F(r)/r^2,1,0)$. Physically, this null vector field is defined so that it points only in the radial and time directions, and so that translation by the vector field produces

[14]This is not equivalent to what is usually called the averaged null energy condition, which involves an average over null geodesics.

the same (additive) change in the scale factor everywhere. In terms of this null vector, the energy condition is also expressed as (4.23). In this case, the condition (4.23) may be expressed by saying that the "Radon transform"[15] of $T_{\mu\nu}\hat{u}^\mu\hat{u}^\nu$ is everywhere non-negative.

4.3.2 Non-monotonic scale factors

The coordinate choice (4.15) assumed the scale factor to be monotonic in the radial coordinate. In this section, we briefly consider the case where it is not. Here, we can choose coordinates

$$ds^2 = dr^2 + a(r)^2(-dt^2 + dx^2)\ . \tag{4.24}$$

Asymptotically, $a(r)$ must be increasing, but suppose that $a'(r) < 0$ in some interval with upper bound r_c, such that $a'(r_c) = 0$. Note that any such geometry violates the null energy condition $d^2/dr^2(ln(a)) \leq 0$ which forbids local minima of a. However, we would like to understand whether such a geometry can still satisfy the constraints coming from strong subadditivity.

It is straightforward to check that $a'(r_c) = 0$ implies that $r = r_c$ is an extremal surface, so as r_0 approaches r_c, there will be a family of extremal surfaces ending on boundary intervals whose length diverges. These extremal surfaces are restricted to the region $r \geq r_c$, so their regulated length will scale with the interval size R in the limit of large R. This is inconsistent with our assumption that the IR physics is some conformal fixed point, so it must be that beyond some R_*, these extremal surfaces are no longer minimal. Let $a_1 = lim_{R\to R_*^-} a(r_0(R))$ be the minimal value of a attained by this branch of extremal surfaces.

In the present coordinates, the equations for an extremal surface penetrating to some minimum radial value r_0 are

$$\left(\frac{dr}{dx}\right)^2 = a^2(r)\left(\frac{a^2(r)}{a^2(r_0)} - 1\right)\ .$$

Thus, we see that only when $a(r_0) = \min_{r\geq r_0} a(r)$ can an extremal surface reach

[15] Here we mean the map from a function on a space to a function on the space of geodesic curves obtained by integrating the original function over the curve.

the boundary. Otherwise, the previous equation would imply some negative value for $\left(\frac{dr}{dx}\right)^2$ at locations where $a(r) < a(r_0)$. Thus, the branch of extremal surfaces which become minimal for $R > R_*$ have r_0 greater than the value where $a(r)$ again decreases past $a(r_c)$. Let a_2 be the maximal value of a for this $R > R_*$ branch of solutions. We see that $a_2 < a_1$.

Using the result (4.17) in the previous section, we have

$$\frac{dS}{dR} = a(r_0) \qquad\qquad c(R) = Ra(r_0)$$

so we see that non-monotonic scale factors, the entanglement c-function is discontinuous, jumping from $R_* a_1$ to $R_* a_2$ at $R = R_*$. This was emphasized previously in [97].

Despite the discontinuous behavior of the RT-surfaces, the constraint from monotonicity of the c-function can still be expressed as (4.23), as we can show by repeating the calculations from the previous section in the coordinates (4.24). In this case, the constraint applies only to the extremal surfaces with minimal area.

4.4 Constraints on spacetimes dual to states of 1+1D CFTs

In this section, we place restrictions on translation and time-translation invariant spacetimes dual to states of 1+1 dimensional holographic CFTs on Minkowski space.

4.4.1 Constraints from positivity and monotonicity of relative entropy

We start by considering constraints arising from the positivity and monotonicity of relative entropy for spacelike intervals.

For our CFT state Ψ, we can choose to work in a frame of reference where the stress tensor is diagonal. We consider the density matrices ρ_I for a spacelike interval I from $(0,0)$ to (R_x, R_t). We will compare these to the density matrices $\sigma_T^{\beta,v}$ calculated from a reference state, which we take to be a boosted thermal state with temperature β and boost parameter v. For these states the relative entropy

$S(\rho_T||\sigma_T^{\beta,v})$ must be positive and increase with the size of the interval,

$$\delta_I^+ S(\rho_I||\sigma_I^{\beta,v}) \geq 0 \tag{4.25}$$

where δ_I^+ represents a deformation $(R_x, R_t) \to (R_x + \delta x, R_t + \delta t)$ that increases the proper length of the interval. Note that positivity follows from this monotonicity condition since the relative entropy is zero for a vanishing interval.

According to the result (4.14) and the discussion in that section, the optimal relative entropy constraints will be obtained by choosing the reference state parameters (β, v) such that the stress tensor of the boosted thermal state matches the stress-tensor of our state. This requires $v = 0$ and $\beta = \beta^*$ such that the energy density of the thermal state matches that of our state. From (4.14) the optimal monotonicity constraint reduces simply to

$$\delta_I^+ \left\{ S(\rho_I) - S(\sigma_I^{\beta^*}) \right\} \leq 0 \tag{4.26}$$

A general expression for the variation of the holographic entanglement entropy under a variation in the interval is given in Appendix C. The result is:

$$\delta_I^+ S = \delta x [A_0^x \gamma_0] - \delta t [A_0^t \gamma_0 \beta_0] \tag{4.27}$$

where A_x^0 and A_t^0 are the spatial and temporal scale factors at the deepest point r_0 on the extremal surface, defined for a general diagonal choice of the metric by $A_x^0 = \sqrt{g_{xx}(r_0)}$ and $A_t^0 = \sqrt{-g_{tt}(r_0)}$, and $\gamma_0 = (1-\beta_0^2)^{-\frac{1}{2}}$ with $\beta_0 = (A_t dt)/(A_x dx)$ measuring the "tilt" of the geodesic at the point r_0.

Using this result, the monotonicity constraint may be expressed as

$$\delta x \left\{ [A_0^x \gamma_0]_I - [A_0^x \gamma_0]_I^{\beta^*} \right\} - \delta t \left\{ [A_0^t \gamma_0 \beta_0]_I - [A_0^t \gamma_0 \beta_0]_I^{\beta^*} \right\} \leq 0 \tag{4.28}$$

where Δ refers to difference between our state and the reference thermal state with the same stress-tensor expectation values. Here we require $\delta x > 0$ and $|\delta t| \leq \delta x$, so the strongest constraint will either be for $\delta t = \delta x$ or $\delta t = -\delta x$. Thus, an equivalent statement is

$$\Delta[\gamma_0 (A_0^x \pm \beta_0 A_0^t)]_I \leq 0 \,, \tag{4.29}$$

where Δ refers to the result for our state minus the result for the thermal state.

Spatial constraint

It is interesting to write the our constraint more explicitly for the special case of a spatial interval. We choose coordinates for which the metric takes the form

$$ds^2 = \frac{F^2(r)}{r^2}dr^2 + r^2dx^2 - r^2G^2(r)dt^2 \,, \tag{4.30}$$

so that the radial coordinate measures the spatial scale factor. In this case, the geodesics lie on constant time slices, so $\beta_0 = 0$, $\gamma_0 = 1$, and the constraint (4.28) gives

$$r_0(R) \leq r_0^{\beta^*}(R) \,, \tag{4.31}$$

Thus, the monotonicity of relative entropy constraint for spatial intervals is equivalent to the statement that the minimum scale factor reached by an extremal surface in the geometry associated with $|\Psi\rangle$ is never less than the value in the thermal state geometry with the same $\langle T_{00}\rangle$.

Since r is a decreasing function of R according to (4.21), the condition (4.31) is equivalent to

$$R(r_0) \leq R_\beta(r_0) \,, \tag{4.32}$$

Using the coordinates (4.30) and the result (4.19), we can express this as

$$\int_1^\infty dx \frac{1}{x^2\sqrt{x^2-1}}(F(r_0x) - F_\beta(r_0x)) \leq 0 \,. \tag{4.33}$$

As we show in the next section, this constraint agrees asymptotically with the condition of positive energy $T_{00} \geq 0$.

More generally, we can show that the condition (4.33) is implied by but does not imply the constraint of positive energy. To see this, we note that $F(\infty) = F_\beta(\infty) = 1$ and that for large r, $F(r) - F_\beta(r) = ar^{-n} + O(r^{-(n+1)})$ with $n \geq 3$. In our coordinates, the positive energy constraint gives $rF'(r) - F(r) + F^3(r) \geq 0$ with equality for $F_\beta(r)$ describing the thermal state. Thus,

$$(F - F_\beta)' \geq \frac{1}{r}(F_\beta - F)(F_\beta^2 + F_\beta F + F^2 - 1) \,.$$

To leading order in large r this is $a(n-2) \leq 0$, so that $F(r) - F_\beta(r)$ must initially decrease below zero as we move in from $r = \infty$. Then since $F_\beta(r) \geq 1$, $(F(r) - F_\beta(r))' \geq 0$ and $F(r) - F_\beta(r)$ must continue to decrease as r decreases, ensuring that (4.33) holds.

Asymptotic Constraints

It is interesting to work out the implications of the relative entropy constraint (4.29) on the asymptotic geometry of the spacetime. For this purpose, we choose Fefferman-Graham coordinates

$$ds^2 = \frac{1}{z^2}(dz^2 + f(z)dx^2 - g(z)dt^2) \,. \tag{4.34}$$

To apply the constraint (4.29) we need an expression relating the parameters β_0, A_0^x, and A_0^t to the parameters (R_x, R_t) describing the boundary interval. Starting from the area functional

$$\text{Area}(\tilde{B}) = \int \frac{dz}{z} \sqrt{1 - g(z)\left(\frac{dt}{dz}\right)^2 + f(z)\left(\frac{dx}{dz}\right)^2} \,, \tag{4.35}$$

we find that the surface is extremal if

$$\begin{aligned} \frac{d}{dz}\left\{ \frac{f(z)\frac{dx}{dz}}{z\sqrt{1 - g(z)\left(\frac{dt}{dz}\right)^2 + f(z)\left(\frac{dx}{dz}\right)^2}} \right\} &= 0 \\ \frac{d}{dz}\left\{ \frac{g(z)\frac{dt}{dz}}{z\sqrt{1 - g(z)\left(\frac{dt}{dz}\right)^2 + f(z)\left(\frac{dx}{dz}\right)^2}} \right\} &= 0 \,. \end{aligned} \tag{4.36}$$

Let z_0 be the maximum value of z reached by the surface, and define as above

$$\beta_0 = \sqrt{\frac{g(z_0)}{f(z_0)}} \frac{dt}{dx}(z = z_0) \,,$$

such that $|\beta_0| < 1$ for a spacelike path. In terms of these parameters, we get

$$\begin{aligned}\left(\frac{dx}{dz}\right)^2 &= \frac{z^2 f_0}{z_0^2 f^2}\frac{1}{\left[1-\frac{z^2 f_0}{z_0^2 f}\right]-\beta_0^2\left[1-\frac{z^2 g_0}{z_0^2 g}\right]} \\ \left(\frac{dt}{dz}\right)^2 &= \beta_0^2\frac{z^2 g_0}{z_0^2 g^2}\frac{1}{\left[1-\frac{z^2 f_0}{z_0^2 f}\right]-\beta_0^2\left[1-\frac{z^2 g_0}{z_0^2 g}\right]}\end{aligned} \tag{4.37}$$

where we have defined $f_0 = f(z_0)$ and $g_0 = g(z_0)$. Using these, we obtain

$$\begin{aligned}R_x &= \int_0^{z_0} dz \frac{z\sqrt{f_0}}{z_0 f}\frac{1}{\sqrt{\left[1-\frac{z^2 f_0}{z_0^2 f}\right]-\beta_0^2\left[1-\frac{z^2 g_0}{z_0^2 g}\right]}} \\ R_t &= \int_0^{z_0} dz \frac{z\beta_0\sqrt{g_0}}{z_0 g}\frac{1}{\sqrt{\left[1-\frac{z^2 f_0}{z_0^2 f}\right]-\beta_0^2\left[1-\frac{z^2 g_0}{z_0^2 g}\right]}}\end{aligned} \tag{4.38}$$

To understand the asymptotic constraints, we can write f and g asymptotically as[16]

$$f(z) = 1 + z^2 f_2 + z^3 f_3 + z^4 f_4 + \ldots \qquad g(z) = 1 - z^2 f_2 + z^3 g_3 + z^4 g_4 + \ldots . \tag{4.39}$$

where we have used tracelessness of the CFT stress tensor to conclude that

$$[g]_{z^2} + [f]_{z^2} \propto \langle -T_{tt} + T_{xx}\rangle = 0 .$$

Defining the proper length $L = \sqrt{R_x^2 - R_t^2}$ and $v = R_t/R_x$, we can use (4.38) to express L and v as power series in z_0 with β_0-dependent coefficients. Inverting these, we can express z_0 and β_0 as power series in L with v-dependent coefficients. Finally, we can write the expression

$$\delta_I S = \gamma_0(A_0^x \pm \beta_0 A_0^t) = \frac{1}{\sqrt{1-\beta_0^2}}\left(\frac{\sqrt{f(z_0)}}{z_0} + \beta_0\frac{\sqrt{g(z_0)}}{z_0}\right)$$

[16]Note that in purely gravitational solutions, f_3 and g_3 vanish, but more generally, these could be sourced by another bulk field corresponding to an operator with sufficiently low dimension.

appearing in (4.29) as a power series in L with v-dependent coefficients. Here we have chosen the plus sign in (4.29) without loss of generality, since the constraint is invariant under a swap of the sign and $v->-v$. The monotonicity constraint implies a negative difference between this expression for general f and g and the expression with the thermal state values

$$f_{\beta^*} = 1 + f_2 z^2 + \frac{1}{4} f_2^2 z^4 \qquad\qquad g_{\beta^*} = 1 - f_2 z^2 + \frac{1}{4} f_2^2 z^4 \,.$$

Since we are working in the limit of small L, the negativity implies that the leading order nonzero terms in the power series must have a negative coefficient.

In the case where f_3 and g_3 are nonzero, the leading order term is at order L^2, and negativity of the coefficient gives:

$$v(3v-2)g_3 + (2v-3)f_3 \geq 0$$

This is required to be true for all $|v| < 1$ (corresponding to the tilt of the interval), and we find that the combination of these conditions is equivalent to

$$f_3 \leq g_3 \qquad\qquad f_3 \leq \frac{3\sqrt{5}-7}{2} g_3 \approx -0.1459 g_3 \tag{4.40}$$

In the case where f_3 and g_3 vanish, the constraint becomes the positivity of the L^3 term, which gives

$$v(2v-1)(g_4 - \frac{1}{4}f_2^2) + (v-2)(f_4 - \frac{1}{4}f_2^2) \geq 0$$

Again, this is required to be true for all $|v| < 1$, and the combination of constraints gives

$$f_4 \leq g_4 \qquad\qquad (f_4 - \frac{1}{4}f_2^2) \leq (4\sqrt{3}-7)(g_4 - \frac{1}{4}f_2^2) \approx -.07178(g_4 - \frac{1}{4}f_2^2) \tag{4.41}$$

Comparison with standard energy conditions

We can compare our results to the standard weak and null energy conditions $T_{\mu\nu}u^\mu u^\nu \geq 0$ for various timelike or null vectors u. The non-vanishing components of the stress

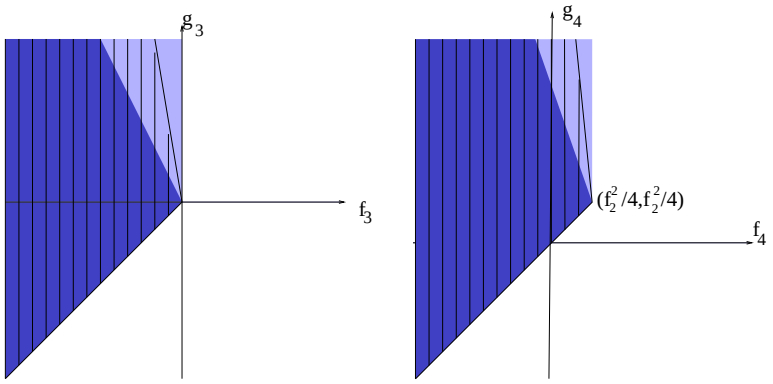

Figure 4.3: Relative entropy constraints on coefficients in the Fefferman-Graham expansion of the metric (striped region). Constraints on the right apply only if $f_3 = g_3 = 0$. Dark blue shaded region are the constraints from the null-energy condition. Full shaded region corresponds to constraints from positivity of relative entropy, equivalent to constraints from the weak energy condition for timelike vectors with no component in the radial direction.

tensor are

$$\begin{aligned} T_{zz} &= -\frac{1}{2z}\frac{g'}{g} - \frac{1}{2z}\frac{f'}{f} + \frac{1}{4}\frac{f'}{f}\frac{g'}{g} \\ T_{tt} &= \frac{g}{4z}\left(2\frac{f'}{f} + z\left(\frac{f'}{f}\right)^2 - 2z\frac{f''}{f}\right) \\ T_{xx} &= -\frac{f}{4z}\left(2\frac{g'}{g} + z\left(\frac{g'}{g}\right)^2 - 2z\frac{g''}{g}\right) \end{aligned} \tag{4.42}$$

Assuming that f_3 and g_3 are nonzero, the weak energy condition applied to timelike vectors with no radial component (i.e. the non-negativity of energy for observers moving in the field theory directions) gives

$$f_3 \leq g_3 \qquad\qquad f_3 \leq 0\,, \tag{4.43}$$

while including u^μ in the radial direction strengthens the conditions to

$$f_3 \leq g_3 \qquad\qquad f_3 \leq -\frac{1}{2}g_3\,. \tag{4.44}$$

When $f_3 = g_3 = 0$, the weak energy condition applied to timelike vectors with no radial component gives

$$f_4 \leq g_4 \qquad\qquad f_4 - \frac{1}{4} f_2^2 \leq 0 \,, \tag{4.45}$$

while the full weak/null energy condition gives

$$f_4 \leq g_4 \qquad\qquad f_4 - \frac{1}{4} f_2^2 \leq -\frac{1}{3}(g_4 - \frac{1}{4} g_2^2) \,. \tag{4.46}$$

The conditions (4.40) and (4.41) coming from monotonicity of relative entropy are intermediate between the weak/null energy condition considering only u in the field theory directions and the conditions for general u. An interesting point is that the weaker conditions (4.43) and (4.45) are exactly equivalent to the conditions obtained by positivity of relative entropy (without demanding monotonicity).

4.4.2 Constraints from strong subadditivity

We now consider the constraints arising from the strong subadditivity of entanglement entropy. For a state invariant under spacetime translations, the entanglement entropy for any spacelike interval will be a single function $S(R_x, R_t)$ where (R_x, R_t) represents the difference between the two endpoints. According to the discussion in Section 4.2, the requirements of strong subadditivity in this case are implied by the minimal set of strong subadditivity constraints (4.2). In these formulae, we have defined $R_\pm = R_x \pm R_t$. To obtain explicit expressions for these, we can evaluate the first derivatives using the result (4.27). We have

$$\partial_\pm S = \gamma_0 (A_0^x \mp \beta_0 A_0^t) \tag{4.47}$$

where A_t, A_x, β_0, and γ_0 are defined in the previous subsection. From here, we can write the constraints (4.2) explicitly by taking one more derivative. For example, we have

$$\begin{aligned} \partial_+ \partial_- S &= \frac{\partial}{\partial R_+} \left[\gamma_0 (A_0^x + \beta_0 A_0^t) \right] \\ &= \frac{\partial r_0}{\partial R_+} \frac{\partial}{\partial r_0} \left[\gamma_0 (A_0^x + \beta_0 A_0^t) \right] + \frac{\partial \beta_0}{\partial R_+} \frac{\partial}{\partial \beta_0} \left[\gamma_0 (A_0^x + \beta_0 A_0^t) \right] \end{aligned}$$

$$= \frac{1}{\Delta}\left\{-\frac{\partial R_-}{\partial \beta_0}\frac{\partial}{\partial r_0}\left[\gamma_0(A_0^x+\beta_0 A_0^t)\right]+\frac{\partial R_-}{\partial r_0}\frac{\partial}{\partial \beta_0}\left[\gamma_0(A_0^x+\beta_0 A_0^t)\right]\right\}$$

where

$$\Delta = \det\begin{pmatrix} \frac{\partial R_-}{\partial r_0} & \frac{\partial R_-}{\partial \beta_0} \\ \frac{\partial R_+}{\partial r_0} & \frac{\partial R_+}{\partial \beta_0} \end{pmatrix} .$$

The strong subadditivity constraint is then that $\partial_+\partial_- S \leq 0$. Here, the determinant Δ is positive for geometries in some neighborhood of pure AdS (and possibly more generally); in this case, the constraint simplifies to the statement that the expression in curly brackets is non-positive.

We can write an explicit expressions for R_- and R_+ using the steps leading to (4.38). We find

$$R_\pm = \int_\gamma ds \gamma_0 \left\{ \frac{A_0^x}{(A^x)^2} \pm \beta_0 \frac{A_0^t}{(A^t)^2} \right\} \tag{4.48}$$

where the integral is along the extremal surface, with length element

$$ds = \frac{dr\sqrt{g_{rr}}}{\gamma_0\sqrt{\left[1-\frac{(A^x(r_0))^2}{(A^x(r))^2}\right]-\beta_0^2\left[1-\frac{(A^t(r_0))^2}{(A^t(r))^2}\right]}} .$$

From this, the constraint $\partial_+\partial_- S \leq 0$ for each spacelike interval I can be expressed as an integral over the extremal curve γ ending on I. It is natural to expect that the result can be expressed in a covariant form similar to (4.23), but we leave this for future work.

Asymptotic constraints

Using the tools from Section 4.4.1, it is straightforward to work out the constraints on the asymptotic geometry implied by the strong subadditivity constraint $\partial_+\partial_- S \leq 0$. Note that the conditions $\partial_+\partial_+ S \leq 0$ and $\partial_-\partial_- S \leq 0$ are always satisfied asymptotically.

We work again in the Fefferman-Graham expansion (4.34) with metric functions expanded as (4.39). We can write the expression (4.47) as a power series in the proper length L of the interval, with coefficients depending on the ratio

$\beta = R_t/R_x$ and the coefficients appearing in (4.39). Acting with

$$\begin{aligned}\partial_+ &= \frac{\partial L}{\partial R_+}\partial_L + \frac{\partial v}{\partial R_+}\partial_v \\ &= \frac{1}{2}\sqrt{\frac{1-v}{1+v}}\left\{\partial_L + (1-v^2)\frac{1}{L}\partial_v\right\}\end{aligned}$$

gives a power series for $\partial_+\partial_- S$, and the strong subadditivity constraint implies that the leading non-zero coefficient must be negative.

In the case where f_3 and g_3 are nonzero, the leading order term is at order L, and negativity of the coefficient gives:

$$(2-7v^2)g_3 \leq -(7-2v^2)f_3$$

This is required to be true for all $|v| < 1$ (corresponding to the tilt of the interval), and we find that the combination of these conditions is equivalent to

$$f_3 \leq g_3 \qquad\qquad f_3 \leq -\frac{2}{7}g_3 \tag{4.49}$$

In the case where f_3 and g_3 vanish, the constraint becomes the negativity of the L^2 term, which gives

$$(1-7v^2)(g_4 - \frac{1}{4}f_2^2) \leq -(7-v^2)(f_4 - \frac{1}{4}f_2^2) \geq 0 \tag{4.50}$$

Again, this is required to be true for all $|v| < 1$, and the combination of constraints gives

$$f_4 \leq g_4 \qquad\qquad (f_4 - \frac{1}{4}f_2^2) \leq -\frac{1}{7}(g_4 - \frac{1}{4}f_2^2) \tag{4.51}$$

These constraints take a similar form to the constraints (4.40) and (4.41) from monotonicity of relative entropy, but are slightly stronger. However, they are still weaker than the constraints (4.44) and (4.46) arising from the null energy condition.

4.5 Constraints on spherically-symmetric asymptotically AdS spacetimes

In this section, we point out a simple constraint on the geometries of static, spherically symmetric asymptotically AdS_{d+2} spacetimes. This would apply for example to spherically symmetric "stars" made of any allowable type of matter in a theory of gravity whose classical limit is Einstein gravity coupled to matter.

For these spacetimes, the dual state is an excited state of the dual CFT on a sphere with a homogeneous stress tensor. If the mass of the spacetime (relative to empty AdS) is M, the field theory energy is $M\ell$ (taking the sphere radius equal to one for the CFT), so we can say that the energy density expectation value for this state relative to the vacuum state is

$$\Delta\langle T_{00}\rangle = \frac{M\ell}{\Omega_d}\,, \tag{4.52}$$

where Ω_d is the volume of a d-sphere.

Now, consider a ball-shaped region B_θ of angular radius θ_0 on the sphere. For this region, the relative entropy for our state with respect to the vacuum state is

$$\begin{aligned} S_{B_\theta}(\rho||0) &= \Delta\langle H_{mod}\rangle - \Delta S \\ &= 2\pi \int_B d\Omega_d \frac{\cos(\theta)-\cos(\theta_0)}{\sin(\theta_0)} \Delta\langle T_{00}\rangle - \Delta S \end{aligned}$$

where we have used the expression (4.7) for the modular Hamiltonian.

Since the stress tensor (4.52) is constant on the sphere, we can perform the integral explicitly to obtain

$$S_{B_\theta}(\rho||0) = -\Delta S + \frac{2\pi M\ell\Omega_{d-1}}{\Omega_d} I_d(\theta_0)$$

where

$$I_d(\theta_0) = \int_0^{\theta_0} d\theta \sin(\theta)^{d-1} \frac{\cos(\theta)-\cos(\theta_0)}{\sin(\theta_0)} = \frac{(\sin\theta_0)^{d-1}}{d}\left[1 - {}_2F_1\left(\frac{1}{2},\frac{d}{2};\frac{d}{2}+1;\sin^2\theta_0\right)\cos\theta_0\right].$$

Then, using the Ryu-Takayanagi formula, the positivity of relative entropy gives

the constraint

$$\Delta\text{Area}(\theta_0) \leq 8\sqrt{\pi} G_N M \ell I_d(\theta_0) \frac{\Gamma\left(\frac{d}{2}+\frac{1}{2}\right)}{\Gamma\left(\frac{d}{2}\right)} \, .$$

where ΔArea is the area of the bulk extremal surface with boundary δB_θ.

For the special case of a hemisphere ($\theta_0 = \pi/2$), we have that

$$\Delta\text{Area}(\pi/2) \leq 8\sqrt{\pi} G_N M \ell \frac{\Gamma\left(\frac{d}{2}+\frac{1}{2}\right)}{d\Gamma\left(\frac{d}{2}\right)} \, .$$

which reduces for 3+1 dimensional gravity to

$$\Delta A \leq 2\pi G_N M \ell_{AdS} \, .$$

Typically, the minimal area extremal surface bounded by an equator on the sphere will be the surface bisecting the spacetime symmetrically, so this constraint bounds the change in area for this bisecting surface by the mass contained in the spacetime.[17] Roughly, the constraint places a bound on how much a certain amount of total energy in the spacetime can curve the spacetime.

4.6 Discussion

In this paper, we have explored constraints from entanglement inequalities on highly symmetric spacetimes. It will be interesting to see how these results generalize to less symmetric cases. In our analysis, we have used only the classical term in the Ryu-Takayanagi formula, so our constraints apply to gravitational theories in the classical limit. It would be interesting to understand how the constraints are corrected when the contribution of bulk quantum fields are taken into account. This should be possible using the quantum-corrected holographic entanglement entropy formula proposed by [28].

[17] In some cases, however, there may exist more than one extremal surface bounded by an equator, and in this case, the minimal area surface may not be the symmetrical one.

4.6.1 Constraints on entanglement structure from geometry

Before concluding, we offer a few remarks on the orthogonal research direction of understanding which entanglement structures are consistent with the existence of a geometrical dual spacetime. In the language of Figure 4.1, we would like to precisely characterize the image of $\mathscr{G}$ in $\mathscr{S}$ (or in ($\mathscr{S}_{phys}$). Here, we make a few qualitative observations that hopefully illuminate how severe these constraints are.

Consider a general asymptotically AdS_{d+2} spacetime. In a Fefferman-Graham description of the metric,

$$ds^2 = \frac{1}{z^2}\left[dz^2 + \Gamma_{\mu\nu}(z,x)dx^\mu dx^\nu\right]$$

the information about the geometry is contained in the functions $\Gamma_{\mu\nu}(z,x)$ of $(d+1)$ variables.

A set of entanglement entropies that includes a similar amount of information as one of these functions is the set $\{S(R,x)\}$ for ball-shaped regions with any radius R centered at any point x. At least close to the boundary (where the geometry is similar to AdS), we expect that there is a one-to-one correspondence between pairs (R,x) and bulk points (z,x_{bulk}), obtained by choosing the point on the RT surface with the largest value of z. For pure AdS, we have simply $(z,x_{bulk}) = (R,x)$. Thus, given the entanglement entropies for ball-shaped regions in one spatial slice, it is plausible that we can reconstruct some combination of the metric functions $\Gamma_{\mu\nu}(z,x)$. The other combinations are related by Lorentz-transformations, so it is further plausible that we can reconstruct the remaining functions (in some neighborhood of the boundary) by considering entanglement entropies for ball-shaped regions in other Lorentz frames.

Assuming this reconstruction is possible, we now have enough information (the full geometry in a neighborhood of the boundary) to calculate entanglement entropies for regions of any other shape. Thus, it is plausible that *for a quantum state with gravity dual, the entanglement entropies for regions of arbitrary shape (assuming they are not too large) are completely determined from the entanglement entropies for ball-shaped regions* (in the various frames of reference). Furthermore, they are determined in a very specific way, via construction of a dual geometry and calculation of extremal surface areas. A natural question is then to

understand which field theory Hamiltonians can give rise to low-energy states with this entanglement structure, and/or why the known examples of holographic CFTs have this property.

Chapter 5

Entanglement Entropy of Holographic States in Terms of One-point Functions

5.1 Introduction

In holographic conformal field theories, states with a simple classical gravity dual interpretation have a remarkable structure of entanglement: according to the holographic entanglement entropy formula [6, 7, 9], their entanglement entropies for arbitrary regions (at leading order in large N) are completely encoded in the extremal surface areas of an asymptotically AdS spacetime. In general, the space of possible entanglement entropies (functions on a space of subsets of the AdS boundary) is far larger than the space of possible asymptotically AdS metrics (functions of a few spacetime coordinates), so this property of geometrically-encodable entanglement entropy should be present in only a tiny fraction of all quantum field theory states [35]. It is an interesting question to understand better which CFT states have this property[1], and which properties of a CFT will guarantee that fami-

[1] Even in holographic CFTs, it is clear that not all states will have this property. For example, if $|\Psi_1\rangle$ and $|\Psi_2\rangle$ are two such states, corresponding to different spacetimes M_{Ψ_1} and M_{Ψ_2}, the superposition $|\Psi_1\rangle + |\Psi_2\rangle$ is not expected to correspond to any single classical spacetime but rather to a superposition of M_{Ψ_1} and M_{Ψ_2}. Thus, the set of "holographic states" is not a subspace, but some

lies of low-energy states with geometric entanglement exist.

For a hint towards characterizing these holographic states, consider the gravity perspective. A spacetime M_Ψ dual to a holographic state $|\Psi\rangle$ is a solution to the bulk equations of motion. Such a solution can be characterized by a set of initial data on a bulk Cauchy surface (and appropriate boundary conditions at the AdS boundary). The solution away from the Cauchy surface is determined by evolving this initial data forwards (or backwards) in time using the bulk equations. Alternatively, we can think of the bulk solution as being determined by evolution in the holographic radial direction, with "initial data" specified at the timelike boundary of AdS. In this case, the existence and uniqueness of a solution is more subtle, but the asymptotic behavior of the fields determines the metric at least in a perturbative sense (e.g. perturbatively in deviations from pure AdS, or order-by-order in the Fefferman-Graham expansion). It is plausible that in many cases, this boundary data is enough to determine a solution nonperturbatively to some finite distance into the bulk, or even for the whole spacetime. Thus, for geometries dual to holographic states, we can say that the bulk spacetime (at least in a perturbative sense) is encoded in the boundary behavior of the various fields.

According to the AdS/CFT dictionary, this boundary behavior is determined by the one-point functions of low-dimension local operators associated with the light bulk fields. On the other hand, the bulk spacetime itself allows us to calculated entanglement entropies (and many other non-local quantities). Thus, the assumption that a state is holographic allows us (via gravity calculations) to determine the entanglement entropies and other non-local properties of the state (again, at least perturbatively) from the local data provided by the one-point functions:

$$|\Psi\rangle \to \langle \mathcal{O}_\alpha(x^\mu)\rangle \to \phi_\alpha \text{ asymptotics} \to \phi_\alpha(x^\mu, z) \to \text{entanglement entropies } S(A) \tag{5.1}$$

where ϕ here indicates all light fields including the metric.[2]

The recipe (5.1) could be applied to any state, but for states that are not holographic, the results will be inconsistent with the actual CFT answers. Thus, we

general subset.

[2]Here, the region A should be small enough so that the bulk extremal surface associated with A should be contained in the part of the spacetime determined through the equations of motion by the boundary values; we do not need this restriction if we are working perturbatively.

have a stringent test for whether a CFT state has a dual description well-described by a classical spacetime: carry out the procedure in (5.1) and compare the results with a direct CFT calculation of the entanglement entropies; if there is a mismatch for any region, the state is not holographic.[3]

In this paper, our goal is to present some more explicit results for the gravity prediction $S_A^{grav}(\langle \mathcal{O}_\alpha \rangle)$ in cases where the gravitational equations are Einstein gravity with matter and the region is taken to be a ball-shaped region B. We will work perturbatively around the vacuum state to obtain an expression as a power series in the one-point functions of CFT operators. At first-order, the result depends only on the CFT stress tensor expectation value [102]:

$$S_B(|\Psi\rangle) = S_B^{vac} + 2\pi \int_B d^{d-1}x \frac{R^2 - r^2}{2R} \langle T_{00} \rangle + \mathcal{O}(\langle \mathcal{O}_\alpha \rangle^2) \,. \tag{5.2}$$

This well-known expression is universal for all CFTs since it follows from the first law of entanglement $\delta^{(1)} S_B = \delta \langle H_B \rangle$, where

$$H_B \equiv -\log \rho_B^{vac} = 2\pi \int_B d^{d-1}x \frac{R^2 - r^2}{2R} T_{00} \tag{5.3}$$

is the vacuum modular Hamiltonian for a ball-shaped region. Thus, to first-order, the gravity procedure (5.1) always gives the correct CFT result for ball-shaped regions, regardless of whether the state is holographic.

General second-order result for ball entanglement entropy

Our focus will be on the second-order answer; in this case, it is less clear whether the gravity results from (5.1) should hold for any CFT or whether they represent a constraint from holography. To obtain explicit formulae at this order, we begin by writing

$$S_B(|\Psi\rangle) = S_B^{vac} + \Delta \langle H_B \rangle - S(\rho_B || \rho_B^{vac}) \tag{5.4}$$

which follows immediately from the definition of relative entropy $S(\rho_B || \rho_B^{vac})$ reviewed in Section 5.2 below. We then make use of a recent result in [105]: to

[3] Another interesting possibility is that the one-point functions could give boundary data that is not consistent with any solution of the classical bulk equations; this possibility exists since the "initial data" for the radial evolution problem obeys certain constraints.

second-order in perturbations from the vacuum state, the relative entropy for a ball-shaped region in a holographic state[4] is equal to the "canonical energy" associated with a corresponding wedge of the bulk spacetime. We provide a brief review of this in Section 5.2 below. On shell, the latter quantity can be expressed as a quadratic form on the space of first-order perturbations to pure AdS spacetime, so we have

$$S(\rho_B||\rho_B^{vac}) = \Delta\langle H_B\rangle - \Delta S_B = \frac{1}{2}\mathscr{E}(\delta\phi_\alpha, \delta\phi_\alpha) + \mathscr{O}(\delta\phi^3)\,. \tag{5.5}$$

Rearranging this, we have a second-order version of (5.2):

$$\begin{aligned} S_B(|\Psi\rangle) &= S_B^{vac} + \delta^{(1)}S_B + \delta^{(2)}S_B + \mathscr{O}(\delta\phi^3) \\ &= S_B^{vac} + \Delta\langle H_B\rangle - \frac{1}{2}\mathscr{E}(\delta\phi_\alpha, \delta\phi_\alpha) + \mathscr{O}(\delta\phi^3) \\ &= S_B^{vac} + 2\pi\int_B d^{d-1}x \frac{R^2 - r^2}{2R}\langle T_{00}\rangle - \frac{1}{2}\mathscr{E}(\delta\phi_\alpha, \delta\phi_\alpha) + \mathscr{O}(\delta\phi^3)\,. \end{aligned} \tag{5.6}$$

As we review in Section 5.2 below, the last term can be written more explicitly as

$$\mathscr{E}(\delta\phi_\alpha, \delta\phi_\alpha) = \int_\Sigma \omega(\delta g, \pounds_\xi \delta g) - \int_\Sigma \xi^a T^{(2)}_{ab}\varepsilon^b\,, \tag{5.7}$$

where Σ is a bulk spatial region between B and the bulk extremal surface $\tilde{B}$ with the same boundary, ω is the "presymplectic form" whose integral defines the symplectic form on gravitational phase space, $T^{(2)}_{ab}$ is the matter stress tensor at second-order in the bulk matter fields, and ξ is a bulk Killing vector which vanishes on $\tilde{B}$. The first-order bulk perturbations $\delta\phi_\alpha$ (including the metric perturbation) may be expressed in terms of the boundary one-point functions via bulk-to-boundary propagators

$$\delta\phi_\alpha(x,z) = \int_{D_B} K_\alpha(x,z;x')\langle\mathscr{O}_\alpha(x')\rangle\,, \tag{5.8}$$

where D_B is the domain of dependence of the ball B. Given the one-point functions within D_B, we can use (5.8) to determine the linearized bulk perturbation in Σ and evaluate (5.7).

The expression (5.6), (5.7), and (5.8) together provide a formal result for the

[4]This second-order relative entropy is known as quantum Fisher information.

ball entanglement entropy of a holographic state, expanded to second-order in the boundary one-point functions.

Explicit results for 1+1 dimensional CFTs

In order to check the general formula and provide more explicit results, we focus in Section 5.3 on the case of 1+1 dimensional CFTs, carrying out an explicit calculation of the gravitational contributions to (5.7) starting from a general boundary stress tensor. We find the result

$$\delta^{(2)} S_B^{grav} = -\frac{1}{2}\int_{B'} dx_1^+ \int_{B'} dx_2^+ \, K_2(x_1^+, x_2^+)\langle T_{++}(x_1^+)\rangle\langle T_{++}(x_2^+)\rangle + \{+ \leftrightarrow -\} \tag{5.9}$$

where the integrals can be taken over any spatial surface B' with boundary ∂B, and the kernel is given by

$$K_2(x_1,x_2) = \frac{6\pi^2}{cR^2}\begin{cases} (R-x_1)^2(R+x_2)^2 & x_1 \geq x_2 \\ (R+x_1)^2(R-x_2)^2 & x_1 < x_2 \end{cases}, \tag{5.10}$$

where c is the central charge. In this special case, the conservation equations determine the stress tensor expectation values throughout the region D_B from the expectation values on B', so as in the first-order result (5.2), our final expression involves integrals only over B'. This will not be the case for the terms involving matter fields, or in higher dimensions. As a consistency check, we show that the expression (5.10) is always negative, as required by its interpretation as the second-order contribution to relative entropy.

We can also check the formula (5.10) via a direct CFT calculation by considering states that are obtained from the CFT vacuum by a local conformal transformation. In two dimensions, states with an arbitrary traceless conserved stress-tensor can be obtained, and the entanglement entropy for these states can also be calculated explicitly. We carry out this calculation in Section 5.4, and show that the result (5.10) is exactly reproduced.

In Section 5.3.2, we consider the matter terms in (5.7) providing some explicit results for the quadratic contributions of scalar operator expectation values. Here,

as in the generic case, the result takes the form

$$\delta^{(2)} S_B^{matter} = -\frac{1}{2}\int_{D_B}\int_{D_B} G_{\alpha\beta}(x,x')\langle \mathscr{O}_\alpha(x)\rangle\langle \mathscr{O}_\beta(x')\rangle \tag{5.11}$$

with integrals over the entire domain of dependence region.

Auxiliary de Sitter Space Interpretation

Recently, in [43] it has been pointed out that the first-order result $\delta^{(1)}S(x^\mu, R)$ for the entanglement entropy of a ball with radius R and center x^μ can be obtained as the solution to the equation of motion for a free scalar field on an auxiliary de Sitter space $ds^2 = \frac{L_{dS}^2}{R^2}(-dR^2 + dx_\mu dx^\mu)$ with the CFT energy density $\langle T_{00}(x^\mu)\rangle$ acting as a source term at $R = 0$. In Section 5.5, we show that in the 1+1 dimensional case, the stress tensor term (5.10) for the entanglement entropy at second-order can also results from solving a scalar field equation on the auxiliary de Sitter space if we add a simple cubic interaction term. In an upcoming paper [106], it is shown that this agreement extends to all orders for a suitable choice of the scalar field potential. The resulting nonlinear wave equation also reproduces the second-order entanglement entropy near a thermal state in the auxiliary kinematic space recently described in [107].

Including the contributions from matter fields or moving to higher dimensions, the expression for entanglement entropy involves one-point functions on the entire causal diamond D_B, so reproducing these results via some local differential equation will require a more complicated auxiliary space that takes into account the time directions in the CFT. This direction is pursued further in [108, 106].

Discussion

While the explicit two-dimensional stress tensor contribution (5.10) can be obtained by a direct CFT calculation for a special class of states, we emphasize that in general the holographic predictions from (5.1) are expected to hold only for holographic states in CFTs with gravity duals. It would be interesting to understand better whether all of the second order contributions we considered here are universal for all CFTs or whether they represent genuine constraints/predictions

from holography.[5] In the latter case, and for the results at higher order in perturbation theory, it is an interesting question to understand better which CFT states and/or which CFT properties are required to reproduce the results through direct CFT calculations. This should help us understand better which theories and which states in these theories are holographic.

5.2 Background

Our holographic calculation of entanglement entropy to second-order in the boundary one-point functions makes use of the direct connection between CFT quantum Fisher information and canonical energy on the gravity side, pointed out recently in [105]. We begin with a brief review of these results.

5.2.1 Relative entropy and quantum Fisher information

Our focus will be on ball-shaped subsystems B of the CFT$_d$, for which the the vacuum density matrix is known explicitly through (5.3). More generally, we can write it as

$$\rho_B^{vac} = e^{-H_B}\,, \qquad\qquad H_B = \int_{B'} \zeta_B^\mu T_{\mu\nu}\varepsilon^\nu\,, \tag{5.12}$$

where $T_{\mu\nu}$ is the CFT stress tensor operator and ε is defined as

$$\varepsilon_\nu = \frac{1}{(d-1)!}\varepsilon_{\nu\nu_1\cdots\nu_{d-1}}dx^{\nu_1}\wedge\cdots\wedge dx^{\nu_{d-1}}\,, \tag{5.13}$$

so that $n^\mu\varepsilon_\mu$ is the volume form on the surface perpendicular to a unit vector n^μ, and ζ_B is a conformal Killing vector defined in the domain of dependence region D_B, with $\zeta_B = 0$ on ∂B. For the ball B with radius R and center x_0^μ in the $t = t_0$ slice, we have

$$\zeta_B = -\frac{2\pi}{R}(t-t_0)(x^i - x_0^i)\partial_i + \frac{\pi}{R}[R^2 - (t-t_0)^2 - (\vec{x}-\vec{x_0})^2]\,\partial_t\,. \tag{5.14}$$

[5] There is evidence in [109, 110, 111] that at least some of the contributions at this order can be reproduced by CFT calculations in general dimensions, since they arise from CFT two and three-point functions, though the results there most directly apply to the case where the perturbation is to the theory rather than the state.

By the conservation of the current $\zeta_B^\mu T_\mu{}^\nu$ associated with this conformal Killing vector, the integral in (5.12) can be taken over any spatial surface B' in D_B with the same boundary as B.

For excited states, the density matrix ρ_B will generally be different than ρ_B^{vac}. One measure of this difference is the relative entropy

$$\begin{aligned} S(\rho_B||\rho_B^{vac}) &= \mathrm{tr}(\rho_B \log \rho_B) - \mathrm{tr}(\rho_B \log \rho_B^{vac}) \\ &= \Delta\langle H_B\rangle - \Delta S_B\,, \end{aligned} \tag{5.15}$$

where H_B is the vacuum modular Hamiltonian given in (5.12), $S_B = -\mathrm{tr}(\rho_B \log \rho_B)$ is the entanglement entropy for the region B and Δ indicates the difference with the vacuum state.

For a one-parameter family of states near the vacuum, we can expand ρ_B as

$$\rho_B(\lambda) = \rho_B^{vac} + \lambda\ \delta\rho_1 + \lambda^2 \delta\rho_2 + \mathscr{O}(\lambda^3)\,. \tag{5.16}$$

The first-order contribution to relative entropy vanishes (this is the first law of entanglement $\delta^{(1)} S_B = \delta\langle H_B\rangle$) so the leading contribution to relative entropy appears at second-order in λ. This quadratic in $\delta\rho_1$ with no contribution from $\delta\rho_2$,

$$S(\rho_B(\lambda)||\rho_B^{vac}) = \lambda^2\, \langle \delta\rho_1, \delta\rho_1\rangle_{\rho_B^{vac}} + \mathscr{O}(\lambda^3)\,, \tag{5.17}$$

where

$$\langle \delta\rho, \delta\rho\rangle_\sigma \equiv \frac{1}{2}\,\mathrm{tr}\left(\delta\rho \frac{d}{d\lambda}\log(\sigma + \lambda\,\delta\rho)\Big|_{\lambda=0}\right)\,. \tag{5.18}$$

This quadratic form, which is positive by virtue of the positivity of relative entropy, defines a positive-(semi)definite metric on the space of perturbations to a general density matrix σ. This is known as the quantum Fisher information metric.

Rearranging (5.15) and making use of (5.17), we have

$$S_B = S_B^{vac} + \int_{B'} \zeta_B^\mu \langle T_{\mu\nu}\rangle \varepsilon^\nu - \lambda^2 \langle \delta\rho_1, \delta\rho_1\rangle_{\rho_B^{vac}} + \mathscr{O}(\lambda^3)\,. \tag{5.19}$$

This general expression is valid for any CFT, but the $\mathscr{O}(\lambda^2)$ term generally has no simple expression in terms of local operator expectation values. However, for

holographic states we can convert this term into an expression quadratic in the CFT one-point functions by using the connection between quantum Fisher information and canonical energy.

5.2.2 Canonical energy

Consider now a holographic state, which by definition is associated with some dual asymptotically AdS spacetime M. Near the boundary, we can describe M using a metric in Fefferman-Graham coordinates as

$$ds^2 = \frac{\ell_{AdS}^2}{z^2}\left(dz^2 + dx_\mu dx^\mu + z^d\,\Gamma_{\mu\nu}(x,z)dx^\mu dx^\nu\right) \tag{5.20}$$

where $\Gamma_{\mu\nu}(z,x)$ has a finite limit as $z\to 0$ and $\Gamma = 0$ for pure AdS.

The relative entropy $S(\rho_B||\rho_B^{vac})$ can be computed at leading order in large N by making use of the holographic entanglement entropy formula, which relates the entanglement entropy for a region A to the area of the minimal-area extremal surface $\tilde{A}$ in M with boundary ∂A,

$$S_A \equiv \frac{\text{Area}(\tilde{A})}{4G_N}\,. \tag{5.21}$$

This yields immediately that $\Delta S_A = (\text{Area}(\tilde{A})_M - \text{Area}(\tilde{A})_{AdS})/(4G_N)$. The result (5.21) also allows us to relate the $\Delta\langle H_B\rangle$ term in relative entropy to a gravitational quantity, since it implies that the expectation value of the CFT stress tensor is related to the asymptotic behaviour of the metric through [37]

$$\langle T_{\mu\nu}\rangle = \frac{d\,\ell_{AdS}^{d-1}}{16\pi G_N}\Gamma_{\mu\nu}(x,z=0)\,. \tag{5.22}$$

Thus, for holographic states, we can write

$$S(\rho_B||\rho_B^{vac}) = \frac{d\,\ell_{AdS}^{d-1}}{16\pi G_N}\int_B \zeta_B^\mu \Gamma_{\mu\nu}(x,0)\,\varepsilon^\nu - \frac{\text{Area}(\tilde{A})_M - \text{Area}(\tilde{A})_{AdS}}{4G_N}\,. \tag{5.23}$$

For a one-parameter family of holographic states $|\Psi(\lambda)\rangle$ near the CFT vacuum, the dual spacetimes $M(\lambda)$ can be described via a metric and matter fields $\phi_\alpha =$

(g, ϕ^{matter}) with some perturbative expansion

$$g = g_{AdS} + \lambda \delta g_1 + \lambda^2 \delta g_2 + \mathcal{O}(\lambda^3) \,,$$
$$\phi^{matter} = \lambda \delta \phi_1^{matter} + \lambda^2 \delta \phi_2^{matter} + \mathcal{O}(\lambda^3) \,. \tag{5.24}$$

By the result (5.19) from the previous section, the second-order contribution to entanglement entropy is equal to the leading order contribution to relative entropy. This is related to a gravitational quantity via (5.23). The main result in [105] is that this second-order quantity can be expressed directly as a bulk integral over the spatial region Σ between B and $\tilde{B}$ where the integrand is a quadratic form on the linearized bulk perturbations δg_1 and $\delta \phi_1^{matter}$.

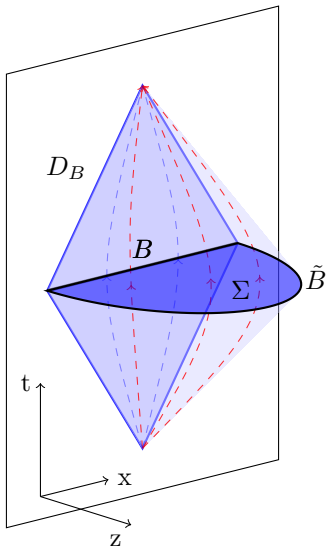

Figure 5.1: The Rindler wedge R_B associated to the ball-shaped region B on the boundary. The blue lines indicate the flow of ζ_B, and the red lines ξ_B. The surface Σ lies between B and the extremal surface $\tilde{B}$.

To describe the general result, consider the region Σ between B and $\tilde{B}$ in pure AdS spacetime, and define R_B as the domain of dependence of this region, as shown in Figure 5.1. Alternatively, R_B is the intersection of the causal past and the causal future of D_B; it can be thought of as a Rindler wedge of AdS associated with B. On R_B, there exists a Killing vector which vanishes at $\tilde{B}$ and approaches the conformal

Killing vector ζ_B at the boundary. In Fefferman-Graham coordinates, this is

$$\xi_B = -\frac{2\pi}{R}(t-t_0)[z\partial_z + (x^i - x_0^i)\partial_i] + \frac{\pi}{R}[R^2 - z^2 - (t-t_0)^2 - (\vec{x}-\vec{x_0})^2]\,\partial_t \quad (5.25)$$

The vector ξ_B is timelike hence defines a notion of time evolution within the region R_B; the "Rindler time" associated with this Rindler wedge.

The "canonical energy", dual to relative entropy at second-order, can be understood as the perturbative energy associated with this time, as explained in [112]. This is quadratic in the perturbative bulk fields including the graviton, and given explicitly by

$$\begin{aligned}
\mathscr{E}(\delta g_1, \delta\phi_1) &= W_\Sigma\left(\delta\phi_1, \pounds_{\xi_B}\delta\phi_1\right) \\
&= \int_\Sigma \omega^{full}\left(\delta\phi_1, \pounds_{\xi_B}\delta\phi_1\right) \\
&= \int_\Sigma \omega\left(\delta g_1, \pounds_{\xi_B}\delta g_1\right) + \int_\Sigma \omega^{matter}\left(\delta\phi_1, \pounds_{\xi_B}\delta\phi_1\right) \\
&= \int_\Sigma \omega(\delta g_1, \pounds_{\xi_B}\delta g_1) - \int_\Sigma \xi_B^a T^{(2)}_{ab}\varepsilon^b\,. \qquad (5.26)
\end{aligned}$$

In the first line, W_Σ is the symplectic form associated with the phase space of gravitational solutions on Σ, and $\pounds_{\xi_B}\delta\phi_1$ is the Lie derivative with respect to ξ on $\delta\phi_1$, the first-order perturbation in metric and matter fields. The symplectic form is equal to the integral over Σ of a "presymplectic" form ω^{full} which splits into a gravitational part and a matter part as in the third line. The matter part can be written explicitly in terms of $T^{(2)}_{ab}$, the matter stress tensor at quadratic order in the fields, while the gravitational part ω is given explicitly by

$$\begin{aligned}
\omega(\gamma^1, \gamma^2) &= \frac{1}{16\pi G_N}\varepsilon_a P^{abcdef}(\gamma^2_{bc}\nabla_d\gamma^1_{ef} - \gamma^1_{bc}\nabla_d\gamma^2_{ef}) \qquad (5.27) \\
P^{abcdef} &= g^{ae}g^{fb}g^{cd} - \frac{1}{2}g^{ad}g^{be}g^{fc} - \frac{1}{2}g^{ab}g^{cd}g^{ef} - \frac{1}{2}g^{bc}g^{ae}g^{fd} + \frac{1}{2}g^{bc}g^{ad}g^{ef}\,.
\end{aligned}$$

In deriving (5.26) it has been assumed that the metric perturbation has been expressed in a gauge for which the coordinate location of the extremal surface $\tilde{B}$ does not change (so that ξ_B continues to vanish there), and the vector ξ_B continues to

satisfy the Killing equation at $\tilde{B}$. Thus, we require that

$$\xi_B|_{\tilde{B}(\lambda)} = 0, \tag{5.28}$$

$$\pounds_{\xi_B} g(\lambda)|_{\tilde{B}(\lambda)} = 0. \tag{5.29}$$

As shown in [112], it is always possible to satisfy these conditions; we will see an explicit example below.

5.3 Second-order contribution to entanglement entropy

Using the result (5.7), we can now write down a general expression for the ball entanglement entropy of a general holographic state up to second-order in perturbations to the vacuum state, in terms of the CFT one-point functions. According to (5.19) and (5.26), the second-order term in the entanglement entropy for a ball B can be expressed as an integral over the bulk spatial region Σ between B and the corresponding extremal surface $\tilde{B}$, where the integrand is quadratic in first-order bulk perturbations.

These linearized perturbations are determined by the boundary behavior of the fields via the linearized bulk equations. In general, to determine the linearized perturbations in the region Σ (or more generally in the Rindler wedge R_B), we only need to know the boundary behavior in the domain of dependence region D_B, as discussed in detail in [113]. The relevant boundary behaviour of each bulk field is captured by the one-point function of the corresponding operator. We can express the results as

$$(\delta\phi_1)_\alpha(x,z)|_\Sigma = \int_{D_B} d^d x' K_\alpha(x,z;x')\langle \mathcal{O}_\alpha(x')\rangle_{CFT} \tag{5.30}$$

where $K_\alpha(x,z;x')$ is the relevant bulk-to-boundary propagator. As discussed in [114, 113, 70], K_α should generally be understood as a distribution to be integrated against consistent CFT one-point functions, rather than a function. Since the expression (5.30) is linear in the CFT expectation values, the result (5.7) is quadratic in these one-point functions and represents our desired second-order result.

To summarize, for a holographic state, the second-order contribution to entanglement entropy in the expansion (5.19) is the leading order contribution to the

relative entropy $S(\rho_B||\rho_B^{vac})$. This is dual to canonical energy, given explicitly by:

$$\delta^{(2)}S_B = -\langle\delta\rho_1,\delta\rho_1\rangle_{\rho_B^{vac}} = -\frac{1}{2}\mathscr{E}(\delta\phi_1,\delta\phi_1) = -\frac{1}{2}\int_\Sigma \omega(\delta g_1, \pounds_{\xi_B}\delta g_1) + \frac{1}{2}\int_\Sigma \xi_B^a T_{ab}^{(2)}\varepsilon^b \,. \tag{5.31}$$

This is quadratic in the linearized perturbations $\delta\phi_\alpha$ (including the metric perturbation, and these can be expressed in terms of the CFT one-point functions on D_B as (5.30).

5.3.1 Example: CFT_2 stress tensor contribution

In this section, as a sample application of the general formula, we provide an explicit calculation of the quadratic stress tensor contribution to the entanglement entropy for holographic states in two-dimensional conformal field theories. This arises from the first term in (5.7).

For a general CFT state, the stress tensor is traceless and conserved,

$$\langle T^\mu{}_\mu\rangle = \langle\partial_\mu T^{\mu\nu}\rangle = 0\,. \tag{5.32}$$

In two dimensions, these constraints can be expressed most simply using light-cone coordinates $x^\pm = x \pm t$, where we have

$$\langle T_{+-}\rangle = \partial_+\langle T_{--}\rangle = \partial_-\langle T_{++}\rangle = 0\,. \tag{5.33}$$

Thus, a general CFT stress tensor can be described by the two functions, $\langle T_{++}(x^+)\rangle$ and $\langle T_{--}(x^-)\rangle$.

Assuming that the state is holographic, there will be some dual geometry of the form (5.20). According to (5.22), the stress tensor expectation values determine the asymptotic form of the metric as

$$\Gamma_{++}(x,0) = 8\pi\frac{G_N}{\ell_{AdS}}\langle T_{++}(x^+)\rangle \qquad \Gamma_{--}(x,0) = 8\pi\frac{G_N}{\ell_{AdS}}\langle T_{--}(x^-)\rangle \tag{5.34}$$

Now, suppose that our state represents a small perturbation to the CFT vacuum, so that the stress tensor expectation values and the asymptotic metric perturbations

are governed by a small parameter λ:

$$\Gamma_{++}(x,0) \equiv \lambda h_+(x^+) \qquad \Gamma_{--}(x,0) \equiv \lambda h_-(x^-) \,. \tag{5.35}$$

Then the metric perturbation throughout the spacetime is determined by this asymptotic behavior by the Einstein equations linearized about AdS. Here, we need only the components in the field theory directions, which give

$$\frac{1}{z^3}\partial_z(z^3\partial_z\Gamma_{\mu\nu}) + \partial_\rho\partial^\rho\Gamma_{\mu\nu} = 0 \,. \tag{5.36}$$

The solution in our Fefferman-Graham coordinates with boundary behaviour (5.35) is

$$\Gamma^{(1)}_{++}(x,z) = \lambda h_+(x^+) \qquad \Gamma^{(1)}_{--}(x,z) = \lambda h_-(x^-) \tag{5.37}$$

with the linearized perturbation $\Gamma^{(1)}_{\mu\nu}$ independent of z.

Satisfying the gauge conditions

We would now like to evaluate the metric contribution to (5.7)

$$\delta^{(2)}S_B^{grav} = -\frac{1}{2}\int_\Sigma \omega^{grav}(\delta g_1, \pounds_{\xi_B}\delta g_1) \,. \tag{5.38}$$

This formula assumes the gauge conditions (5.28) which differ from the Fefferman-Graham gauge conditions we have been using so far. Thus, we must find a gauge transformation to bring our metric perturbation to the appropriate form. In general, we can write

$$\gamma_{ab} = h_{ab} + (\pounds_V g)_{ab} = h_{ab} + \nabla_a V_b + \nabla_b V_a \,. \tag{5.39}$$

where γ is the desired metric perturbation satisfying the gauge condition, and h is the perturbation in Fefferman-Graham coordinates (equivalent to Γ for $d = 2$).

The procedure for finding an appropriate V and evaluating (5.38) is described in detail in [105], but we review the main points here. Defining coordinates (X^A, X^i) so that the extremal surface lies at some fixed value of X^A with X^i describing coordinates along the surface, the gauge condition (5.28) (equivalent to requiring that

the coordinate location of the extremal surface remains fixed) gives

$$(\nabla_i \nabla^i V_A + [\nabla_i, \nabla_A] V^i + \nabla_i h^i_A - \frac{1}{2} \nabla_A h^i{}_i)|_{\tilde{B}} = 0 \tag{5.40}$$

while the condition (5.29) that ξ_B continues to satisfy the Killing equation at $\tilde{B}$ gives

$$(h_{iA} + \nabla_i V_A + \nabla_A V_i)\,|_{\tilde{B}} = 0\,, \tag{5.41}$$

$$\left(h^A_D - \frac{1}{2} \delta^A_D h^C_C + \nabla^A V_D + \nabla_D V^A - \delta^D_D \nabla_C V^C_C \right) \Big|_{\tilde{B}} = 0\,. \tag{5.42}$$

To solve these, we first expand our general metric perturbation in a Fourier basis.

$$h_{\mu\nu}(t,x,z) = \lambda \int \left[\delta^+_\mu \delta^+_\nu \hat{h}_+(k) e^{ikx^+} + \delta^-_\mu \delta^-_\nu \hat{h}_-(k) e^{ikx^-} \right] dk\,, \tag{5.43}$$

with a gauge choice $h_{za}(t,x,z) = 0$.

For each of the basis elements, we use the equations (5.40), (5.41) and (5.42) to determine V and its first derivatives at the surface V. For these calculations, it is useful to define polar coordinates $(z,x) = (r\cos\theta, r\sin\theta)$. Since the gauge conditions are linear in V, the conditions on V for a general perturbation are obtained from these by taking linear combinations as in (5.43),

$$V_a(t,x,z) = \lambda \int \left[\hat{V}^+_a(k) e^{ikx^+} + \hat{V}^-_a(k) e^{ikx^-} \right] dk\,. \tag{5.44}$$

After requiring V_a remain finite at $\theta = \pm\frac{\pi}{2}$, we find

$$\begin{aligned}
\hat{V}_t^-(k;t,r,\theta) &= \frac{e^{-ikt}}{k^3 r^2 \cos^2\theta}\left(-i\cos(kr) + \sin\theta\sin(kr) - i\frac{(k^2r^2\cos^2\theta - 1)e^{ikr\sin\theta}}{2}\right) \\
\hat{V}_r^-(k;t,r,\theta) &= \frac{e^{-ikt}}{k^3 r^2 \cos^2\theta}\left(\sin(kr) - i\sin\theta\cos(kr)\right. \\
&\qquad \left. - \frac{(k^2r^2\cos^2\theta\sin\theta + ikr\cos^2\theta + 2i\sin\theta)e^{ikr\sin\theta}}{2}\right) \\
\partial_t\hat{V}_\theta^-(k;t,r,\theta) &= \frac{e^{-ikt}}{2k^2 r\cos\theta}\left((2 + k^2r^2\cos^2\theta - 2ikr\sin\theta)e^{ikr\sin\theta} - \frac{2\sin(kr)}{k^3r^2}\right) \\
\partial_r\hat{V}_\theta^-(k;t,r,\theta) &= \frac{e^{-ikt}}{k^3 r^2\cos\theta}\Big(2i\cos(kr) \\
&\qquad + \left[2kr\sin\theta + r^3k^3\sin\theta\cos^2\theta + i\left(r^2k^2\cos^2\theta - kr^2 + 2\right)\right]e^{ikr\sin\theta}\Big)
\end{aligned} \tag{5.45}$$

where the $V^\pm$ solutions are related through $\hat{V}_r^+(k;t,r,\theta) = \hat{V}_r^-(k;-t,r,\theta)$ and $\hat{V}_t^-(k;t,r,\theta) = -\hat{V}_t^+(k;-t,r,\theta)$. The results here give the behavior of V and its derivatives only at the surface $\tilde{B}$ ($r = R$ in polar coordinates). Elsewhere, V can be chosen arbitrarily, but we will see that our calculation only requires the behavior at $\tilde{B}$.

Evaluating the canonical energy

Given the appropriate V, we can evaluate (5.38) using

$$\begin{aligned}
\omega(g,\gamma,\pounds_\xi\gamma) &= \omega(h + \pounds_V g, \pounds_{\xi_B}(h + \pounds_V g)) \\
&= \omega(g,h,\pounds_\xi h) + \omega(g,h+\pounds_V g,\pounds_{[\xi,V]}g) - \omega(g,\pounds_\xi h,\pounds_V g)
\end{aligned} \tag{5.46}$$

where

$$[\xi,V]^a = \xi^b\partial_b V^a - V^b\partial_b\xi^a \tag{5.47}$$

and we have used that $\pounds_\xi g = 0$. We can simplify this expression using the gravitational identity

$$\omega(g,\gamma,\pounds_\xi g) = d\chi(\gamma,X) \tag{5.48}$$

where

$$\chi(\gamma,X)=\frac{1}{16\pi G_N}\varepsilon_{ab}\left\{\gamma^{ac}\nabla_c X^b-\frac{1}{2}\gamma_c{}^c\nabla^a X^b+\nabla^b\gamma^a{}_c X^c-\nabla_c\gamma^{ac}X^b+\nabla^a\gamma^c{}_c X^b\right\}. \tag{5.49}$$

Thus, we have

$$\omega(g,\gamma,\pounds_\xi\gamma)=\omega(g,h,\pounds_\xi h)+d\rho \tag{5.50}$$

where

$$\rho=\chi(h+\pounds_V g,[\xi,V])-\chi(\pounds_\xi h,V)\,. \tag{5.51}$$

Finally, choosing V so that it vanishes at B, we can rewrite (5.38) as

$$\mathscr{E}=\int_\Sigma\omega(g,h,\pounds_\xi h)+\int_{\tilde{B}}\rho(h,V)\,. \tag{5.52}$$

In this final expression, we only need V and its derivatives at the surface $\tilde{B}$. Thus, we can now calculate the result explicitly for a general perturbation. In the Fourier basis, the final result in terms of the boundary stress tensor is

$$\mathscr{E}=\int dk_1\int dk_2\,\hat{K}_2(k_1,k_2)\,\langle T_{++}(k_1)\rangle\langle T_{++}(k_2)\rangle+\{+\leftrightarrow-\}\,, \tag{5.53}$$

where the kernel is

$$\hat{K}_2(k_1,k_2)=\frac{256\pi^2R^4G_N}{\ell_{AdS}K^3(K-\kappa)^3(K+\kappa)^3}\Big[(K^5-2\,(\kappa^2+4)K^3+\kappa^4K)\cos K \\ -(5K^4-6K^2\kappa^2+\kappa^4)\sin K+8\,K^3\cos\kappa\Big]\,, \tag{5.54}$$

with $K\equiv R(k_1+k_2),\kappa\equiv R(k_1-k_2)$. We note in particular that the result splits into a left-moving part and a right-moving part with no cross term.

Transforming back to position space

$$\mathscr{E}=\int_{B'}dx_1^+\int_{B'}dx_2^+\,K_2(x_1^+,x_2^+)\,\langle T_{++}(x_1^+)\rangle\langle T_{++}(x_2^+)\rangle+\{+\leftrightarrow-\}\,, \tag{5.55}$$

where the kernel K_2 is symmetric under exchange of $x_1^\pm$ and $x_2^\pm$, and has support

only on $x_i^{\pm} \in [-R,R]$. Focusing only on the domain of support, we have

$$K_2(x_1,x_2) = \frac{4\pi^2 G_N}{R^2 \ell_{AdS}} \begin{cases} (R-x_1)^2(R+x_2)^2 & x_1 \geq x_2 \\ (R+x_1)^2(R-x_2)^2 & x_1 < x_2 \end{cases} . \tag{5.56}$$

Using the relation $c = 3\ell_{AdS}/(2G_N)$ between the CFT central charge and the gravity parameters, we recover the result (5.10) from the introduction.

Like the leading order result in (5.19), the integrals can be taken over any surface B' with boundary ∂B. The fact that we only need the stress tensor on a Cauchy surface for D_B is special to the stress tensor in two dimensions, since the conservation relations allow us to find the stress tensor expectation value everywhere in D_B from its value on a Cauchy surface. For other operators, or in higher dimensions, the result will involve integrals over the full domain of dependence. We will see an explicit example in the next subsection.

5.3.2 Example: scalar operator contribution

We now consider an explicit example making use of the bulk matter field term in (5.7) in order to calculate the terms in the entanglement entropy formula quadratic in the scalar operator expectation values. The discussion for other matter fields would be entirely parallel. This example is more representative, since the formula will involve scalar field expectation values in the entire domain of dependence D_B, i.e. a boundary spacetime region rather than just a spatial slice. The results here are similar to the recent work in [109, 110, 111], but we present them here to show that they follow directly from the canonical energy formula.

We suppose that the CFT has a scalar operator of dimension Δ with expectation value $\langle \mathcal{O}(x) \rangle$. According to the usual AdS/CFT dictionary, this corresponds to a bulk scalar field with mass $m^2 = \Delta(\Delta - d)$ and asymptotic behavior

$$\phi(x,z) \to \gamma z^{\Delta} \langle \mathcal{O}(x) \rangle , \tag{5.57}$$

where γ is a constant depending on the normalization of the operator $\mathcal{O}$. The leading effects of the bulk scalar field on the entanglement entropy (5.7) come

from the matter term in the canonical energy

$$\delta^{(2)} S_B^{matter} = \frac{1}{2} \int_\Sigma \xi_B^a T_{ab}^{(2)} \varepsilon^b \, . \tag{5.58}$$

Using the explicit form of ξ_B from (5.25) and ε from (5.13), this gives (for a ball centered at the origin)

$$\delta^{(2)} S_B^{matter} = -\frac{\ell_{AdS}^{d-1}}{2} \int_0^R \frac{dz}{z^{d-1}} \int_{x^2<R^2-z^2} d^{d-1}x \frac{\pi}{R}(R^2 - z^2 - x^2) T_{00}^{(2)}(x,z) \, . \tag{5.59}$$

This expression is valid for a general bulk matter field. For a scalar field, we have

$$T_{ab}^{(2)} = \partial_a \phi_1 \partial_b \phi_1 - \frac{1}{2} g_{ab} (g^{cd} \partial_c \phi_1 \partial_d \phi_1 + m^2 \phi_1^2) \, , \tag{5.60}$$

where g_{ab} is the background AdS metric and ϕ_1 represents the solution of the linearized scalar field equation on AdS,

$$\frac{1}{z^{d-1}} \partial_z \left\{ z^{d-1} \partial_z \phi \right\} + \partial_\mu \partial^\mu \phi - \frac{m^2}{z^2} \phi = 0 \, , \tag{5.61}$$

with boundary behavior as in (5.57). This solution is given most simply in Fourier space, where we have

$$\phi_1(k,z) = \frac{2^\nu \Gamma(\nu+1)}{(2\pi)^d} \int_{k_0^2 > \vec{k}^2} d^d k \frac{e^{i k_\mu x^\mu}}{\left(k_0^2 - \vec{k}^2\right)^{\nu/2}} z^{\frac{d}{2}} J_\nu \left(\sqrt{k_0^2 - \vec{k}^2} z \right) \gamma \langle \mathscr{O}(k) \rangle \, , \tag{5.62}$$

where $\nu = \Delta - d/2$, but we can formally write a position-space expression using a bulk-to-boundary propagator $K(x,z;x')$ as [115, 116]

$$\phi_1(x,z) = \gamma \int dx' K(x,z;x') \langle \mathscr{O}(x') \rangle \, . \tag{5.63}$$

The integral here is over the boundary spacetime, however it has been argued (see, for example [113, 114]) that to reconstruct the bulk field throughout the Rindler wedge R_B (and specifically on Σ), we need only the boundary values on the domain of dependence region. We recall some explicit formulae for this "Rindler bulk reconstruction" in Appendix D. Combining these results, we have a general

expression for the scalar field contribution to entanglement entropy at second-order in the scalar one-point functions,

$$\delta^{(2)}S_B^{scalar} = -\frac{\ell_{AdS}^{d-1}}{2}\int_0^R \frac{dz}{z^{d-1}}\int_{x^2<R^2-z^2} d^{d-1}x\frac{\pi}{R}(R^2-z^2-x^2) \left\{(\partial_0\phi_1)^2+(\partial_i\phi_1)^2+(\partial_z\phi_1)^2+\frac{m^2}{z^2}\phi_1^2\right\} \tag{5.64}$$

where ϕ_1 is given in (5.62) or (5.63) .

As a simple example, consider the case where the scalar field expectation value is constant. In this case it is simple to solve (5.61) everywhere to find that

$$\phi_1(x,z) = \gamma\langle\mathscr{O}\rangle z^{\Delta}\,. \tag{5.65}$$

Inserting this into the general formula (5.64), and performing the integrals, we obtain

$$\delta^{(2)}S_B^{scalar} = -\frac{\pi\ell_{AdS}^{d-1}}{4}\gamma^2\langle\mathscr{O}\rangle^2 R^{2\Delta}\Omega_{d-2}\frac{\Delta\Gamma(\frac{d}{2}-\frac{1}{2})\Gamma(\Delta-\frac{d}{2}+1)}{\Gamma(\Delta+\frac{3}{2})}\,. \tag{5.66}$$

This reproduces previous results in the literature [100, 110].

5.4 Stress tensor contribution: direct calculation for $\mathbf{CFT}_2$

In Section 5.3.1, we used the equivalence between quantum Fisher information and canonical energy to obtain an explicit expression for the second-order stress tensor contribution to the entanglement entropy for holographic states in two-dimensional CFTs. This is applicable for general holographic states, whether or not other matter fields are present in the dual spacetime (in which case there are additional terms in the expression for entanglement entropy). In special cases where there are no matter fields, the spacetime is locally AdS and we can understand the dual CFT state as being related to the vacuum state by a local conformal transformation. We show in this section that in this special case, we can reproduce the holographic result (5.56) through a direct CFT calculation, providing a strong consistency check. We note that the result does not rely on taking the large N limit or on any special properties

of the CFT, so the formula holds universally for this simple class of states.

Our approach will be to develop an iterative procedure to express the entanglement entropy as an expansion in the stress tensor expectation value for this special class of states. We evaluate the entanglement entropy for these states from a correlation function of twist operators obtained by transforming the result for the vacuum state.[6] Similarly, the stress tensor expectation values follow directly from the form of the conformal transformation. Inverting the relationship between the required conformal transformation and the stress tensor expectation value allows us to express the entanglement entropy as a perturbative expansion in the expectation value of the stress tensor.

5.4.1 Conformal transformations of the vacuum state

In two-dimensional CFT, under a conformal transformation $w = f(z)$, the stress tensor transforms as

$$T'(w) = \left(\frac{dw}{dz}\right)^{-2} \left(T(z) + \frac{c}{12}\{f(z);z\}\right). \tag{5.67}$$

Here c is the central charge of the CFT and the inhomogeneous part is the Schwarzian derivative

$$\{f(z);z\} \equiv \frac{f'''(z)}{f'(z)} - \frac{3f''(z)^2}{2f'(z)^2}. \tag{5.68}$$

For an infinitesimal transformation $f(z) = z + \lambda\,\varepsilon(z)$, the Schwarzian derivative can be expanded as

$$\{z+\lambda\varepsilon(z);z\} = \lambda\,\varepsilon'''(z) - \lambda^2\left(\varepsilon'''(z)\varepsilon'(z) + \frac{3}{2}\varepsilon''(z)^2\right) + \lambda^3\left(\varepsilon'(z)^2\varepsilon'''(z) + 3\varepsilon'(z)\varepsilon''(z)^2\right) + \cdots \tag{5.69}$$

The CFT vacuum is invariant under the $SL(2,\mathbb{C})$ subgroup of global conformal transformations. However, for transformations which are not part of this subgroup, the vacuum state transforms into *excited states*. The action of the full conformal group includes the full Virasoro algebra which involves arbitrary products and

[6] A similar approach was recently used to derive the modular Hamiltonian of these excited states in [117].

derivatives of the stress tensor

$$\mathrm{Id} \sim 1, T, \partial^m T, T^2, T\partial^n T, \cdots . \tag{5.70}$$

These states capture the gravitational sector of the gravity dual. Other excited states can be obtained by the action of other primary operators and their descendants. However we restrict ourselves to the class states that are related to 'pure gravity' excitations, which are the states obtained by conformal transformation of the vacuum state.

We denote the excited state as $|f\rangle = U_f |0\rangle$ where U_f is the action of a conformal transformation on the vacuum $|0\rangle$. The expectation value of the stress tensor for the state perturbed state $|f\rangle$ is

$$\langle f|T(z)|f\rangle = \langle 0|U_f^\dagger T(z) U_f|0\rangle = \langle 0|T'(w)|0\rangle = \left(\frac{df}{dz}\right)^{-2} \frac{c}{12}\{f(z);z\}, \tag{5.71}$$

where we used that $\langle 0|T(z)|0\rangle = 0$. The anti-holomorphic component of the stress tensor $\bar{T}(\bar{z})$ is similarly related to the anti-holomophic part of the conformal transformation $\bar{f}$.

To leading order in a conformal transformation near the identity, this equation relates the conformal transformation to $\langle T(z)\rangle$ by a third-order ordinary differential equation. The three integration constants correspond to the invariance of $\langle T(z)\rangle$ under the global conformal transformations. Thus we have an invertible relationship between the conformal transformations modulo their global part and $\langle T(z)\rangle$, at least near the identity.

5.4.2 Entanglement entropy of excited states

In a two-dimensional CFT, the entanglement entropy can be explicitly computed using the replica method [118, 83]. The computation can be reduced to a correlation function of twist operators $\Phi_\pm$, which are conformal primaries with weight $(h_n, \bar{h}_n) = \frac{c}{24}(n-1/n, n-1/n)$.

The Rényi entropy is

$$\exp\left((1-n)S^{(n)}\right) = \langle \Phi_+(z_1)\Phi_-(z_2)\rangle = (z_2 - z_1)^{-2h_n}. \tag{5.72}$$

The entanglement entropy is obtained by taking the $n \to 1$ limit of $S^{(n)}$.

$$S_{\text{vac}} = \lim_{n\to 1} S^{(n)} = \lim_{n\to 1} (1-n)^{-1} \log(z_2 - z_1)^{-2h_n} = \frac{c}{12} \log \frac{(z_2-z_1)^2}{\delta^2}\,. \tag{5.73}$$

For the excited states obtained by conformal transformations $z \to w = f(z)$ the Rényi entropy is

$$\exp\left((1-n)S_{\text{ex}}^{(n)}\right) = \langle f|\Phi_+(z_1)\Phi_-(z_2)|f\rangle \tag{5.74}$$

$$= \left(\frac{df}{dz}\right)_{z_1}^{-h_n} \left(\frac{df}{dz}\right)_{z_2}^{-h_n} \left(\frac{d\bar{f}}{d\bar{z}}\right)_{\bar{z}_1}^{-\bar{h}_n} \left(\frac{d\bar{f}}{d\bar{z}}\right)_{\bar{z}_2}^{-\bar{h}_n} \langle 0|\Phi_+(z_1)\Phi_-(z_2)|0\rangle\,. \tag{5.75}$$

Here z_1, z_2 are the points $f(z_1) = \bar{f}(\bar{z}_1) = -R$, $f(z_2) = \bar{f}(\bar{z}_2) = R$. The entanglement entropy of the excited state is

$$S_{\text{ex}} = \lim_{n\to 1} S_{\text{ex}}^{(n)} = \frac{c}{12} \log \left| \frac{f'(z_1) f'(z_2) \bar{f}'(\bar{z}_1) \bar{f}'(\bar{z}_2) (z_2 - z_1)^2}{\delta^2} \right|. \tag{5.76}$$

Therefore the change in entanglement entropy respect to the vacuum state is

$$\delta S \equiv S_{\text{ex}} - S_{\text{vac}} = \frac{c}{12} \log \left| \frac{f'(f^{-1}(R)) f'(f^{-1}(-R)) (f^{-1}(R) - f^{-1}(-R))^2}{(2R)^2} \right| + \frac{c}{12} \log \left| \frac{\bar{f}'(\bar{f}^{-1}(R)) \bar{f}'(\bar{f}^{-1}(-R)) (\bar{f}^{-1}(R) - \bar{f}^{-1}(-R))^2}{(2R)^2} \right|. \tag{5.77}$$

By inverting (5.71), the conformal transformation required to reach the state $|f\rangle$ can be expressed as a function of the expectation value of the stress tensor. Plugging this f into (5.77), allows us to express the entanglement entropy as a function of the expectation value of the stress tensor alone, as we set out to do.

In practice, we will invert (5.71) order by order in a small conformal transformation and express the entanglement entropy as an expansion in the resulting small stress tensor. The second-order term in this expansion will be the Fisher information metric.

In the following, we will focus on the holomorphic term in (5.71), noting that

the anti-holomorphic part follows identically.[7]

5.4.3 Perturbative expansion

Consider a conformal transformation perturbation near the identity transformation

$$w = f(z) = z + \lambda f_1(z) + \lambda^2 f_2(z) + \lambda^3 f_3(z) + \cdots , \tag{5.78}$$

where λ is a small expansion parameter.

In this expansion,

$$\frac{12}{c}\langle T(w)\rangle = \lambda\, f_1'''(w) + \lambda^2 \left(-\frac{3}{2} f_1''(w)^2 - 3 f_1'(w) f_1'''(w) + f_2'''(w) - f_1(w) f_1''''(w) \right) + \mathcal{O}(\lambda^3) , \tag{5.79}$$

and the entanglement entropy is

$$\begin{aligned} \frac{12}{c} S_{\text{ex}} &= \log \left| \frac{f'(z_1) f'(z_2)(z_2 - z_1)^2}{\delta^2} \right| \\ &= \log \frac{(2R)^2}{\delta^2} + \lambda \left[\frac{R\,(f_1'(-R) + f_1'(R)) + f_1(-R) - f_1(R)}{R} \right] \\ &\quad + \lambda^2 \Big(- \frac{(f_1(R) - f_1(-R))^2}{4R^2} + \frac{-f_1(-R) f_1'(-R) + f_1(R) f_1'(R) + f_2(-R) - f_2(R)}{R} \\ &\qquad - \frac{1}{2} f_1'(-R)^2 - \frac{1}{2} f_1'(R)^2 + f_2'(-R) + f_2'(R) - f_1(-R) f_1''(-R) - f_1(R) f_1''(R) \Big) \\ &\quad + \mathcal{O}(\lambda^3) . \end{aligned} \tag{5.80}$$

Linear order

To first-order in λ, the stress tensor is given by

$$\langle T(z)\rangle = \lambda \frac{c}{12} f_1'''(z) + \mathcal{O}(\lambda^2) , \tag{5.81}$$

[7] Note that the potential cross-term between left and right moving contributions vanished in the gravitational computation of $\delta^{(2)} S$.

so that change in the expectation value of the modular Hamiltonian becomes

$$\begin{aligned}\delta\langle H_B\rangle &= \frac{\lambda\, c}{24R}\int_{-R}^{R} dz\,(R^2-z^2)f_1'''(z)\\ &= \frac{\lambda\, c}{24R}\left[(R^2-z^2)f_1''(z)+2\left(zf_1'(z)-f_1(z)\right)\right]_{-R}^{R}\\ &= \frac{\lambda\, c}{12R}\left[R(f_1'(R)+f_1'(-R))-(f_1(R)-f_1(-R))\right]. \end{aligned} \tag{5.82}$$

From (5.77) we also have that the first-order change in entanglement entropy is

$$\delta^{(1)}S = \frac{\lambda\, c}{12R}\left[R(f_1'(R)+f_1'(-R))-(f_1(R)-f_1(-R))\right]. \tag{5.83}$$

Comparing with (5.82) we see that the first law of entanglement holds

$$\delta^{(1)}S = \delta\langle H_B\rangle\,. \tag{5.84}$$

Second-order

The second-order change in entanglement entropy gives the second-order relative entropy as the modular Hamiltonian is linear in the expectation value of the stress tensor. This is the quantum Fisher metric in the state space, which is dual to the canonical energy in gravity [105]. In this section, we obtain the expression for canonical energy from the CFT side and find an exact match to the results of Section 5.3.1.

Our procedure so far yields the entanglement entropy of a subregion in terms of a perturbative expansion in small stress tensor expectation value

$$\begin{aligned}\delta S = \quad & \int_B \frac{dz}{2\pi}K_1(z)\langle T(z)\rangle - \frac{1}{2}\int_B\frac{dz_1}{2\pi}\int_B\frac{dz_2}{2\pi}K_2(z_1,z_2)\langle T(z_1)\rangle\langle T(z_2)\rangle+\cdots\\ & +\{z\leftrightarrow\bar{z}\}\,.\end{aligned} \tag{5.85}$$

To obtain $K_2(z_1,z_2)$, we need to invert the relationship in (5.79) order by order, the lower order solutions $f_{i-1}, f_{i-2},\cdots f_1$ becoming sources for the i-th order solution.

Taking the explicit expression for $\langle T(z)\rangle$ to simplify solving the differential

equations,

$$\langle T(z)\rangle = \lambda \left(c_1 e^{ik_1 z} + c_2 e^{ik_2 z} \right), \tag{5.86}$$

is sufficient to extract the Fourier transformed kernel.

The first-order solution is

$$f_1(z) = F_1 + F_2 z + F_3 z^2 + \frac{12i}{c}\left(c_1 \frac{e^{ik_1 z}}{k_1^3} + c_2 \frac{e^{ik_2 z}}{k_2^3} \right), \tag{5.87}$$

where F_i are constants that corresponds to the global part of the conformal transformation and do not effect the final result. We take these constants to be zero for simplicity. The second-order solution is

$$f_2(z) = -\frac{9}{c^2}\left[\frac{11i}{16}(c_1^2 \frac{e^{2ik_1 z}}{k_1^5} + c_2^2 \frac{e^{2ik_2 z}}{k_2^5}) + i\frac{c_1 c_2}{k_1^3 k_2^3} \frac{e^{i(k_1+k_2)z}\left(k_1^4 + 3k_2 k_1^3 + 3k_2^2 k_1^2 + 3k_2^3 k_1 + k_2^4\right)}{(k_1+k_2)^3} \right]. \tag{5.88}$$

With these solutions, we obtain

$$\tilde{K}_1(k) = \quad \frac{2}{k^2}\frac{\sin(kR) - kR\cos(kR)}{kR}, \tag{5.89}$$

as well as

$$\tilde{K}_2(k_1,k_2) = \frac{96R^4}{c}\frac{(K^5 - 2(\kappa^2+4)K^3 + \kappa^4 K)\cos K - (5K^4 - 6K^2\kappa^2 + \kappa^4)\sin K + 8K^3\cos\kappa}{K^3(K-\kappa)^3(K+\kappa)^3}, \tag{5.90}$$

with $K \equiv R(k_1+k_2)$ and $\kappa \equiv R(k_1-k_2)$.

Taking the inverse Fourier transformation of $\tilde{K}_1(k)$

$$K_1(z) \quad = \quad \int dk\, \tilde{K}_1(k) e^{-ikz} = \pi \frac{R^2 - z^2}{R} W(R,z) \tag{5.91}$$

where

$$W(R,x) \equiv \frac{(\mathrm{sgn}(R+x) + \mathrm{sgn}(R-x))}{2} \tag{5.92}$$

is a window function with support $x \in [-R,R]$.

The second-order position space kernel is

$$K_2(z_1,z_2)=\frac{6\pi^2}{cR^2}\begin{cases}(R-z_1)^2(R+z_2)^2 & -R\le z_2\le z_1\le R\\ (R+z_1)^2(R-z_2)^2 & -R\le z_1< z_2\le R\end{cases}. \tag{5.93}$$

The anti-holomorphic part is the same with $z\to\bar{z}$, and the cross term vanishes. With the relation

$$c=\frac{3\ell_{AdS}}{2G_N} \tag{5.94}$$

this reproduces the kernel for canonical energy in (5.56).

This result holds for regions defined on any spatial slice of the CFT. If we choose the $t=0$ slice, $z=\bar{z}=x$ and our result becomes

$$\delta S_{EE}^{(2)} \;=\; -\frac{1}{2}\int_B dx_1\int_B dx_2\,K_2(x_1,x_2)\left[\langle T_{++}(x_1)\rangle\langle T_{++}(x_2)\rangle+\langle T_{--}(x_1)\rangle\langle T_{--}(x_2)\rangle\right].$$

Changing variables using $x_1=x-r$, $x_2=x+r$, the kernel is simply

$$K_2(x,r)=K_2(x,-r)=\frac{12\pi^2}{cR^2}\left[(R-|r|)^2-x^2\right]^2\Theta\left(R-|r|-|x|\right). \tag{5.95}$$

5.4.4 Excited states around thermal background

A similar analysis can be applied to perturbations around a thermal state with temperature $T=\beta^{-1}$. If we denote homogeneous thermal state $|\beta\rangle$, the stress tensor one-point function is

$$\langle\beta|T|\beta\rangle=\frac{\pi^2 c}{6\beta^2}. \tag{5.96}$$

This can be obtained by a conformal transformation from the vacuum with

$$f_\beta(z)=\frac{\beta}{2\pi}\log(z). \tag{5.97}$$

On top of this transformation, one could also apply an infinitesimal conformal transformation to obtain non-homogeneous perturbation around thermal state.

A similar computation as the previous section leads to the first-order kernel

$$K_1^\beta(z) = \frac{2\beta}{\sinh(\frac{2\pi R}{\beta})} \sinh\left(\frac{\pi(R-z)}{\beta}\right) \sinh\left(\frac{\pi(R+z)}{\beta}\right), \tag{5.98}$$

which is the modular hamiltonian of thermal state in 2d CFT.

Furthermore, the second-order kernel is

$$K_2^\beta(z_1,z_2) = \frac{24\beta^2}{c\sinh^2(\frac{2\pi R}{\beta})} \begin{cases} \sinh^2\left(\frac{\pi(R-z_1)}{\beta}\right)\sinh^2\left(\frac{\pi(R+z_2)}{\beta}\right) & -R \le z_2 \le z_1 \le R \\ \sinh^2\left(\frac{\pi(R+z_1)}{\beta}\right)\sinh^2\left(\frac{\pi(R-z_2)}{\beta}\right) & -R \le z_1 < z_2 \le R \end{cases}. \tag{5.99}$$

Consistency check : homogeneous BTZ perturbation

As a check, consider the homogeneous perturbation example, where $\langle T\rangle = \langle\bar{T}\rangle = \frac{\lambda}{8G_N}$.[8]

In the AdS_3 this is a perturbation towards the planar BTZ black hole geometry,

$$ds^2 = \frac{1}{z^2}\left(dz^2 + (1+\lambda z^2/2)^2 dx^2 - (1-\lambda z^2/2)^2 dt^2\right) \tag{5.100}$$

in Fefferman-Graham coordinates. Holographic renormalization (5.22) tells us the stress tensor expectation value of the dual CFT is

$$\langle T_{tt}\rangle = \frac{1}{2\pi}\left(\langle T\rangle + \langle\bar{T}\rangle\right) = \frac{\lambda}{8\pi G_N}. \tag{5.101}$$

As the black hole corresponds to the thermal state in CFT, the dual state be obtained by the conformal transformation (5.97).

First, applying (5.77) for this conformal transformation, the change in entanglement entropy with respect to the vacuum is

$$\delta S = \lambda\frac{R^2}{6G} - \lambda^2\frac{R^4}{90G} + \lambda^3\frac{4R^6}{2835G} + \mathcal{O}(\lambda^4), \tag{5.102}$$

which matches the previous known results [100, 105].

[8] $\lambda = \frac{2\pi^2}{\beta}$ sets the temperature.

The linear order equals $\delta\langle H_B\rangle$ as expected from the entanglement first law.

The second-order term gives the quantum Fisher information or the canonical energy

$$\mathscr{E} = \frac{d^2}{d\lambda^2}(\Delta E - \Delta S)\Big|_{\lambda=0} = \frac{R^4}{45G_N}\,. \tag{5.103}$$

Using the formula using the second-order kernel (5.85) and (5.93), we obtain the same canonical energy

$$\mathscr{E} \;=\; 2\frac{d^2}{d\lambda^2}\left[\frac{1}{2}\int_B \frac{dz_1}{2\pi}\int_B \frac{dz_2}{2\pi}\,K_2(x_1,x_2)\langle T\rangle\langle T\rangle\right]_{\lambda=0} = \frac{R^4}{45G_N}\,. \tag{5.104}$$

5.5 Auxiliary de Sitter space interpretation

In [43], it was pointed out that the leading order perturbative expression (5.2) for entanglement entropy, expressed as a function of the center point x and radius R of the ball B, is a solution to the wave equation for a free scalar field on an auxiliary de Sitter space, with $\langle T_{00}(x)\rangle$ acting as a source.

It was conjectured that higher order contributions might be accounted for by local propagation in this auxiliary space with the addition of self-interactions for scalar field. In this section, we show that for two-dimensional CFTs, the second-order result (5.10) can indeed be reproduced by moving to a non-linear wave equation with a simple cubic interaction to this scalar field. A slight complication is that we actually require two-scalar fields; one sourced by the holomorphic stress tensor T_{++}, and the other sourced by the anti-holomorphic part T_{--}; the perturbation to the entanglement entropy is then the sum of these two scalars, $\delta S = \delta S_+ + \delta S_-$, reproducing both terms in (5.10). We will focus on δS_+ since δS_- follows identically.

To reproduce the second-order results for entanglement entropy, we consider an auxiliary de Sitter space with metric

$$ds^2_{dS} = \frac{L^2_{dS}}{R^2}\left(-dR^2 + dx^2\right)\,. \tag{5.105}$$

and consider a scalar field δS_+ with mass $m^2 L_{dS}^2 = -2$ and action

$$\mathscr{L} = \frac{1}{2}\nabla_a(\delta S_+)\nabla^a(\delta S_+) + \frac{1}{2}m^2(\delta S_+)^2 + \frac{4}{cL_{dS}^2}(\delta S_+)^3 . \tag{5.106}$$

The equation of motion is

$$\left(\nabla_{dS}^2 - m^2\right)\delta S_+(R,x) = \frac{12}{cL_{dS}^2}(\delta S_+(R,x))^2 . \tag{5.107}$$

As shown in [43], the first-order perturbation (5.2) obeys the linearized wave equation

$$\left(\nabla_{dS}^2 - m^2\right)\delta^{(1)}S_+(R,x) = 0 . \tag{5.108}$$

We can immediately check that the second-order perturbation (5.10) is consistent with the nonlinear equation by acting with the dS wave equation on the second-order kernel (5.93)

$$\left(\nabla_{dS}^2 - m^2\right)K_2(x_1 - x, x_2 - x) = -\frac{24}{cL_{dS}^2}K_1(x_1 - x)K_1(x_2 - x) . \tag{5.109}$$

Integration against the CFT stress tensor then gives (5.107).

Alternatively, introducing the retarded[9] bulk-to-bulk propagator [119]

$$G_{dS}(\eta, x; \eta', x') = -\frac{\eta^2 + \eta'^2 - (x - x')^2}{4\eta\eta'} \tag{5.110}$$

and bulk-to-boundary propagator

$$K_{dS}(\eta, x; x') = \lim_{\varepsilon\to 0}\left[-4\pi\varepsilon \lim_{\eta'\to\varepsilon} G_{dS}(\eta, x; \eta', x')\right] = \pi\frac{\eta^2 - (x - x')^2}{\eta} \tag{5.111}$$

we can show directly that the solution with boundary behavior

$$\delta S_+ = \frac{4\pi}{3}\langle T_{++}\rangle R^2 + \mathscr{O}(R^3) \tag{5.112}$$

[9] These propagators are defined to be non-zero only within the future directed light-cone. This is important in reproducing both the support and the exact form of $K_2(x_1, x_2)$.

for $R \to 0$ is

$$\delta^{(1)} S_+(R,x_0) = \int dx K_{dS}(R,x_0;x)\langle T_{++}(x)\rangle \tag{5.113}$$

at first-order and

$$\delta^{(2)} S_+(R,x_0) = \frac{12}{cL_{dS}^2}\int_{dS} d\eta' dx' \sqrt{|g_{dS}|}\, G_{dS}(R,x_0;\eta',x') \left(\int dx K_{dS}(\eta',x';x)\langle T_{++}(x)\rangle\right)^2, \tag{5.114}$$

at second-order, where the latter term comes from the diagram shown in Figure 5.2.

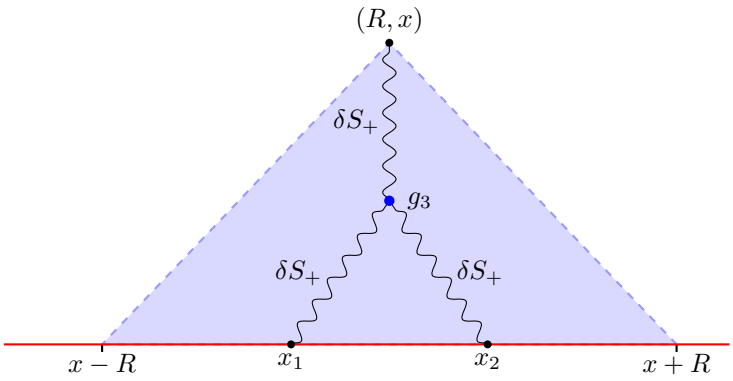

Figure 5.2: Feynman diagram which computes $\delta^{(2)}S$. The δS_+ field propagates in de Sitter with a cubic interaction given by (5.106). The bold (red) line is the conformal boundary of de Sitter which is identified with a time slice of the CFT. δS_+ is sourced by the CFT stress tensor on this boundary.

The integrals can be performed directly to show that these results match with the expressions (5.2) and (5.10) respectively.

A useful advantage of writing the second-order result in the form (5.114) is that it is manifestly negative. More explicitly, we have

$$\delta^{(2)} S_+(R,x_0) \quad = \quad -\frac{3}{cL_{dS}^2}\int d\eta dy \sqrt{|g_{dS}|}\, \frac{R^2+\eta^2-(x_0-y)^2}{R\eta}\left[\int_{B_y} dx K_{dS}(\eta,y;x)\langle T_{++}(x)\rangle\right]^2. \tag{5.115}$$

where $\sqrt{|g_{dS}|}$ and the squared expression are manifestly positive and the bulk-to-bulk propagator (5.110) is positive over the range of integration where $(y - x_0)^2 \leq (R - \eta)^2$. That this expression is negative is required by the positivity of relative entropy, since we showed above that $-\delta^{(2)}S$ represents the leading order perturbative expression for the relative entropy.

Recently, it has been realized that the modular Hamiltonian in certain non-vacuum states in two dimensional CFTs can be described by propagation in a dual geometry [107] matching the kinematic space found in [120, 121]. We find that the results of Section 5.4.4 can be explained by the same interacting theory (5.106) on this kinematic space. The kinematic space dual to the thermal state is [107]

$$ds^2 = \frac{4\pi^2 L_{dS}^2}{\beta^2 \sinh^2\left(\frac{2\pi R}{\beta}\right)} \left(-dR^2 + dx^2\right) . \tag{5.116}$$

The second-order perturbation to the entanglement entropy from (5.99) obeys the wave equation (5.107) with the same interactions in this kinematic space.

We could imagine adding additional fields propagating in de Sitter to capture the contributions to the entanglement entropy from scalar operators discussed in Section 5.3.2. However, unlike the contribution from the stress tensor, this contribution involves integration of the one-point functions over the full domain of dependence D_B. In higher-dimensions, this will also be true for the stress tensor contribution. The $R = 0$ boundary of the auxiliary de Sitter space does not include the time direction of the CFT, so any extension of these results to contributions of other operators or higher dimensional cases will require a more sophisticated auxiliary space. Promising work in this direction is discussed in [108, 106].

Chapter 6

Conclusion

This thesis investigated entanglement entropy using holographic duality focusing on its applications to a particular class of noncommutative theories in Part I and on general properties of the holographic formula for entanglement entropy in Part II.

In Part I, Chapter 2 applied the holographic Ryu-Takayanagi formula for entanglement entropy to noncommutative theories. A violation of the area law was found as is to be expected in nonlocal theories. We interpreted our results as an indication that the vacuum states of these noncommutative theories are entangled on length scales of the nonlocality leading to an enhancement in the effective number of degrees of freedom involved in the entanglement entropy between two spatial regions.

Chapter 3 followed up on the study of entanglement entropy in this class of noncommutative theories by studying them in a different perturbative regime. The aim was to explore in what regimes similar violations to the area law could be found. It was found that noncommutative interactions did not induce long range entanglement in the vacuum state of these theories to leading order in perturbations theory.

Part I fits into a larger effort to apply this holographic formula to better understand the entanglement entropy in the full range of field theories with holographic duals. The class of noncommutative theories studied are interesting as they involve many unusual ingredients in the context of gauge-gravity duality. These include a nontrivial dilaton profile and compact dimensions and the presence of a bulk two-

form field in the gravitational dual. In addition, entanglement entropy is interesting in its own right in the larger context of the study of noncommutative field theories. It would be interesting to investigate the onset of long range entanglement in these theories, perturbatively at large N and through further holographic studies.

Part II focused on the properties of entanglement entropy in general holographic states. Chapter 4 explores the constraints imposed by the existence the holographic formula for entanglement entropies on the geometries of holographic duals. A number of constraints were identified. In particular, the strong subadditivity of entanglement entropy implies that the dual geometry must obey an averaged null energy condition in three dimensional gravity.

Chapter 4 describes the first step in a programme of relating the constraints on geometries imposed by the holographic entanglement entropy formula to physically motivated constraints like energy conditions. It would be particularly interesting to extend our results to higher dimension or to explore the implication of other field theoretic entanglement identities. The technical difficulties of dealing with the nonlocal nature of the holographic formula provide the major barrier to such extension. It may be that recent approaches to reorganising the data in holographic dualities using an auxiliary kinematic space along the lines of [108] may provide some insight into these technical difficulties.

In the classical limit, the dual holographic geometry is determined by the one-point functions of the field theory. This geometry allows us to compute the entanglement entropies through the holographic Ryu-Takayanagi formula. Chapter 5 expresses the entanglement entropies of holographic states directly in terms of these one-point functions. In particular the entanglement entropy in a class of purely gravitational asymptotically AdS_3 states is expressed in an expansion in the one-point function of the stress tensor of the field theory. This is confirmed directly in the dual conformal field theory. This result is then interpreted in terms of the propagation of a self-interacting scalar field in an auxiliary de Sitter space.

Chapter 5 describes the first steps in a program of relating entanglement entropy to one-point functions in holographic field theories. Finding the explicit form of this relationship could provide insights into the structure of entanglement in these field theories as well as providing constraints on the class of states which have holographic duals. In this way Chapter 4 can be though of as providing con-

straints on the geometries which can be dual to field theories, while Chapter 5 provides constraints on the states which can have gravitational duals. Finally, Chapter 5 has extended the intriguing fact noticed in [43] that the entanglement entropy of near vacuum states can be interpreted in terms of the propagation of a field in an auxiliary de Sitter space by adding interactions to the field. This provides some support to the idea that this auxiliary de Sitter space contains interesting physics and that what is so far a curious fact should be investigated further.

Bibliography

[1] S. W. Hawking, *Breakdown of Predictability in Gravitational Collapse*, *Phys. Rev.* **D14** (1976) 2460–2473.

[2] J. D. Bekenstein, *A Universal Upper Bound on the Entropy to Energy Ratio for Bounded Systems*, *Phys. Rev.* **D23** (1981) 287.

[3] R. Bousso, *A Covariant entropy conjecture*, *JHEP* **07** (1999) 004, [hep-th/9905177].

[4] J. M. Maldacena, *The Large N limit of superconformal field theories and supergravity*, *Int. J. Theor. Phys.* **38** (1999) 1113–1133, [hep-th/9711200]. [Adv. Theor. Math. Phys.2,231(1998)].

[5] O. Aharony, S. S. Gubser, J. M. Maldacena, H. Ooguri, and Y. Oz, *Large N field theories, string theory and gravity*, *Phys. Rept.* **323** (2000) 183–386, [hep-th/9905111].

[6] S. Ryu and T. Takayanagi, *Holographic derivation of entanglement entropy from AdS/CFT*, *Phys. Rev. Lett.* **96** (2006) 181602, [hep-th/0603001].

[7] S. Ryu and T. Takayanagi, *Aspects of Holographic Entanglement Entropy*, *JHEP* **08** (2006) 045, [hep-th/0605073].

[8] T. Nishioka, S. Ryu, and T. Takayanagi, *Holographic Entanglement Entropy: An Overview*, *J. Phys.* **A42** (2009) 504008, [arXiv:0905.0932].

[9] V. E. Hubeny, M. Rangamani, and T. Takayanagi, *A Covariant holographic entanglement entropy proposal*, *JHEP* **07** (2007) 062, [arXiv:0705.0016].

[10] P. Calabrese and J. L. Cardy, *Entanglement entropy and quantum field theory: A Non-technical introduction*, *Int. J. Quant. Inf.* **4** (2006) 429, [quant-ph/0505193].

[11] A. Kitaev and J. Preskill, *Topological entanglement entropy*, *Phys. Rev. Lett.* **96** (2006) 110404, [hep-th/0510092].

[12] L. Bombelli, R. K. Koul, J. Lee, and R. D. Sorkin, *A Quantum Source of Entropy for Black Holes*, *Phys. Rev.* **D34** (1986) 373–383.

[13] M. Van Raamsdonk, *Building up spacetime with quantum entanglement*, *Gen. Rel. Grav.* **42** (2010) 2323–2329, [arXiv:1005.3035]. [Int. J. Mod. Phys.D19,2429(2010)].

[14] M. A. Nielsen and I. L. Chuang, *Quantum computation and quantum information*. Cambridge university press, 2010.

[15] H. Casini, M. Huerta, and J. A. Rosabal, *Remarks on entanglement entropy for gauge fields*, *Phys. Rev.* **D89** (2014), no. 8 085012, [arXiv:1312.1183].

[16] P. V. Buividovich and M. I. Polikarpov, *Entanglement entropy in gauge theories and the holographic principle for electric strings*, *Phys. Lett.* **B670** (2008) 141–145, [arXiv:0806.3376].

[17] W. Donnelly, *Decomposition of entanglement entropy in lattice gauge theory*, *Phys. Rev.* **D85** (2012) 085004, [arXiv:1109.0036].

[18] J. Eisert, M. Cramer, and M. B. Plenio, *Area laws for the entanglement entropy - a review*, *Rev. Mod. Phys.* **82** (2010) 277–306, [arXiv:0808.3773].

[19] B. Swingle, *Entanglement Entropy and the Fermi Surface*, *Phys. Rev. Lett.* **105** (2010) 050502, [arXiv:0908.1724].

[20] E. H. Lieb and M. B. Ruskai, *A Fundamental Property of Quantum-Mechanical Entropy*, *Phys. Rev. Lett.* **30** (1973) 434–436.

[21] E. H. Lieb and M. B. Ruskai, *Proof of the strong subadditivity of quantum-mechanical entropy*, *J. Math. Phys.* **14** (1973) 1938–1941.

[22] J. Polchinski, *String theory. Vol. 1: An introduction to the bosonic string*. Cambridge University Press, 2007.

[23] E. Witten, *Anti-de Sitter space and holography*, *Adv. Theor. Math. Phys.* **2** (1998) 253–291, [hep-th/9802150].

[24] T. Sakai and S. Sugimoto, *Low energy hadron physics in holographic QCD*, *Prog. Theor. Phys.* **113** (2005) 843–882, [hep-th/0412141].

[25] A. Bergman, K. Dasgupta, O. J. Ganor, J. L. Karczmarek, and G. Rajesh, *Nonlocal field theories and their gravity duals*, *Phys. Rev.* **D65** (2002) 066005, [hep-th/0103090].

[26] I. R. Klebanov and E. Witten, *AdS / CFT correspondence and symmetry breaking*, *Nucl. Phys.* **B556** (1999) 89–114, [hep-th/9905104].

[27] A. Lewkowycz and J. Maldacena, *Generalized gravitational entropy*, *JHEP* **08** (2013) 090, [arXiv:1304.4926].

[28] T. Faulkner, A. Lewkowycz, and J. Maldacena, *Quantum corrections to holographic entanglement entropy*, *JHEP* **11** (2013) 074, [arXiv:1307.2892].

[29] A. Hashimoto and N. Itzhaki, *Noncommutative Yang-Mills and the AdS / CFT correspondence*, *Phys. Lett.* **B465** (1999) 142–147, [hep-th/9907166].

[30] J. M. Maldacena and J. G. Russo, *Large N limit of noncommutative gauge theories*, *JHEP* **09** (1999) 025, [hep-th/9908134].

[31] J. L. Karczmarek and C. Rabideau, *Holographic entanglement entropy in nonlocal theories*, *JHEP* **10** (2013) 078, [arXiv:1307.3517].

[32] J. L. F. Barbon and C. A. Fuertes, *Holographic entanglement entropy probes (non)locality*, *JHEP* **04** (2008) 096, [arXiv:0803.1928].

[33] J. L. F. Barbon and C. A. Fuertes, *A Note on the extensivity of the holographic entanglement entropy*, *JHEP* **05** (2008) 053, [arXiv:0801.2153].

[34] C. Rabideau, *Perturbative entanglement entropy in nonlocal theories*, *JHEP* **09** (2015) 180, [arXiv:1502.0382].

[35] N. Lashkari, C. Rabideau, P. Sabella-Garnier, and M. Van Raamsdonk, *Inviolable energy conditions from entanglement inequalities*, *JHEP* **06** (2015) 067, [arXiv:1412.3514].

[36] N. Lashkari, M. B. McDermott, and M. Van Raamsdonk, *Gravitational dynamics from entanglement 'thermodynamics'*, *JHEP* **04** (2014) 195, [arXiv:1308.3716].

[37] T. Faulkner, M. Guica, T. Hartman, R. C. Myers, and M. Van Raamsdonk, *Gravitation from Entanglement in Holographic CFTs*, *JHEP* **03** (2014) 051, [arXiv:1312.7856].

[38] B. Swingle and M. Van Raamsdonk, *Universality of Gravity from Entanglement*, arXiv:1405.2933.

[39] R. M. Wald, *Black hole entropy is the Noether charge*, *Phys. Rev.* **D48** (1993) 3427–3431, [gr-qc/9307038].

[40] V. Iyer and R. M. Wald, *Some properties of Noether charge and a proposal for dynamical black hole entropy*, *Phys. Rev.* **D50** (1994) 846–864, [gr-qc/9403028].

[41] J. Lin, M. Marcolli, H. Ooguri, and B. Stoica, *Locality of Gravitational Systems from Entanglement of Conformal Field Theories*, *Phys. Rev. Lett.* **114** (2015) 221601, [arXiv:1412.1879].

[42] J. Bhattacharya, V. E. Hubeny, M. Rangamani, and T. Takayanagi, *Entanglement density and gravitational thermodynamics*, *Phys. Rev.* **D91** (2015), no. 10 106009, [arXiv:1412.5472].

[43] J. de Boer, M. P. Heller, R. C. Myers, and Y. Neiman, *Holographic de Sitter Geometry from Entanglement in Conformal Field Theory*, *Phys. Rev. Lett.* **116** (2016), no. 6 061602, [arXiv:1509.0011].

[44] M. J. S. Beach, J. Lee, C. Rabideau, and M. Van Raamsdonk, *Entanglement entropy from one-point functions in holographic states*, *JHEP* **06** (2016) 085, [arXiv:1604.0530].

[45] T. Takayanagi, *Entanglement Entropy from a Holographic Viewpoint*, *Class. Quant. Grav.* **29** (2012) 153001, [arXiv:1204.2450].

[46] T. Nishioka and T. Takayanagi, *AdS Bubbles, Entropy and Closed String Tachyons*, *JHEP* **01** (2007) 090, [hep-th/0611035].

[47] I. R. Klebanov, D. Kutasov, and A. Murugan, *Entanglement as a probe of confinement*, *Nucl. Phys.* **B796** (2008) 274–293, [arXiv:0709.2140].

[48] N. Lashkari, *Equilibration of Small and Large Subsystems in Field Theories and Matrix Models*, *Commun. Math. Phys.* **333** (2015), no. 3 1199–1224, [arXiv:1304.6416].

[49] Y. Sekino and L. Susskind, *Fast Scramblers*, *JHEP* **10** (2008) 065, [arXiv:0808.2096].

[50] M. Requardt, *Entanglement-Entropy for Groundstates, Low-lying and Highly Excited Eigenstates of General (Lattice) Hamiltonians*, hep-th/0605142.

[51] V. Alba, M. Fagotti, and P. Calabrese, *Entanglement entropy of excited states*, *J. Stat. Mech.* **0910** (2009) P10020, [arXiv:0909.1999].

[52] M. Edalati, W. Fischler, J. F. Pedraza, and W. Tangarife Garcia, *Fast Scramblers and Non-commutative Gauge Theories*, *JHEP* **07** (2012) 043, [arXiv:1204.5748].

[53] W. Fischler, A. Kundu, and S. Kundu, *Holographic Entanglement in a Noncommutative Gauge Theory*, *JHEP* **01** (2014) 137, [arXiv:1307.2932].

[54] S. Minwalla, M. Van Raamsdonk, and N. Seiberg, *Noncommutative perturbative dynamics*, *JHEP* **02** (2000) 020, [hep-th/9912072].

[55] N. Seiberg and E. Witten, *String theory and noncommutative geometry*, *JHEP* **09** (1999) 032, [hep-th/9908142].

[56] M. Li and Y.-S. Wu, *Holography and noncommutative Yang-Mills*, *Phys. Rev. Lett.* **84** (2000) 2084–2087, [hep-th/9909085].

[57] S. Chakravarty, K. Dasgupta, O. J. Ganor, and G. Rajesh, *Pinned branes and new nonLorentz invariant theories*, *Nucl. Phys.* **B587** (2000) 228–248, [hep-th/0002175].

[58] A. Bergman and O. J. Ganor, *Dipoles, twists and noncommutative gauge theory*, *JHEP* **10** (2000) 018, [hep-th/0008030].

[59] K. Dasgupta, O. J. Ganor, and G. Rajesh, *Vector deformations of N=4 superYang-Mills theory, pinned branes, and arched strings*, *JHEP* **04** (2001) 034, [hep-th/0010072].

[60] E. Bergshoeff, C. M. Hull, and T. Ortin, *Duality in the type II superstring effective action*, *Nucl. Phys.* **B451** (1995) 547–578, [hep-th/9504081].

[61] K. Dasgupta and M. M. Sheikh-Jabbari, *Noncommutative dipole field theories*, *JHEP* **02** (2002) 002, [hep-th/0112064].

[62] K. Narayan, T. Takayanagi, and S. P. Trivedi, *AdS plane waves and entanglement entropy*, *JHEP* **04** (2013) 051, [arXiv:1212.4328].

[63] V. E. Hubeny, H. Maxfield, M. Rangamani, and E. Tonni, *Holographic entanglement plateaux*, *JHEP* **08** (2013) 092, [arXiv:1306.4004].

[64] M. Headrick, *Entanglement Renyi entropies in holographic theories*, *Phys. Rev.* **D82** (2010) 126010, [arXiv:1006.0047].

[65] E. Tonni, *Holographic entanglement entropy: near horizon geometry and disconnected regions*, *JHEP* **05** (2011) 004, [arXiv:1011.0166].

[66] W. Fischler, A. Kundu, and S. Kundu, *Holographic Mutual Information at Finite Temperature*, *Phys. Rev.* **D87** (2013), no. 12 126012, [arXiv:1212.4764].

[67] R. Bousso, S. Leichenauer, and V. Rosenhaus, *Light-sheets and AdS/CFT*, *Phys. Rev.* **D86** (2012) 046009, [arXiv:1203.6619].

[68] B. Czech, J. L. Karczmarek, F. Nogueira, and M. Van Raamsdonk, *The Gravity Dual of a Density Matrix*, *Class. Quant. Grav.* **29** (2012) 155009, [arXiv:1204.1330].

[69] V. E. Hubeny and M. Rangamani, *Causal Holographic Information*, *JHEP* **06** (2012) 114, [arXiv:1204.1698].

[70] R. Bousso, B. Freivogel, S. Leichenauer, V. Rosenhaus, and C. Zukowski, *Null Geodesics, Local CFT Operators and AdS/CFT for Subregions*, *Phys. Rev.* **D88** (2013) 064057, [arXiv:1209.4641].

[71] A. Hashimoto and N. Itzhaki, *Traveling faster than the speed of light in noncommutative geometry*, *Phys. Rev.* **D63** (2001) 126004, [hep-th/0012093].

[72] B. Durhuus and T. Jonsson, *Noncommutative waves have infinite propagation speed*, *JHEP* **10** (2004) 050, [hep-th/0408190].

[73] A. C. Wall, *Maximin Surfaces, and the Strong Subadditivity of the Covariant Holographic Entanglement Entropy*, *Class. Quant. Grav.* **31** (2014), no. 22 225007, [arXiv:1211.3494].

[74] M. Headrick and T. Takayanagi, *A Holographic proof of the strong subadditivity of entanglement entropy*, *Phys. Rev.* **D76** (2007) 106013, [arXiv:0704.3719].

[75] W. Li and T. Takayanagi, *Holography and Entanglement in Flat Spacetime*, *Phys. Rev. Lett.* **106** (2011) 141301, [arXiv:1010.3700].

[76] V. E. Hubeny, *Extremal surfaces as bulk probes in AdS/CFT*, *JHEP* **07** (2012) 093, [arXiv:1203.1044].

[77] D.-W. Pang, *Holographic entanglement entropy of nonlocal field theories*, *Phys. Rev.* **D89** (2014), no. 12 126005, [arXiv:1404.5419].

[78] D. Dou and B. Ydri, *Entanglement entropy on fuzzy spaces*, *Phys. Rev.* **D74** (2006) 044014, [gr-qc/0605003].

[79] D. Dou, *Comments on the Entanglement Entropy on Fuzzy Spaces*, *Mod. Phys. Lett.* **A24** (2009) 2467–2480, [arXiv:0903.3731].

[80] J. L. Karczmarek and P. Sabella-Garnier, *Entanglement entropy on the fuzzy sphere*, *JHEP* **03** (2014) 129, [arXiv:1310.8345].

[81] P. Sabella-Garnier, *Mutual information on the fuzzy sphere*, *JHEP* **02** (2015) 063, [arXiv:1409.7069].

[82] N. Shiba and T. Takayanagi, *Volume Law for the Entanglement Entropy in Non-local QFTs*, *JHEP* **02** (2014) 033, [arXiv:1311.1643].

[83] P. Calabrese and J. L. Cardy, *Entanglement entropy and quantum field theory*, *J. Stat. Mech.* **0406** (2004) P06002, [hep-th/0405152].

[84] H. Casini and M. Huerta, *Entanglement entropy in free quantum field theory*, *J. Phys.* **A42** (2009) 504007, [arXiv:0905.2562].

[85] M. P. Hertzberg, *Entanglement Entropy in Scalar Field Theory*, *J. Phys.* **A46** (2013) 015402, [arXiv:1209.4646].

[86] M. R. Douglas and N. A. Nekrasov, *Noncommutative field theory*, *Rev. Mod. Phys.* **73** (2001) 977–1029, [hep-th/0106048].

[87] "NIST Digital Library of Mathematical Functions." http://dlmf.nist.gov/, Release 1.0.8 of 2014-04-25. Online companion to [122].

[88] A. Erdélyi et al., *Tables of Integral Transforms*, vol. I and II. McGraw Hill, New York, NY, 1954. Available at http://authors.library.caltech.edu/43489/.

[89] P. Hayden, M. Headrick, and A. Maloney, *Holographic Mutual Information is Monogamous*, *Phys. Rev.* **D87** (2013), no. 4 046003, [arXiv:1107.2940].

[90] J. Hammersley, *Extracting the bulk metric from boundary information in asymptotically AdS spacetimes*, *JHEP* **12** (2006) 047, [hep-th/0609202].

[91] S. Bilson, *Extracting spacetimes using the AdS/CFT conjecture*, *JHEP* **08** (2008) 073, [arXiv:0807.3695].

[92] V. Balasubramanian, B. D. Chowdhury, B. Czech, J. de Boer, and M. P. Heller, *Bulk curves from boundary data in holography*, *Phys. Rev.* **D89** (2014), no. 8 086004, [arXiv:1310.4204].

[93] M. Nozaki, T. Numasawa, A. Prudenziati, and T. Takayanagi, *Dynamics of Entanglement Entropy from Einstein Equation*, *Phys. Rev.* **D88** (2013), no. 2 026012, [arXiv:1304.7100].

[94] J. Bhattacharya and T. Takayanagi, *Entropic Counterpart of Perturbative Einstein Equation*, *JHEP* **10** (2013) 219, [arXiv:1308.3792].

[95] S. Banerjee, A. Kaviraj, and A. Sinha, *Nonlinear constraints on gravity from entanglement*, *Class. Quant. Grav.* **32** (2015), no. 6 065006, [arXiv:1405.3743].

[96] S. Banerjee, A. Bhattacharyya, A. Kaviraj, K. Sen, and A. Sinha, *Constraining gravity using entanglement in AdS/CFT*, *JHEP* **05** (2014) 029, [arXiv:1401.5089].

[97] R. C. Myers and A. Singh, *Comments on Holographic Entanglement Entropy and RG Flows*, *JHEP* **04** (2012) 122, [arXiv:1202.2068].

[98] R. Callan, J.-Y. He, and M. Headrick, *Strong subadditivity and the covariant holographic entanglement entropy formula*, *JHEP* **06** (2012) 081, [arXiv:1204.2309].

[99] E. Caceres, A. Kundu, J. F. Pedraza, and W. Tangarife, *Strong Subadditivity, Null Energy Condition and Charged Black Holes*, *JHEP* **01** (2014) 084, [arXiv:1304.3398].

[100] D. D. Blanco, H. Casini, L.-Y. Hung, and R. C. Myers, *Relative Entropy and Holography*, *JHEP* **08** (2013) 060, [arXiv:1305.3182].

[101] H. Casini and M. Huerta, *A Finite entanglement entropy and the c-theorem*, *Phys. Lett.* **B600** (2004) 142–150, [hep-th/0405111].

[102] H. Casini, M. Huerta, and R. C. Myers, *Towards a derivation of holographic entanglement entropy*, *JHEP* **05** (2011) 036, [arXiv:1102.0440].

[103] B. Swingle and I. H. Kim, *Reconstructing quantum states from local data*, *Phys. Rev. Lett.* **113** (2014), no. 26 260501, [arXiv:1407.2658].

[104] M. Parikh and J. P. van der Schaar, *Derivation of the Null Energy Condition*, *Phys. Rev.* **D91** (2015), no. 8 084002, [arXiv:1406.5163].

[105] N. Lashkari and M. Van Raamsdonk, *Canonical Energy is Quantum Fisher Information*, arXiv:1508.0089.

[106] J. de Boer, F. Hael, M. P. Heller, and R. C. Myers, *Holography for Entanglement and Causal Diamonds, to appear*, .

[107] C. T. Asplund, N. Callebaut, and C. Zukowski, *Equivalence of Emergent de Sitter Spaces from Conformal Field Theory*, arXiv:1604.0268.

[108] B. Czech, L. Lamprou, S. McCandlish, B. Mosk, and J. Sully, *A Stereoscopic Look into the Bulk*, arXiv:1604.0311.

[109] T. Faulkner, *Bulk Emergence and the RG Flow of Entanglement Entropy*, *JHEP* **05** (2015) 033, [arXiv:1412.5648].

[110] A. J. Speranza, *Entanglement entropy of excited states in conformal perturbation theory and the Einstein equation*, arXiv:1602.0138.

[111] T. Faulkner, R. G. Leigh, and O. Parrikar, *Shape Dependence of Entanglement Entropy in Conformal Field Theories*, *JHEP* **04** (2016) 088, [arXiv:1511.0517].

[112] S. Hollands and R. M. Wald, *Stability of Black Holes and Black Branes*, *Commun. Math. Phys.* **321** (2013) 629–680, [arXiv:1201.0463].

[113] A. Almheiri, X. Dong, and D. Harlow, *Bulk Locality and Quantum Error Correction in AdS/CFT*, *JHEP* **04** (2015) 163, [arXiv:1411.7041].

[114] I. A. Morrison, *Boundary-to-bulk maps for AdS causal wedges and the Reeh-Schlieder property in holography*, *JHEP* **05** (2014) 053, [arXiv:1403.3426].

[115] A. Hamilton, D. N. Kabat, G. Lifschytz, and D. A. Lowe, *Holographic representation of local bulk operators*, *Phys. Rev.* **D74** (2006) 066009, [hep-th/0606141].

[116] A. Hamilton, D. N. Kabat, G. Lifschytz, and D. A. Lowe, *Local bulk operators in AdS/CFT: A Holographic description of the black hole interior*, *Phys. Rev.* **D75** (2007) 106001, [hep-th/0612053]. [Erratum: Phys. Rev.D75,129902(2007)].

[117] N. Lashkari, *Modular Hamiltonian of Excited States in Conformal Field Theory*, arXiv:1508.0350.

[118] C. Holzhey, F. Larsen, and F. Wilczek, *Geometric and renormalized entropy in conformal field theory*, *Nucl. Phys.* **B424** (1994) 443–467, [hep-th/9403108].

[119] X. Xiao, *Holographic representation of local operators in de sitter space*, *Phys. Rev.* **D90** (2014), no. 2 024061, [arXiv:1402.7080].

[120] B. Czech, L. Lamprou, S. McCandlish, and J. Sully, *Tensor Networks from Kinematic Space*, arXiv:1512.0154.

[121] B. Czech, L. Lamprou, S. McCandlish, and J. Sully, *Integral Geometry and Holography*, *JHEP* **10** (2015) 175, [arXiv:1505.0551].

[122] F. W. J. Olver, D. W. Lozier, R. F. Boisvert, and C. W. Clark, eds., *NIST Handbook of Mathematical Functions*. Cambridge University Press, New York, NY, 2010. Print companion to [87].

[123] M. Headrick, R. C. Myers, and J. Wien, *Holographic Holes and Differential Entropy*, *JHEP* **10** (2014) 149, [arXiv:1408.4770].

[124] K. Papadodimas and S. Raju, *An Infalling Observer in AdS/CFT*, *JHEP* **10** (2013) 212, [arXiv:1211.6767].

Appendix A

Analysis of the Potential Divergences from the $j > 1$ Terms

This analysis follows that of [83], where it is found that the leading divergence when the Green's function is evaluated at coincident points is entirely contained in the $j = 1$ term.

The Green's function for the scalar field on the n-sheeted space was given in (3.25):

$$\begin{aligned} G_n(x,x') = &\int_0^\infty \frac{dk}{\pi} \int \frac{d^{d_\perp}p^\perp}{(2\pi)^{d_\perp}} \int_0^\infty dqq \frac{J_k(qr)J_k(qr')}{q^2+p_\perp^2+m^2} \cos(k(\theta-\theta')) e^{ip_\perp(x_\perp - x'_\perp)} \\ &- \frac{1}{12\pi n^2} \int \frac{d^{d_\perp}p^\perp}{(2\pi)^{d_\perp}} \int_0^\infty dqq \frac{\partial_\nu [J_\nu(qr)J_\nu(qr')]_{\nu=0}}{q^2+p_\perp^2+m^2} e^{ip_\perp(x_\perp - x'_\perp)} \qquad \text{(A.1)} \\ &- \sum_{j>1} \frac{B_{2j}}{\pi n^{2j}(2j)!} \int \frac{d^{d_\perp}p^\perp}{(2\pi)^{d_\perp}} \int_0^\infty dqq \frac{(\partial_\nu)^{2j-1}[J_\nu(qr)J_\nu(qr')\cos(\nu(\theta-\theta'))]_{\nu=0}}{q^2+p_\perp^2+m^2} e^{ip_\perp(x_\perp - x'_\perp)}. \end{aligned}$$

The first term is independent of n and did not enter into the calculation of the entanglement entropy. The second term was the subject of our investigation. However, the third term was dropped with the claim that it could not introduce any new divergences. This appendix will justify this claim.

We start by revisiting the entanglement entropy in the commutative theory. In

this case from (3.42)

$$S \sim \int r dr G_1(r,r) f_n(r,r), \tag{A.2}$$

where only the contributions to the divergences in the final result have been kept.

The Green's function when evaluated at coincident points gives a Λ^2 divergence

$$\begin{aligned} G_1(r,r) \sim & \int d^4p \frac{1}{p^2+m^2} \sim \int d\alpha \; p^3 dp \; e^{-\alpha(p^2+m^2)-\frac{1}{\alpha\Lambda^2}} \\ & \sim \Lambda^2 - m^2 \log\Lambda^2. \end{aligned} \tag{A.3}$$

The f_n term has the form

$$f_n(r,r) \sim \int d^2p^\perp \; qdq \; \frac{\partial_\nu [J_\nu(qr)J_\nu(qr)]_{\nu=0}}{q^2+p_\perp^2+m^2} + \sum_{j>1} \int d^2p^\perp \; qdq \; \frac{\partial_\nu^{2j-1} [J_\nu(qr)J_\nu(qr)]_{\nu=0}}{q^2+p_\perp^2+m^2}. \tag{A.4}$$

The momentum integrals can be evaluated when the function is evaluated at coincident points

$$\begin{aligned} \int d^2p^\perp \; qdq \; \frac{J_\nu(qr)J_\nu(qr)}{q^2+p_\perp^2+m^2} &= \int d\beta \; pdp \; qdq \; J_\nu(qr)J_\nu(qr) e^{-\beta(q^2+p^2+m^2)-\frac{1}{\beta\Lambda^2}} \\ & \sim e^{-\frac{1}{2}r^2} I_\nu(\frac{1}{2}r^2) \log\Lambda^2. \end{aligned} \tag{A.5}$$

This must be integrated over r

$$\int_0^\infty r dr e^{-\frac{1}{2}r^2} I_\nu(\frac{1-\varepsilon^2}{2}r^2) = \frac{1}{\sqrt{2}\varepsilon} - \nu + O(\varepsilon), \tag{A.6}$$

where a small ε has been added to regulate the integral. It is only divergent because ∂_ν^{2j-1} was passed though the integral sign. Once this derivative is applied, ε can be safely taken to zero. A calculation of terms $O(\Lambda^0)$ would require a more careful

analysis, but this is sufficient for extracting the leading $O(\log\Lambda^2)$ divergence. Thus

$$\int d^4x f_n(x,x) \sim A_\perp \log\Lambda^2 \left[\partial_\nu(-\nu) + \sum_{j>1} \partial_\nu^{2j-1}(-\nu)\right] = A_\perp \log\Lambda^2 \left[-1 + \sum_{j>1} 0\right]. \tag{A.7}$$

This shows that all the $j > 1$ terms vanish when the Green's function is evaluated at coincident points and the divergence is entirely contained in the $j = 1$ term.

In the noncommutative and dipole theories, the Green's functions are evaluated at points separated by the length scale of the nonlocality rather than at coincident points. However, we saw that the source of divergences in the entanglement entropy was regions in the integral where this separation vanishes. This analysis shows that these divergences are contained in the $j = 1$ term.

Appendix B

Modular Hamiltonian for an Interval in a Boosted Thermal State of a 1+1D CFT

In this appendix, we derive the modular Hamiltonian for a spatial interval $[-R,R]$ in the boosted thermal state. To do this, we start by considering the domain of dependence D_1 of the interval $[-r,r]$ for the vacuum state in Minkowski space with coordinates (t',x'). For this interval, the modular Hamiltonian is quantum operator associated with the conformal isometry generated by

$$H_1 = \frac{\pi}{r}((r^2-(t')^2-(x')^2)\partial_{t'} - 2t'x'\partial_{x'}) \ .$$

We can now apply a boost

$$x' = \gamma(x-vt) \qquad\qquad t' = \gamma(t-vx) \ .$$

In this case, the region D_1 maps to the domain of dependence D_2 of the interval from $-(r_t,r_x)$ to (r_t,r_x), where $r^2 = r_x^2 - r_t^2$ and $v = r_t/r_x$. In this case, the generator H_1 maps to

$$H_2 = \frac{\pi}{r_x^2-r_t^2}\left[(r_x(r_x^2-r_t^2)+2txr_t - r_x(t^2+x^2))\partial_t + (r_t(r_x^2-r_t^2) - 2txr_x + r_t(x^2+t^2))\partial_x\right]$$

Next, we perform a transformation for which the causal development of the interval $[-1,1]$ maps to the full Minkowski space (with coordinates (u,τ)), such that the resulting state is the thermal state on Minkowski space dual to the planar BTZ geometry with horizon at $z = z_0$.

$$ds^2 = \frac{dz^2 - \left(1 - \frac{z^2}{z_0^2}\right)^2 d\tau^2 + \left(1 + \frac{z^2}{z_0^2}\right)^2 du^2}{z^2} \tag{B.1}$$

The appropriate transformation (which can be obtained by finding the coordinate transformation that maps the bulk region associated with the domain of dependence of $[-1,1]$ to the planar BTZ black hole) is

$$\begin{aligned} t &= \frac{\sinh(2\tau/z_0)}{\cosh(2u/z_0)+\cosh(2\tau/z_0)} \\ x &= \frac{\sinh(2u/z_0)}{\cosh(2u/z_0)+\cosh(2\tau/z_0)} \,. \end{aligned} \tag{B.2}$$

After the map, the region D_2 maps to the domain of dependence D_3 of the interval from $-(R_t,R_u)$ to (R_t,R_u), where

$$\begin{aligned} r_t &= \frac{\sinh(2R_t/z_0)}{\cosh(2R_u/z_0)+\cosh(2R_t/z_0)} \\ r_x &= \frac{\sinh(2R_u/z_0)}{\cosh(2R_u/z_0)+\cosh(2R_t/z_0)} \,. \end{aligned} \tag{B.3}$$

The generator H_2 maps to

$$\begin{aligned} H_3 \quad = \quad & \frac{\pi z_0}{C_u^2 - C_t^2} \left[\{ C_u S_u + C_u S_t \sinh(2u/z_0)\sinh(2\tau/z_0) - C_t S_u \cosh(2u/z_0)\cosh(2\tau/z_0) \} \partial_\tau \right. \\ & \left. \{ -C_t S_t + C_u S_t \cosh(2u/z_0)\cosh(2\tau/z_0) - C_t S_u \sinh(2u/z_0)\sinh(2\tau/z_0) \} \partial_u \right] \end{aligned} \tag{B.4}$$

where

$$C_u = \cosh(2R_u/z_0) \qquad S_u = \sinh(2R_u/z_0) \,.$$

Finally, we can perform one further Lorentz transformation

$$u = \gamma(u' + v\tau') \qquad\qquad \tau = \gamma(\tau' + vu') \,.$$

with velocity $v = R_t/R_x$, such that the region D_3 is mapped to the domain of dependence of the interval $[-R,R]$, where $R^2 = R_x^2 - R_t^2$. In terms of v, z_0, and R, we find that the generator H_3 restricted to $\tau' = 0$ gives

$$\begin{aligned} H_4 = \frac{\pi\gamma z_0}{C_u^2 - C_t^2}\{ & -\partial_{\tau'} \quad (\cosh(\gamma v U)\cosh(\gamma U)(C_u S_t v + S_u C_t) \\ & \quad -\sinh(\gamma v U)\sinh(\gamma U)(S_u C_t v + S_t C_u) \\ & \quad -(S_t C_t v + C_u S_u)) \\ & +\partial_{u'} \quad (\cosh(\gamma v U)\cosh(\gamma U)(C_u S_t + S_u C_t v) \\ & \quad -\sinh(\gamma v U)\sinh(\gamma U)(S_u C_t + S_t C_u v) \\ & \quad -(S_t C_t + C_u S_u v))\} \end{aligned} \tag{B.5}$$

where we define $U = 2u'/z_0$ and

$$C_t = \cosh(2R\gamma v/z_0) \qquad C_u = \cosh(2R\gamma/z_0) \qquad S_t = \sinh(2R\gamma v/z_0) \qquad S_u = \sinh(2R\gamma/z_0)\,.$$

The modular Hamiltonian is obtained by making the replacements $\partial_{\tau'} \to T_{\tau'\tau'}$ and $\partial_{u'} \to T_{\tau' u'}$ and integrating over $[-R,R]$.

Appendix C

Variation in Geodesic Length under Endpoint Variation

In this section, we derive a formula for the variation of the entanglement entropy of a boosted interval for some translation and time-translation invariant state in a holographic 1+1 dimensional field theory under a general variation in the endpoint of the interval.[1] We assume that the field theory lives on Minkowski space with coordinates (x,t).

The dual spacetime will be a 2+1 dimensional spacetime with translational isometries in one spatial direction and one time direction, associated with Killing vectors ξ_t^μ and ξ_x^μ. We assume that the spacetime has a conformal boundary, with a Minkowski space boundary geometry $ds^2 = -dt^2 + dx^2$ such that the Killing vectors ξ_t^μ and ξ_x^μ become $\partial_t = (1,0)$ and $\partial_x = (0,1)$ at the boundary. Consider a spatial geodesic with endpoints on the boundary at points 0 and $R(\gamma, \gamma v)$, where $v < 1$, $\gamma = (1-v^2)^{-1}$. We would like to determine the variation in length of the geodesic under a variation in the proper length R of the boundary interval.

The geodesic is an extremum of the action

$$S = \int_i^f d\lambda \sqrt{g_{\mu\nu} \frac{dx^\mu}{d\lambda} \frac{dx^\nu}{d\lambda}} \,. \tag{C.1}$$

[1] It is interesting to note that techniques similar to those in this section were used in [123] to show a relation between differential entropy and the lengths of bulk curves.

In general, the variation of an action $S = \int d\lambda \mathscr{L}(q_n, \dot{q}_n)$ evaluated for an on-shell configuration under a variation of the boundary conditions (assuming the range of integration remains the same) is given by

$$\delta S = [p_n \delta q_n]_i^f \ ,$$

where q_n are the coordinates and $p_n = \partial \mathscr{L} / \partial q_n$ are the conjugate momenta. This follows immediately since the variation of the action gives a total derivative when the Euler-Lagrange equations are satisfied. Consider a general variation of the endpoints

$$\delta x_f^\mu = \delta x \xi_x^\mu + \delta t \xi_t^\mu \ .$$

Since the conjugate momentum to x^μ is

$$p_\mu = \frac{\partial \mathscr{L}}{\partial x^\mu} = \frac{g_{\mu\nu} \frac{dx^\nu}{d\lambda}}{\sqrt{g_{\mu\nu} \frac{dx^\mu}{d\lambda} \frac{dx^\nu}{d\lambda}}} \ .$$

we have

$$\delta S = \delta x \xi_x^\mu p_\mu + \delta t \xi_t^\mu p_\mu \ . \tag{C.2}$$

Now, for a Killing vector ξ^μ, the action (C.1) is invariant under $x^\mu \to x^\mu + \xi^\mu$. The corresponding conserved quantity is exactly $\xi^\mu p_\mu$. Thus, the right hand side of (C.2) can be evaluated at any point on the trajectory. We choose to evaluate it at the midpoint of the geodesic, where $\partial_\lambda x^\mu$ is a linear combination of ξ_t^μ and ξ_x^μ (i.e. with no component in the radial direction). In this case,

$$\partial_\lambda x^\mu = \xi_t^\mu \frac{\xi_t \cdot \partial_\lambda x}{\xi_t \cdot \xi_t} + \xi_x^\mu \frac{\xi_x \cdot \partial_\lambda x}{\xi_x \cdot \xi_x} \ ,$$

so we find that our expression (C.2) becomes

$$\delta S = \delta x [\gamma_0 A_0^x] + \delta t [\gamma_0 \beta_0 A_0^t] \ . \tag{C.3}$$

where we have defined

$$A_0^x \ = \ \sqrt{\xi_x \cdot \xi_x}$$

$$
\begin{aligned}
A_0^t &= \sqrt{-\xi_t \cdot \xi_t} \\
\beta_0 &= \frac{A_0^x}{A_0^t} \frac{\xi_t \cdot \partial_\lambda x}{\xi_x \cdot \partial_\lambda x} \\
\gamma_0 &= \frac{1}{\sqrt{1-\beta_0^2}} ,
\end{aligned}
$$

which measures the "tilt" of the geodesic at the midpoint.

In the special case of a spatial interval, we will have $\xi_t \cdot \partial_\lambda x = 0$ everywhere, so

$$
\frac{\delta S}{\delta R} = \sqrt{\xi_x^2} = \sqrt{g_{\mu\nu} \xi_x^\mu \xi_x^\nu} \, . \tag{C.4}
$$

Thus, the variation of the entanglement entropy with respect to the size of a spatial interval gives exactly the spatial scale factor.

Appendix D

Rindler Reconstruction for Scalar Operators in CFT_2

In this appendix we find an expression for the matter contribution to the second-order perturbation to the entanglement entropy of a ball B using Rindler reconstruction so as to only use the one-point functions of the scalar operator in the domain of dependence D_B. We specialise to two dimensional CFTs in order to obtain a more explicit expression which can be compared to the gravitational contribution (5.10). Further discussions of Rindler reconstruction can be found in the literature [115, 116, 124, 114, 113].

Coordinates on the Rindler wedge R_B of radius R can be given by (r,τ,ϕ) which map back into Poincaré coordinates by

$$z=\frac{R}{r\cosh\phi+\sqrt{r^2-1}\cosh\tau}\,, \tag{D.1}$$

$$t=\frac{R\sqrt{r^2-1}\sinh\tau}{r\cosh\phi+\sqrt{r^2-1}\cosh\tau}\,, \tag{D.2}$$

$$x=\frac{Rr\sinh\phi}{r\cosh\phi+\sqrt{r^2-1}\cosh\tau}\,, \tag{D.3}$$

where $1<r<\infty$.

The scalar field dual to an operator $\mathcal{O}$ can be reconstructed in this Rindler

wedge using [113]

$$\phi(r,\tau,\phi) = \int d\omega dk\, e^{-i\omega\tau - ik\phi} f_{\omega,k}(r)\mathcal{O}_{\omega,k}\,, \tag{D.4}$$

$$f_{\omega,k}(r) = r^{-\Delta}\left(1-\frac{1}{r^2}\right)^{-i\frac{\omega}{2}} {}_2F_1\left(\frac{\Delta}{2}-\frac{i(\omega+k)}{2}, \frac{\Delta}{2}+\frac{i(\omega+k)}{2}; \Delta; r^{-2}\right), \tag{D.5}$$

where $\mathcal{O}_{\omega,k}$ is the Fourier transform of the CFT expectation value of the operator

$$\mathcal{O}_{\omega,k} = \int d\tau d\phi\, e^{i\omega\tau + ik\phi}\langle\mathcal{O}(\tau,\phi)\rangle\,. \tag{D.6}$$

This can be expressed in terms of the operator in the original coordinates

$$\mathcal{O}_{\omega,k} = \int_{D_B} dt dx \Big[(R+x+t)^{i\frac{k+\omega}{2}}(R-x-t)^{-i\frac{k+\omega}{2}} (R-x+t)^{i\frac{\omega-k}{2}}(R+x-t)^{i\frac{k-\omega}{2}}\Big]\langle\mathcal{O}(t,x)\rangle\,, \tag{D.7}$$

where the region of integration is only over the domain of dependence D_B.

This form of the scalar field can be combined with (5.58) to obtain an an expression for $\delta^{(2)}S^{scalar}$ which only depends on the expectation value of $\mathcal{O}$ in D_B,

$$\delta^{(2)}S^{scalar} = -\frac{1}{4}\int_1^\infty dr dk d\omega_1 d\omega_2\, r\sqrt{r^2-1}\Big[f_{\omega_1,k}(r)f_{\omega_2,-k}(r)\left(-\frac{\omega_1\omega_2}{r^2-1}+\frac{k^2}{r^2}+\Delta(\Delta-2)\right) + \left(r^2-1\right)f'_{\omega_1,k}(r)f'_{\omega_2,-k}(r)\Big]\mathcal{O}_{\omega_1,k}\mathcal{O}_{\omega_2,-k}\,. \tag{D.8}$$